Neotectonics in Central Mexico
from Landsat TM Data:

FINAL REPORT

Christopher G.A. Harrison and Christopher A. Johnson

RSMAS, University of Miami

Department of Marine Geology and Geophysics
4600 Rickenbacker Causeway
Miami, Florida 33149 USA

Neotectonics in Central Mexico
from Landsat TM Data:
FINAL REPORT

Christopher G.A. Harrison and Christopher A. Johnson

RSMAS, University of Miami
Department of Marine Geology and Geophysics
4600 Rickenbacker Causeway
Miami, Florida 33149 USA

_____
Christopher G.A. Harrison
Principal Investigator

_____
Christopher A. Johnson
Co-Investigator

15 December 1988

Popocatepetl from the west.

Table of Contents

1 Introduction

This report is a summary of results from a TM survey of neotectonics in central Mexico, dealing specifically with faulting and its relationship to volcanism there. The Mexican Volcanic Belt (MVB) is the dominant physiographic province in the study area. Late Miocene to Quaternary calc-alkaline volcanics of the MVB have been generated by active subduction of the Cocos plate beneath Mexico along the Middle America (Acapulco) Trench.

The course of human history in central Mexico has always been profoundly influenced by tectonic and volcanic activity in the region, from the time of the earliest human settlements there up through the modern disaster of the Mexico City earthquakes of September 1985. With this in mind, it is surprising to learn that very little is known in detail about the nature of recent crustal deformation and its relationship to volcanism there. In part, this lack of knowledge results from the size and extent of the volcanic province. It straddles a complicated zone comprising the various boundaries between at least four lithospheric plates, and stretches nearly 1000 km from the Gulf of California to the Gulf of Mexico, with an average width of about 100 km. The plates in the area include the North America, Pacific, Cocos, and Rivera plates.

We chose Mexico for this study because of the unusual characteristics of the Mexican volcanic arc, characteristics that had yet to be satisfactorily explained. The MVB is particularly interesting because it does not lie parallel to its trench (Figure 1). This fact has spurred recent speculation concerning the origin of the volcanic belt and its relationship to local and regional tectonics. Some consider the oblique orientation of the MVB to result from variations in the geometry of subduction along the trench (Suarez and Singh, 1986), while others suggest that zones of deformation and/or weakness in the overriding plate are responsible (Cebull and Shurbet, 1987). Previous studies have often focused on the structure and tectonics of parts or segments of the MVB (Allan, 1986; Nieto-Obregon *et al.*, 1985; Pasquare *et al.*, 1988), but so far no clear picture of regional crustal deformation supported by consistent regional observations has emerged. The regional and synoptic coverage and high spatial resolution offered by the Landsat Thematic Mapper (TM) enable a detailed analysis of structures within and around the MVB with a uniform data base. Although the MVB generally covers older rocks and structures, the volcanics provide an excellent surface for expression of neotectonic activity. We have used TM images to describe, map, and interpret recent crustal deformation in central Mexico, in order to better understand the regional tectonic relationships there.

This study used the many advantages provided by TM data to examine the nature and regional extent of recent tectonism in central Mexico. The mapping of neotectonic structures in the region was completed by tracing of fault scarps from digitally enhanced Landsat TM images at scales of 1:1,000,000 to 1:50,000. The TM data used in the study cover most of the MVB and include much of the area between the MVB and the southwestern Pacific coast of Mexico, more than a quarter of a million square kilometers. This report summarizes the information contained in the neotectonic maps derived from the interpretations. The knowledge gained from this regional analysis will be useful to other researchers studying the MVB at all scales. It also provides new perspective on the question of the oblique orientation of the MVB. In the regional sense, this study constitutes the first step toward an understanding of:

- the neotectonic activity (faulting) in central Mexico;

- crustal motions responsible for this faulting;

- the role of this activity in controlling the distribution and character of late Cenozoic volcanics there; and

- the spatial relationship of this activity to earlier zones of deformation.

1
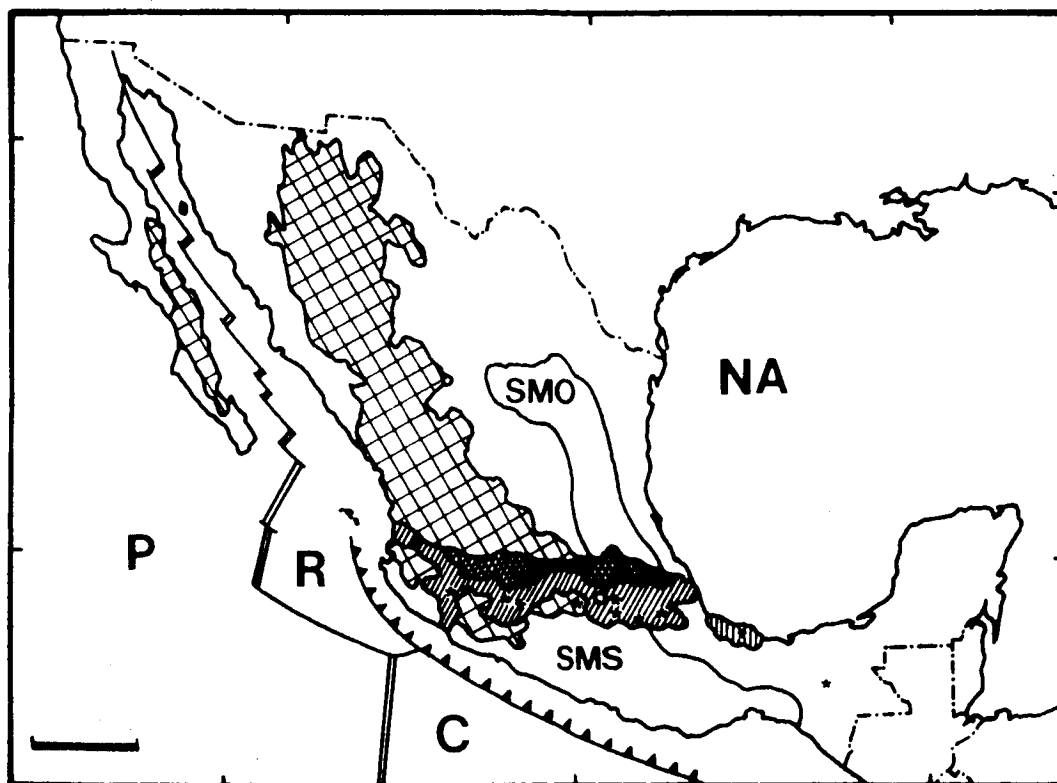
Figure 1: Principal tectonic elements of central Mexico. The oblique orientation of the volcanic belt relative to the Middle America Trench is clear. SMO=Sierra Madre Oriental, SMS=Sierra Madre del Sur, wide cross-hatch=Oligocene-Miocene volcanics of the Sierra Madre Occidental, narrow cross-hatch=northern Mexican Volcanic Belt (Pliocene), narrow diagonal lines=southern Mexican Volcanic Belt (Plio-Quaternary), narrow vertical lines=Tuxtla alkalic province, NA=North American Plate, P=Pacific Plate, C=Cocos Plate, R=Rivera Plate, stars=major volcanic centers, circle=Mexico City. Scale bar is 300 km long.

1.1 Statement of Problem and Approach

Present ideas on the origin and evolution of the MVB are diverse and surprisingly numerous. These include: subduction related volcanism (Molnar and Sykes, 1969; Thorpe, 1977; Hanus and Vanek, 1978; Lomnitz, 1982; Suarez and Singh, 1986); an ancient zone of crustal weakness (Mooser, 1972); a reactivated paleoshear (Le Pichon and Fox, 1971); or geosuture (Mooser, 1969); an extension of the Gulf of California (Mooser *et al.*, 1974); an extension of offshore transform faults (Gastil and Jensky, 1973); a zone of strike-slip displacement (Gastil and Jensky, 1973; Walper, 1980); left-lateral shear (Urrutia-Fucugauchi, 1984); crustal transtension (Shurbet and Cebull, 1984); or rifting and graben structures (Luhr *et al.*, 1985; Allan *et al.*, 1987). The origin of the magmas from which the volcanics are derived is equally the subject of debate, and suggestions include: lower crustal origin (Negendank, 1976); mantle origin (Verma, 1983, 1984); and mixing of magmas of diverse origins (Nelson and Carmichael, 1984).

From this abbreviated list it is clear that there is no lack of interest in this region and over the course of the past two decades many attempts have been made to understand its complexities. The majority of contributions have dealt only with small parts of the volcanic belt, and many of them then attempt to apply their conclusions to the rest of the belt. Verma (1985) has recently summed up the current status of research in central Mexico as follows:

> "in spite of such a large number of studies on the subject of the MVB, we still lack an adequate knowledge of many of its important aspects, problems, and solutions. Further, a large population of Mexico lives here as many important cities are located in the MVB (Mexico, Guadalajara, Puebla, Toluca, Queretaro, Pachuca, Cuernavaca, Veracruz, Colima, and so on). Thus, there exist innumerable problems associated with this densely populated area. Finally, this volcanic province is also very important from geothermal and economic-mineral points of view. Therefore, a systematic effort is very much needed".

One important problem that has emerged is that of the oblique orientation of the MVB relative to the Middle America (Acapulco) Trench, to which it has generally been assumed to be genetically related (see Figure 1). Researchers interested in this particular problem generally can be divided into two groups: the first attributes the anomalous orientation of the volcanic belt to progressive variations in the geometry of subduction along the trench; the second relates the orientation of the MVB to a zone of active deformation and/or crustal weakness within the overriding slab. Most agree that, to some extent, both factors probably contribute to the unusual orientation of the MVB, but it is instructive to examine each alone in more detail.

Cross and Pilger (1982) provide an excellent summary of the first school of thought in a paper where they discuss the various factors that control subduction geometry. They cite the Middle America Trench as an example of the complex interaction of several factors that influence the size of the arc-trench gap along a subduction zone. These factors are:

1. absolute motion of the overriding plate;

2. relative plate convergence rate;

3. anomalies in the subducted oceanic lithosphere such as seamount chains, aseismic ridges and oceanic plateaus; and

4. age of the subducted oceanic lithosphere.

Increasing the first three factors tends to increase the arc-trench gap by reducing the angle of subduction; while increasing the last factor causes two opposing tendencies:

- the high density of older lithosphere leads to high-angle subduction and decreases arc-trench distance; and

- opposing this is its lower temperature, which increases the arc-trench distance because of the additional time necessary for heating.

Cross and Pilger (1982) focus on the contrasting nature of the subduction zone off Mexico and Central America as an example where upper-plate absolute motion (factor 1 above) is the dominant control on the size of the arc-trench gap. Shallow subduction of the Cocos Plate takes place beneath Mexico where the North American Plate is actively overriding the trench, while steeper subduction takes place along Central America where, in the absolute-motion frame, the Caribbean Plate is nearly stationary. The MVB in Mexico is used as an example where the relative convergence rates (of the North American and Cocos Plates in this case) increase along the trench, producing a corresponding increase in the arc-trench gap (factor 2 above). This idea has been recently espoused by Suarez and Singh (1986), who attribute the anomalous orientation of the MVB to the progressive shallowing of the dip of the subducted slab from NW to SE along the Middle America Trench.

Shurbet and Cebull (1986) have argued that this fairly simple hypothesis fails to consider several key observations, drawing attention to complexities in the overriding slab:

- the observation that most of the volcanoes of the MVB are in excess of 50 km beyond (inland of) the limit of intermediate-depth seismicity associated with the downgoing slab (Nixon, 1982);

- geochemical evidence indicates a limited or minimal effect of the subducted slab (altered oceanic crust or sediments) or continental crust on the composition of volcanic rocks erupted along the MVB (Robin, 1982; Verma, 1983);

- perhaps most important, the hypothesis espoused by Cross and Pilger (1982) ignores the very complex pre-volcanic history of the central Mexican basement, in particular the likely possibility of an earlier zone of crustal weakness.

Evidence for tectonic activity in earlier epochs comes from a variety of sources, including likely offset of Pre-Mesozoic rocks and batholithic and mineral belts (de Cserna, 1970; Gastil and Jensky, 1973), paleomagnetic evidence for large-scale block rotations (Urrutia-Fucugauchi, 1981), and geometrical considerations derived from regional tectonic reconstructions (Anderson and Schmidt, 1983). Cebull and Shurbet (1987) discuss the evidence for the Mesozoic development of a zone of crustal weakness in the area of the present MVB. Neotectonic activity, as seen throughout the volcanic belt, may represent the reactivated offspring of such a zone of weakness (Mooser, 1972) as well as the development of an incipient plate boundary (Luhr *et al.*, 1985).

The problem of resolving this dichotomy, as well as assessing the relative contribution of each hypothesis to the actual situation in central Mexico, is made more difficult by the immense size of the region and the lack of regionally continuous data. Mohr (1974) studied a large portion of east Africa, using Landsat I imagery to map regional structures of the entire east African rift system. The general similarities between the two areas (east Africa and central Mexico) are quite striking: both are dominated by Plio-Quaternary volcanism

4

and tectonic activity; both involve a very large region not easily studied in detail by conventional means; and both may involve neotectonic activity that is geometrically controlled by much older inherited zones of weakness in the crust. Mohr (1974) demonstrated that the use of satellite images to study neotectonics of large regions such as this is highly effective.

1.2   Timetable

DATE	EVENT
1 Jul 1985:	contract NAS5-28745 begins;
Jul-Sept 1985:	repeated acquisitions of TM data over northern Venezuela, all of which were cloudy;
Sept 1985:	operational control of Landsat 4 and 5 transferred to EOSAT; all new acquisitions over original study area (Venezuela) are halted;
Jan 1986:	Johnson visits Goddard browse facility, determines that image situation for Venezuela is hopeless without additional acquisitions. Mexico and the Greater Antilles are considered as alternate areas;
29 Jan 1986:	first progress report;
26 Mar 1986:	request permission from NASA to change study area to Mexico;
14 Apr 1986:	change to Mexico accepted by NASA;
Apr 1986	scenes 26/46 26/47 29/46 received in Miami;
Apr-May 1986:	(3 weeks) first field trip to Mexico for reconnaissance and purchase of maps, etc.;
Jul 1986:	scene 27/46 received;
Jul-Aug 1986:	(5 weeks) Johnson goes to Goddard to do image enhancement on first four scenes using IAF;
3-5 Sept 1986:	Landsat TM Workshop, Goddard;
Dec 1986:	large scale TM photographic products arrive in Miami from Goddard;
Dec 1986:	AGU meeting, San Francisco; first presentation of some preliminary results;
Jan 1987:	Barros joins project with funding from NASA's Underrepresented Minority Program
May 1987:	Spring AGU meeting, Baltimore; poster session with more results;
Jun 1987:	(3 weeks) three additional scenes (27/47 28/46 26/48) partially processed at Goddard;
Sept 1987:	Landsat TM Workshop, Santa Barbara;

Oct 1987:	(1 week) trip to Mexico (Johnson/Barros) for purchase of additional maps and to set up closer collaboration with Mexican researchers for future field work and publications;
24 Sept 1987:	Johnson defends thesis: A Study of Neotectonics in Central Mexico from Landsat Thematic Mapper Imagery;
Oct-Dec 1987:	preparation for 3-4 week field trip in early 1988.
Mar-Apr 1988:	(3 weeks) field trip for ground truth and reconnaissance;
May 1988:	Johnson has hepatitis, contracted in Mexico;
Jun-Jul 1988	(3 weeks) last four TM images processed at Goddard;
Jul 1988:	COSPAR meeting in Helsinki, Finland; presentation of results summary;
Aug 1988:	final Landsat Workshop, University of Maryland; final results presented;
Aug 1988:	notification of acceptance of neotectonics paper submitted to Physics of the Earth and Planetary Interiors;
Sept-Nov 1988:	preparation of final report, publications;
Oct 1988:	notification of acceptance of two abstracts on the tectonic evolution of Mexico to be presented at the South-Central Section meeting of the Geological Society of America in March, 1989;
Dec 1988:	AGU Fall meeting, San Francisco, presentation of paper on Chapala-Oaxaca fault zone.

1.3 Satellite Remote Sensing

In the past decade, the speed and efficiency of geologic mapping and resource evaluation have been greatly facilitated by the use of Landsat Multi-Spectral Scanner (MSS) data (Williams, 1983; Ramos, 1977; Halbouty, 1976). Among the advantages of Landsat images over conventional aerial photographs for geologic mapping are (after Halbouty, 1976):

- the digital nature of the images, which permits the use of sophisticated data processing as an aid to geologic interpretation;

- the multispectral character of the images, which allows the discrimination of certain rock types that exhibit different spectral responses to incident light, producing subtle tonal variations that can be digitally enhanced; and

- the ability to use these images to map and interpret, on a regional scale of tens to hundreds of kilometers, geologic information that is often not visible on aerial photographs.

Another advantage that has been frequently overlooked is that for the study of large regions, satellite data can be significantly less expensive than comparable coverage using color aerial photographs (Lang *et al.*, 1987). For many areas, aerial photograph coverage may also be unavailable, inadequate, or totally lacking.

1.4 Landsat Thematic Mapper

In many ways the Thematic Mapper (TM) represents a major improvement over the earlier MSS, producing images that contain even more geologic information. The TM operates in seven spectral bands, three of which are in the range of the MSS (TM bands 2, 3, and 4). Bands for this sensor were selected after considerable study and debate; and the actual bands chosen represent a compromise between the needs of the geological community and those interested in agriculture and forestry. Table 1 shows the band designations, spectral ranges, and principal applications of each. As can be seen from the table, these spectral bands were chosen primarily for monitoring vegetation. An exception is band 7, which was added primarily for geological applications. TM bands 5 and 7 are both useful to geologists because of their capability of distinguishing clay and carbonate minerals (Paylor et $al.$, 1986).

Table 1 Thematic Mapper Spectral Bands

Band 1	(0.45-0.52 μm)	useful for coastal water mapping because of its water penetrating abilities; able to distinguish soil from vegetation
Band 2	(0.52-0.60 μm)	encompasses the visible green reflectance peak of vegetation; useful for assessment of vegetation health
Band 3	(0.63-0.69 μm)	chlorophyll absorption band useful for vegetation discrimination
Band 4	(0.76-0.90 μm)	useful for measuring biomass content and for delineation of water bodies
Band 5	(1.55-1.75 μm)	responds to vegetation and soil water content
Band 6	(10.40-12.50 μm)	thermal infrared band useful in vegetation stress analysis, thermal mapping, and soil moisture discrimination
Band 7	(2.08-2.35 μm)	a band selected for its ability to discriminate between different rock types, particularly various clay minerals, and for hydrothermal alteration mapping

The TM represents a great step forward in earth remote sensing for geological applications. The instantaneous field of view (IFOV) of the TM is 30x30 m (120x120 m for band 5), as opposed to 79x79 m for the MSS. This means that the resolution of the TM data is about 2.6 times that of the MSS (seven times better if the $area$ of each pixel is considered). This better resolution allows observation of much smaller areas, which in turn permits more detailed mapping of small-scale features such as stratigraphy and minor fault scarps. Even though the pixel size is smaller and the spectral bandwidths are narrower for the TM, its radiometric sensitivity is much improved over that of the MSS. Because of this improvement, the number of quantization levels has been increased from 64 for the MSS to 256 for the TM (a 6-bit versus an 8-bit quantization). This finer quantization allows for greater sensitivity to changes in radiometric values, both within a given spectral band and between bands.

These improvements in the TM "allow accurate photogeologic/geomorphic mapping, including relative age dating of alluvial fans, measurement of structural and bedding attitudes, and construction of such things as structural cross sections and stratigraphic columns" (Paylor et $al.$, 1986). Fielding et $al.$ (1986) have corrected regional maps and mapped the structure and stratigraphy of the Argentine Puna with TM imagery. The images allow the detection of clastic units of a thickness (5-10 m) that is below the actual resolution of the sensor, provided the spectral signature of the unit is sufficiently different from that of its surroundings. Lang et $al.$ (1987) report that it has been possible to map detailed structures in the Wind

River and Big Horn basin areas of central Wyoming. They used detailed stratigraphic columns of type sections, derived directly from TM imagery at scales up to 1:24,000, to trace the stratigraphy of the region. Together with strike and dip information (derived from the TM data in combination with topographic maps), this new information defines structures that are not shown on published maps, the details of which could later be confirmed on the ground.

1.5 Image Coverage and Quality

1.5.1 Day Scenes

In the first phase of this study a 1:1,000,000 scale TM image mosaic was constructed using ten black and white images of TM band 5. This band was chosen because of its capacity to penetrate haze and its reputation for higher contrast image products, which aids in structural interpretation. A sketch map showing the approximate aerial coverage of all the images eventually used in this study, and of the mosaic, is shown in Figure 2. For convenience in referencing, each image was assigned a name corresponding to a prominent physiographic or cultural feature within that particular image (see Table 2).

The data, as received from EOSAT, were in the form of 1:1,000,000 scale black and white negatives; and to construct the mosaic, a contact print of each was made and fitted carefully together with its neighbors. The geometric quality of the data was such that scene-to-scene registration was nearly perfect in all cases, with allowances for shadow effects due to variations in sun elevation and azimuth. Table 2 contains more detailed information on all of the TM data used in this study (both digital and photographic).

Table 2 Thematic Mapper data used in this study.

| Path/Row	Scene I.D.	Date Acquired	Sun el/az	Quality	Cloud Cover	Digital Negative	Name
30/45	50444-16540	5/19/85	61° / 88°	—	< 10%	/ N	'Tepic'
30/46	50444-16542	5/19/85	61° / 85°	—	< 10%	/ N	'Jalisco'
29/46	50677-16454	1/7/86	36° / 140°	+	0%	D / N	'Guadalajara'
29/47	50677-16460	1/7/86	37° / 139°	+	0%	/ N	'Colima'
28/46	50782-16371	4/22/86	58° / 99°	0	< 10%	/ N	'Penjamo'
28/46	50766-16373	4/6/86	55° / 108°	0	0%	D /	'Penjamo'
28/47	50782-16373	4/22/86	58° / 96°	0	0%	D / N	'Michoacan'
27/46	50695-16325	1/25/86	37° / 136°	+	0%	D / N	'Morelia'
27/47	50695-16332	1/25/86	38° / 135°	+	0%	D / N	'Tzizio'
26/46	50608-16282	10/30/85	46° / 139°	0	0%	D / N	'Tula'
26/47	50336-16302	1/31/85	40° / 134°	0	< 10%	D / N	'Mexico City'
26/48	50336-16304	1/31/85	41° / 133°	+	0%	D /	'Acapulco'
25/47	50297-16240	12/23/84	37° / 142°	0	< 10%	D /	'Puebla'
25/48	50297-16242	12/23/84	38° / 141°	0	0%	D /	'Oaxaca'
27/48	50743-16324	3/14/86	50° / 116°	+	0%	D /	'Zihuatanejo'
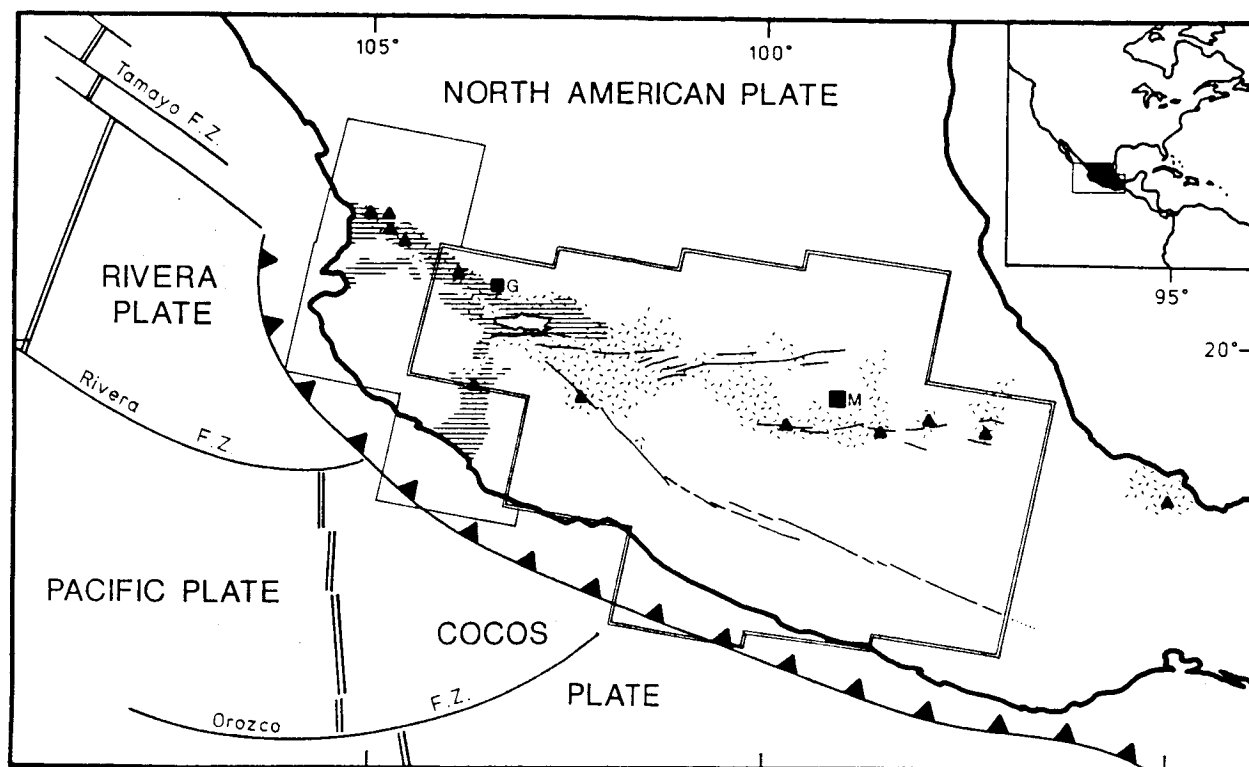
Figure 2: Sketch map showing coverage of the images used in this study. Doubly outlined areas are covered by both digital and photographic data at various scales up to 1:50,000. Single outlines show areas covered by photographic images at 1:1,000,000 scale only. For more detailed information on individual images please refer to Table 2.

9

Cartographically, all of the data used in this study is in the Space Oblique Mercator (SOM) projection. The SOM projection is virtually identical to the Universal Transverse Mercator (UTM) projection used in most standard geologic and topographic maps. It is slightly different, however, because the SOM projection uses meridians with azimuths parallel to the ground track of the satellite. This simplifies the calculations and cuts the time involved during the digital cubic-convolution resampling procedure used to register the data to a standard cartographic grid. Since the orbit of the Landsat 5 spacecraft is near-polar and inclined 98.2° with respect to the equator, the difference between SOM and UTM projections increases with increasing latitude. At the low latitudes involved in this study (18 to 21° N) the difference between the two projections is minimal; and enlargements of the Landsat images can be directly compared to geologic and topographic maps of the same scale.

The quality of the images varies quite a lot, due primarily to cloud cover and to the time of year that each image was acquired. Cloud cover does not exceed 10 percent in any of the images, but in those images where it approaches 10 percent a significant amount of information is lost, due to the additional loss in the cloud shadows. This is particularly troublesome in the 'Tepic' and 'Jalisco' images, where there were additional problems due to the acquisition date. In all cases, the images acquired during the winter months were clearer, primarily because of increased contrast due to low sun elevation, but also because clearer atmospheric conditions tend to prevail in central Mexico during this time of year. Those images acquired during the spring or fall presented a "washed-out" appearance and were more difficult to interpret for structures because of reduced shadow information. These conditions are taken into account in Table 2, where each image is given a relative quality estimate of worse (−), average (0), or better (+), related to their interpretability. Even in the worst images, many previously unmapped fault scarps were visible, although their sense of motion was more difficult to determine.

Besides the photographic data that were used in the mosaic, Table 2 shows the images available in digital format. Four of these (the 'Guadalajara', 'Morelia', 'Tula', and 'Mexico City' scenes) were digitally enhanced in the late Summer of 1986 at NASA's Goddard Space Flight Center (see the following chapter on image processing for a more detailed discussion of the techniques used to enhance the digital data). Other digital images were enhanced during two later visits to Goddard over the next two years. Photographic enlargements of the enhanced scenes were generated at Goddard and shipped to Miami. Full scene enlargements were produced at a scale of 1:250,000. In addition, 1:100,000 and 1:50,000 scale enlargements of portions of the scenes that were of particular interest were also generated.

1.5.2   Night (Thermal) Scenes

Nine thermal (TM band 6) images were acquired over our study area during the period from November 1987 through January 1988. Six of these were successful acquisitions. The other three were too cloudy to use. The path/row coordinates of these scenes are: 129/197; two from 130/198; 131/198; 131/197; 132/198. All scenes were single band photographic products at 1:1 million scale (black and white).

These images were useful for several reasons. First, many of the fault scarps that face southward were difficult to see on the day scenes because they lacked a sharp shadow. On the night thermal scenes, however, these scarps become much more visible due to their warmth, which is caused by solar heating during the day. Thus southward facing scarps stand out as bright (warm) lines against the generally darker (cooler) background. This weakness of the daytime data was largely compensated by their higher resolution, and no major neotectonic features were found on the night scenes that had been missed on the day scenes.

Another interesting feature was observed on the image from path 132, row 198. This scene roughly coincides with the day scene covering the region between Guadalajara and the Colima volcanoes. On the thermal

image there is a bright spot located at the summit of Volcan Colima that appears to reflect ongoing fumarolic activity. A similar, less intense, feature was detected on Volcan Popocatepetl. None of the other volcanoes covered by the thermal images displayed this type of feature. The crater lake at the summit of Nevado de Toluca (extinct) is slightly brighter on the thermal images, primarily because of the surface temperature contrast with the surrounding rocks. It was unfortunate that the digital data was not available for these scenes, since this made it impossible to study these features in more detail.

2 Image Processing

Computers can easily and rapidly manipulate digital images to produce more effective displays of image data for interpretation. Digital processing of digitally acquired images is generally preferred to photographic or optical processing because digital techniques are more flexible and powerful, and because there is no image degradation from repeated digital copying (Gillespie, 1980). The image processing for this study was done on the IAF (Image Analysis Facility) VAX 11/780 at Goddard Space Flight Center. The IAF is equipped with an extensive image processing and analysis software package called the Land Assessment System (LAS). It is an extremely versatile system consisting of over 240 functions for image analysis and enhancement. More detailed information on LAS and its applications may be found in the LAS User's Manual. Details of the image processing done at Goddard will be discussed later in this section.

With regard to this study the most important digital processing techniques are image rectification and enhancement. Rectification procedures remove distortions and degradations that have been introduced by the imaging process, and prepare an image for display and analysis. Standard corrections of this type are usually performed on the raw Landsat images prior to their distribution, so there is no need to go into further detail about them here. Pratt (1978) gives a more thorough discussion of image rectification procedures and their applications.

Image enhancement procedures aid in the extraction and interpretation of data and other information of interest that is often only subtly expressed on unprocessed or conventionally processed images. Enhancement methods can be generally divided into (from Moik, 1980):

- contrast enhancement (gray-scale modification);

- color enhancement (both pseudocolor and false color);

- edge enhancement;

- multi-image enhancement.

All of these have geologic applications, and all were used in one form or another during the course of this study. The following sections describe each in more detail as they relate to this study.

2.1 Contrast Enhancement

A raw image often spans only part of the full dynamic range of brightness values that the display device is capable of representing. Contrast enhancement is applied to the entire image in a uniform way so as to stretch the contrast to the full dynamic range. Such a procedure, termed a contrast stretch, may be implemented several ways using LAS, depending on the desired result. These transformations may also be used selectively to stretch the dark, midrange, or bright regions of the gray scale histogram, thus enhancing the corresponding portions of the Landsat scene. Using these methods to suit the individual image and the area of interest, subtle features that are expressed by very small gray scale changes can be made very clear.

In order to apply a contrast stretch to an image, one must first know the general characteristics of the gray-scale histogram for that image. For each image, these characteristics are unique, and they also vary

considerably between the different spectral bands of an image. The LAS function HISTPLT was used to obtain line printer plots of the gray-scale histograms (256 possible levels) for each of the images used in this study. A larger standard deviation means a broader gray-scale histogram, which directly translates into greater contrast in the image. Because the dynamic range of the TM sensor is 256 gray-scale values, even a standard deviation of 40 means that the majority of pixels in that scene are occupying only a portion of the values possible. Band 5 exhibited the highest contrast in all of the digital images, with band 2 generally showing the least contrast. These facts were taken into consideration later when band combinations were chosen for the color products.

Another important characteristic of the images used in this study is that their gray-scale histograms all tended to lie at the low end of the dynamic range. None of the histograms had an average value of over 100. This property would later cause problems during the edge enhancement of the images, which is discussed separately later.

One of the LAS intensity transformation functions, STRETCH, was used to perform the contrast enhancement of the images. Based on the characteristics of each histogram outlined above, this program generates a look-up table (LUT), which is just a list of linear transformations of input and output gray level values. If the lower valued pixels in an image are transformed to the bottom of the gray level scale, and the higher valued pixels are transformed to the highest values, with the medium valued pixels spread out between them, the result is a contrast stretched image. In practice this routine was the last step after the edge enhancement process. The objective in using it was an overall improvement in image contrast to aid in interpretation.

2.2 Color Enhancement

Any color can be produced through the combination of various amounts of three primary colors (usually red, green, and blue) in a color-additive system such as a CRT, or by subtraction of primaries (cyan, magenta, and yellow) from white in a subtractive system such as photographic film. The actual number of colors that can possibly be displayed are limited by properties of the display device (usually a CRT or color film) and by the number of bits/pixel/band of the image. This is illustrated by the RGB *color cube*, which is a three-dimensional color space defined by three orthogonal axes, each representing the gray levels of a component in the RGB display (Schowengerdt, 1983); RGB stands for the red, green and blue components of the display. For the TM, with 8 bits/pixel/band, a total of 256 gray levels are possible for each pixel, and 256^3 colors are possible in a three-band color combination. Each pixel in the color combination is represented by a vector within the color cube. Vectors that lie along the line between the origin of the color cube and the opposite corner represent pixels in various shades of gray, and thus this line is called the *gray line*. Pixels on this line have equal values in all three of the spectral components that make up the color composite.

The color properties of an object in an image may be described as having different amounts of *hue, saturation*, and *intensity*, which correspond to the subjective sensations of *color, color purity*, and *brightness*, respectively. Various systems have been devised to relate these three parameters on a single diagram, to assist in the understanding of the relationships between them. The Munsell system (Moik, 1980) consists of a cylindrical space defined by an axis, along which variations in intensity (brightness) are represented. The polar angle represents the hue, and the distance from the axis (radius) corresponds to the saturation. Any pixel in a digital image may be plotted within this space using the three parameters above. Gray shades, and therefore monochrome images, lie along the axis of the cylinder, because they have no hue or saturation (Moik, 1980).

The amount of information that can be represented on a display is dramatically increased through the use of color (Moik, 1980), which is the incentive behind color enhancement techniques. These are of two types. Pseudocolor is a technique by which the gray-scale is transformed into a scale of color hues, allowing the detection of many more levels of detail. For multispectral images, another type of enhancement is the combination of any of the bands, projected through appropriate primary filters, to produce a false color composite image.

2.3 Pseudocolor Enhancement

A monochrome image or a single band of a multispectral image contains brightness information that is often in the form of very small gray level differences. A *pseudocolor* operation is performed on the image to enhance these subtle differences in brightness, thus increasing the interpretability of the image. Each gray level is converted to a unique color on a scale encompassing all or part of the spectrum of colors that the display device is capable of generating. There are many logical techniques of assigning colors to gray levels. Most of them involve the generation of three pseudocolor component images, one for each of the primary colors, using a specified relationship between the intensity values of the input image and the corresponding intensity in each of the output component images. Careful consideration of the parameters that determine the above relationship is necessary to take maximum advantage of the added hue and saturation information, in addition to brightness, for the purpose of visual interpretation. The three component images are then recombined to form the pseudocolor image, using the appropriate primary color filters (Moik, 1980).

This technique is particularly effective when used to enhance thermal data, and so it has not seen wide application in the present study. Several night scenes were acquired over our study area (as described earlier); but all were in photographic format, so no digital manipulation of the data was possible.

2.4 False Color

In a multispectral scene where the spectral bands are not restricted to the visible spectrum, a false-color composite is needed to display information in the invisible part of the spectrum. A false-color composite image is generated by using any three spectral components (the TM has seven), combined using appropriate color filters. The reflective properties of the surface being imaged determine the values of the pixels within each spectral band, which will in turn determine the colors in the composite image. Normally, these colors are quite different from the actual color of the surface, because the composite is constructed from spectral bands that are restricted in width, and may also encompass invisible portions of the spectrum. When Landsat TM bands 2, 3, and 4 are displayed together as blue, green, and red, respectively, a standard *false-color infrared* image is generated. This is the standard color composite combination because of its similarity to color infrared photos. In actuality, the selection of spectral bands and their color assignments in the composite are arbitrary, and may be tailored to suit the particular needs of the interpreter. Prior to the combination of the various spectral components, various enhancements, filters, etc., may be used to take maximum advantage of the color information contained within the image. The results of various image transformations such as ratios may also be used as components in false-color composites.

For this study, many band combinations where tried prior to the selection of those that seemed to yield the best contrast and separability of rock units. As a matter of convention, each scene was depicted in the 234 combination (all band combinations in this report are in blue-green-red order). This combination, however, was found to be inferior to the alternative 'standard' combination (bands 134) for all of the TM scenes.

The reason for this was the generally poor contrast of TM band 2. The 134 combination was chosen for production of a print of each full scene at a scale of 1:250,000, in order to have a 'standard' image on which to begin interpretations. Overall, the clear choice as the most useful combination for all four images was the 734 combination. The most important advantage of this combination is its similarity to the standard 234 (or 134) combination as far as the depiction of vegetation in various shades of red, but with band 7 substituted for band 2 much more contrast is obtained throughout the image, even within the vegetated regions. The colors in this combination are much brighter, and many more shades and hues are clearly visible, probably corresponding to variations in the distribution of various clay and carbonate minerals on the ground, to which band 7 is more sensitive. This band combination has the additional useful property of separating volcanic flows and other deposits through contrasting shades of reds and browns, probably related to the differing maturity of the vegetative communities on the flows of different ages, as well as to subtle mineralogical variations between the flows, which may be due to variable clay compositions on the weathered rock surface and in the overlying soil.

The 154 combination is also useful in distinguishing various volcanic units in the 'Mexico City' scene (254 was used for volcanic areas of the 'Chapala' scene). Unlike the standard band combinations, this one is sensitive to the moisture content of the vegetation, and color differences in the image reflect this sensitivity. Plants in and around bodies of water are generally bright red to pink in this combination, while drier vegetation, such as that found on the forested slopes of the volcanoes and other highland areas, appears in shades of darker reds and browns. Vegetation that is drier still, such as the dry grasses and shrubs that cover the much more arid lowland areas, appear in shades dominated by greens, but also including blues and even purples. The potential of this particular band combination for geobotanical discrimination of rock units has not been fully explored yet. This combination was not so useful for all of the images, particularly the 'Morelia' and 'Tula' scenes, perhaps because of atmospheric conditions that severely curtailed the contrast of band 2 in those scenes.

Another combination that was often found useful was that of bands 247. Three of the full scenes were printed in this combination. Its properties include the depiction of vegetation in various shades of green, with drier areas appearing tan to pink. Using this combination, it is also sometimes possible to distinguish between various volcanic rocks based solely on color.

2.5   Edge Enhancement

Lineaments of geologic significance, such as faults, topographic crests and vales, and lithologic and structural contacts, can be sharpened using edge enhancement (Williams, 1983). Sharpening may be achieved through high-pass filtering, which emphasizes spatial frequencies above a chosen cutoff frequency. Noise is also enhanced by this process, so it should be carefully reduced or removed before edge enhancement techniques are applied. The noise level of our Landsat images was generally low enough so that even the strongest edge enhancement filters resulted in a minimum amount of visible noise in the output.

Blurred images may be sharpened by an operation similar to differentiation, because blurring is an averaging process (Moik, 1980) equivalent to integration. For digital images differences, rather than derivatives, must be used. The resulting image is composed of elements representing the magnitude of the gradient at each pixel location. The First Difference method, which is essentially a differentiation process, has been used to highlight the geologic "structural fabric" or the pattern of very small linear features down to the resolution limit of the imaging system (Williams, 1983). The following mathematical summary of simple edge enhancement techniques is largely based on discussions of the subject by Moik (1980) and Rosenfeld and Kak (1982). Other useful summaries of edge enhancement techniques are presented by Pratt (1978) and Schowengerdt (1983).

For a digital image $\mathbf{G}$ at line j and column k, the *first differences* in the x- and y-directions are defined as

$$\Delta_x \mathbf{G}(j,k) = \mathbf{G}(j,k) - \mathbf{G}(j-1,k) \quad \Delta_y \mathbf{G}(j,k) = \mathbf{G}(j,k) - \mathbf{G}(j,k-1) \tag{1}$$

where the quantities $\Delta_x \mathbf{G}(j,k)$ and $\Delta_y \mathbf{G}(j,k)$ are the row and column first differences, respectively. Linear combinations of $\Delta_x \mathbf{G}$ and $\Delta_y \mathbf{G}$ may be used to define first differences in other directions. The magnitude of the *digital gradient* of $\mathbf{G}(j,k)$ is

$$|\nabla \mathbf{G}(j,k)| = \sqrt{[\Delta_x \mathbf{G}(j,k)]^2 + [\Delta_y \mathbf{G}(j,k)]^2} \tag{2}$$

and the first difference enhanced image is obtained by

$$\mathbf{G}_D = |\nabla \mathbf{G}|. \tag{3}$$

Another very useful form of edge enhancement involves a number of methods loosely grouped under the term *Laplacian*. It was a modified form of this method that was used for the enhancement of the digital images in this study. The primary objective of applying this form of enhancement was to improve the visibility of small-scale edge features, particularly fault scarps, which would likely go unnoticed in the raw image data.

At a location (j,k) in an image $\mathbf{G}$, the digital Laplacian is

$$\nabla^2 \mathbf{G}(j,k) = [\mathbf{G}(j+1,k) + \mathbf{G}(j-1,k) + \mathbf{G}(j,k+1) + \mathbf{G}(j,k-1)] - 4\mathbf{G}(j,k). \tag{4}$$

The Laplacian edge image $\mathbf{G}_L$ is then

$$\mathbf{G}_L = \nabla^2 \mathbf{G}. \tag{5}$$

Pixels in the Laplacian image $\mathbf{G}_L$ will have values that are proportional to the difference between the gray level of $\mathbf{G}(j,k)$ and the average gray level of the four horizontal and vertical neighbors of (j,k). For example, if $\mathbf{G}$ were a Landsat image, pixels in broad regions having nearly constant radiance, such as areas of water or smooth plains, will have very low values in the Laplacian $\mathbf{G}_L$. Conversely, at the boundaries of such regions, such as shorelines or fault scarps in shadow, $\mathbf{G}_L$ takes on larger absolute values. Actually, the Laplacian $\mathbf{G}_L$ is negative at the bottom of an edge or ramp and positive at the top for the one-dimensional case.

When the Laplacian of an image is subtracted from the image itself, the result is an edge-enhanced version of the original

$$\mathbf{G}_e = \mathbf{G} - \nabla^2 \mathbf{G} \tag{6}$$

where an element of $\mathbf{G}_e$ is given by

$$\mathbf{G}_e(j,k) = 5\mathbf{G}(j,k) - [\mathbf{G}(j+1,k) + \mathbf{G}(j-1,k) + \mathbf{G}(j,k+1) + \mathbf{G}(j,k-1)]. \tag{7}$$

The enhanced image $\mathbf{G}_e$ is deblurred by the emphasis of high-frequency information, and is termed the *Laplacian Difference* image.

A convenient method of performing the above enhancements is by digital filtering. By convolving $\mathbf{G}$ with a filter function h, the filtered image $\mathbf{G}_F$ is obtained

$$\mathbf{G}_e = \mathbf{G} * h. \tag{8}$$

This type of convolution is extremely flexible because h can be modified to suit any application. For instance, the Laplacian operation of equation (5) is easily computed using the convolution operation (8) along with the proper 3×3 convolution filter matrix h_L:

$$[h_L] = \begin{pmatrix} 0 & 1 & 0 \\ 1 & -4 & 1 \\ 0 & 1 & 0 \end{pmatrix}. \tag{9}$$

Similarly, the Laplacian Difference operation (6) can be implemented using (8) and h_{LD}:

$$[h_{LD}] = \begin{pmatrix} 0 & -1 & 0 \\ -1 & 5 & -1 \\ 0 & -1 & 0 \end{pmatrix}. \tag{10}$$

Notice that (10) is equivalent to the original image (a matrix with a single element: a one in the center) minus the Laplacian matrix (9). Alternative digital "Laplacian Differences" may be used by defining different filter matrices, normally with the stipulation that the sum of their elements is unity.

The LAS function CONVOLVE was used to perform the edge enhancements, and it allows the user to define the elements of the filter matrix to be used in the convolution. The standard Laplacian Difference matrix (10) was tried at first, but it tended to yield results that were unacceptable because the digital grid became too apparent when the enhanced images were enlarged, which tended to distract the eye from important trends on the image. For this reason (and because much of the color contrast was lost during the filtering process, resulting in grayish color composites) it was decided to boost the contribution of the central element in the matrix by a factor of one, producing a more gentle, modified convolution matrix h_M:

$$[h_M] = \begin{pmatrix} 0 & -1 & 0 \\ -1 & 6 & -1 \\ 0 & -1 & 0 \end{pmatrix} \tag{11}$$

but since the sum of the elements should be unity, h_M was divided by 2 to yield

$$[h_{M'}] = \begin{pmatrix} 0 & -.5 & 0 \\ -.5 & 3 & -.5 \\ 0 & -.5 & 0 \end{pmatrix}. \tag{12}$$

This is essentially the same as averaging the Laplacian Difference image with the original, to obtain an enhanced image without the distracting harshness that the standard Laplacian Difference filter produced. An added benefit associated with the use of (12) for the convolution was the restoration of most of the color contrast in the enhanced image.

A problem was encountered early in the edge enhancement work which was related to the generally low average radiance of the TM scenes. The edge enhancement routines used generally widened the gray-level histogram of the image being enhanced, with the result that, for areas such as shadows or water with average pixel values in the neighborhood of zero, many of the pixels in the output image were forced to values below zero. Because each pixel is an 8-bit word, this meant that the value in the output image would be represented as $(256 - x)$, where x is the distance below zero that particular pixel was forced. This wrap-around effect caused the darker regions in the output image to contain a "salting" of bright pixels, which was perhaps unimportant but very distracting. During interpretation the problem was finally solved by linearly moving the histogram to the midrange of brightness values prior to the edge enhancement.

The full procedure that was developed for edge enhancement involved three basic steps, using various functions of LAS. These steps are as follows:

- the raw data was moved to the midrange of the gray scale prior to the edge convolution, to eliminate the "salting" problem mentioned above (see Figure 3);

- the image was then convolved using the convolution matrix (12), which resulted in a slight smoothing and broadening of the image histogram;

- finally, a contrast stretch was applied to the edge enhanced image, accomplished by stretching the lower and upper 0.2% frequency values to gray level values of 40 and 240, respectively (Figure 3).

As a result of the filtering process described above, the enhanced images displayed much greater detail and sharpness than the unenhanced images. When compared directly, the latter almost appear as if they are out of focus, the blurring is so evident (Figure 4). Two possible causes of this blurring effect in the raw data are:

- the cubic convolution used to resample the original data for mapping into the SOM projection on the 'P' tapes probably causes a small blurring effect; and

- there may be a small amount of "leakage" in this data, caused by a portion of the radiance that each pixel detects being contributed by radiance from adjacent pixels.

Whatever the cause of the blurring, features that are hardly visible in the raw data stand out much more sharply following the filtering operation using (12). Upon reexamination, all features found on the enhanced images can also be found on the raw images, although sometimes with difficulty. In general, the enhancement only makes the images more interpretable, but it does not create features that do not exist in the raw images.

2.6 Multi-Image Enhancement

Ratioing is a type of multi-image enhancement technique that has been successfully employed for geologic applications (Goetz et al., 1975; Gillespie, 1980; Stewart et al., 1980). Assuming band to band registration, when the tonal or density values of one band of a multispectral scene are divided by the corresponding values of another, the result is termed a *ratioed image*. Actually the process is not quite so simple because of complications that arise when both images have very low values (areas of shadow in an image are a good example). In this instance, the signal to noise ratio is radically decreased and the values of the ratioed image derived from them fluctuate wildly (and meaninglessly). This problem is usually eliminated by the application of a "shadow mask", which is simply the assignment of all pixels in shadow to a value of zero. Therefore this solution is, at best, only a compromise, because of the loss of important information in areas of shadow. An additional problem arises when considering the possibility of mistaking low-radiance areas of an image for shadows. The shadow masking technique is discussed in more detail by Podwysocki et al. (1983).

Even with these serious problems, this simple method has proven to be one of the most useful (Sabins, 1978), because it enhances subtle tonal variations due to slightly different spectral characteristics of surface materials, while suppressing changes in illumination due to topography. This makes ratioing extremely useful for tracing lithology, and when the appropriate bands are used, for delineating areas of alteration that might point to mineralization and/or faulting. Landsat ratios have been used for a variety of applications, including: minimizing the effects of vegetation in the study of soil conditions (Siegal and Goetz,

'Mexico City' TM band 4
Histograms during edge enhancement
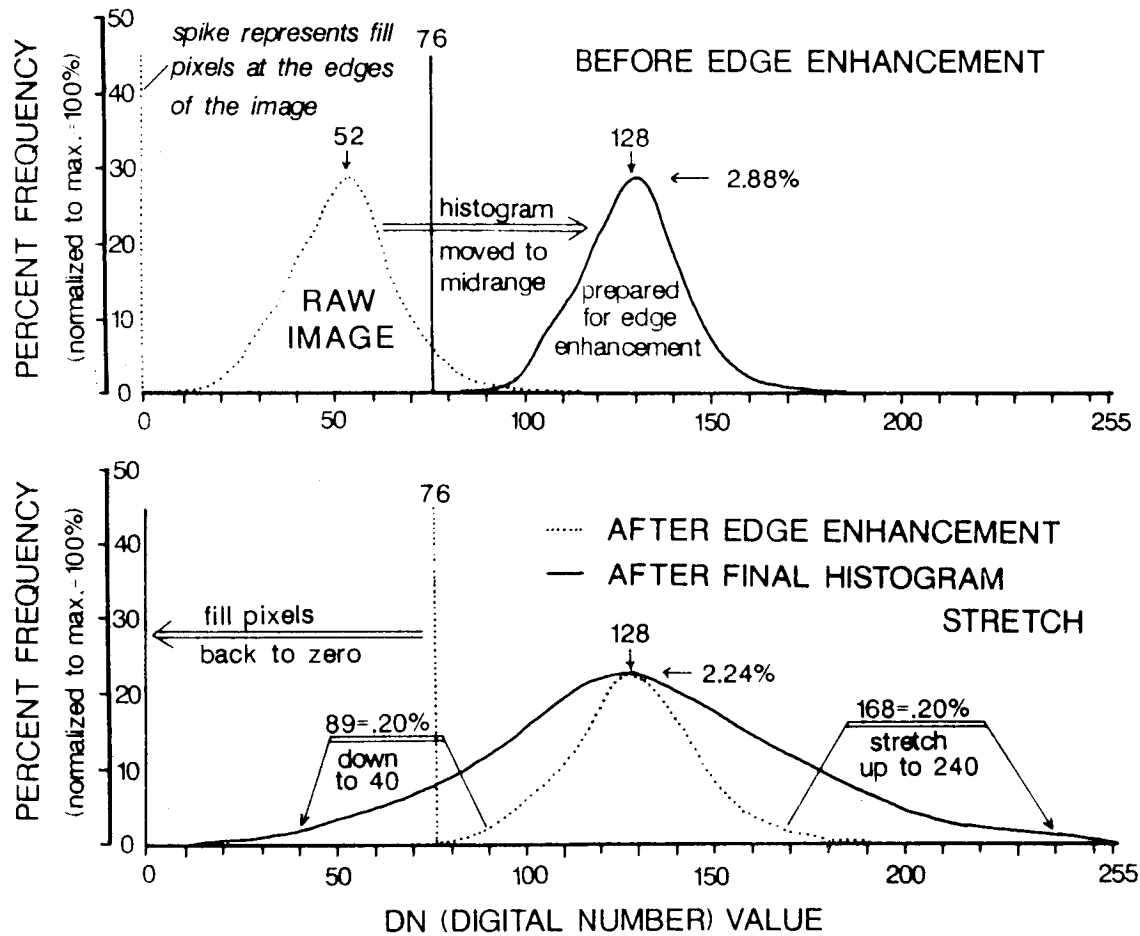
Figure 3: Illustration showing edge enhancement procedure used in this study.

Figure 4: A portion of the Morelia scene 256 pixels long by 128 pixels wide (approximately 7.3 km by 3.65 km). The top half of the figure shows the raw data, and the bottom half shows the same area after the application of the Laplacian Difference filter (eq. 6) using the modified convolution matrix (12). The enhancement of many subtle details is readily apparent.

1977); emphasizing variations in silicate composition using thermal bands (Vincent, 1975); discrimination between hydrothermally altered and unaltered rock (Podwysocki *et al.*, 1983); separation of lithologies and discrimination of hydrothermal alteration associated with porphyry copper deposits (Abrams *et al.*, 1983); and lithologic discrimination and enhancement of structural features (Stewart *et al.*, 1980). For maximum effect, the choice of the appropriate ratio combination depends on the application and desired results.

For an image with P spectral components, the number of ratios that are possible is $n=P(P-1)$, and n equals 42 for the Landsat TM. The number of possible combinations (m) increases when the combination of any three of these ratios into a color composite is considered: $m=n!/[3! \, (n-3)!]$. This number increases further because there are six different ways of assigning each combination to the three primary colors. This means that the most useful ratios are not easily chosen, and that *a priori* knowledge of the best ratios and color combinations is necessary for the most efficient use of ratioing (Moik, 1980).

In view of the shadow problem and others associated with the ratioing of images, it was thought appropriate to attempt more subtle techniques. The method of choice was a simple differencing technique with a few minor modifications. This method is based on a simple premise: that differences in spectral reflectance between bands may be enhanced by the subtraction of one band from another. The difference image should have advantageous properties similar to those of the ratio, including enhancement of subtle spectral variations and suppression of topographic shading (albeit more gently in a standard difference), and none of the disadvantages related to shadows.

The difference between two spectral bands of a multispectral image will naturally have both positive and negative values, so it must be scaled for display and further enhancement. In addition, the scaling should increase the contrast enough to make small changes visible. The standard difference image $\mathbf{G}_{k,D}$ is computed using

$$\mathbf{G}_{k,D} \; = \; a(\mathbf{G}_i - \mathbf{G}_j) + b \tag{13}$$

where $\mathbf{G}_i$ and $\mathbf{G}_j$ are different spectral component images (Moik, 1980). The constant a is used for scaling the image contrast, and may be substituted with any form of contrast enhancement algorythm that may be appropriate. The constant b is determined so that zero difference between $\mathbf{G}_i$ and $\mathbf{G}_j$ results in a medium gray value.

There was not enough time to fully explore the possibilities of this technique during the work at Goddard Space Flight Center, since most of the time was devoted to the edge enhancement of the images. A portion of the 'Mexico City' image covering the area around Taxco was used to experiment with the difference technique, and the most promising procedure discovered so far consists of the following steps:

- after the spectral bands to be differenced have been selected, their histograms are equalized;

- one band is subtracted from the other using the LAS function ADDPIC, with the image to be subtracted multiplied by a factor of negative one;

- the result of zero difference is set to a gray value of 128;

- the final step is a contrast enhancement of the difference image, setting the 0.2 percentile values in its histogram to 40 and 240 (these are arbitrary values determined by characteristics of the display device).

This procedure results in the greatest contrast in the final product; and discrete lithologic units generally have smooth, consistent gray level representation throughout the image. Also, the topographic information is almost completely removed, producing a 'flat' effect similar to a geologic map.

The selection of spectral bands for the difference images began with information found in the literature on the most useful band ratios. After the most likely candidates were tried, additional differences were tried experimentally, based on visual estimations of brightness contrasts between bands. Settle *et al.* (1985) describe several useful band ratios used during the NASA/GEOSAT Test Case Project for discrimination of lithology. The sensor used was the NS-001 Thematic Mapper Simulator, having bands generally equivalent to those on the Landsat TM. The most useful ratios were found to be the equivalents of bands 5/7, 3/2. 4/5, and 2/5. For the various test sites involved in the NASA/GEOSAT Project, these band ratios were determined to be useful for the discrimination and mapping of iron oxidation, vegetation communities, and for relating image spectra to mineralogy.

The equivalent differences (5 − 7, 3 − 2, 4 − 5, and 2 − 5) were tried for the area around Taxco, but the 5 − 7 difference was the only one useful, although 5 − 4 also produced a great amount of contrast. The 3 − 1 difference was found to be superior to the 3 − 2 difference, perhaps because of the very low contrast exhibited by band 2 in this image. A fourth difference, 7 − 3, seemed well suited for discrimination of vegetation types, which in turn should be useful for lithologic mapping using geobotanical considerations.

Three of the differences (5 − 4, 3 − 1, and 5 − 7) were combined in a color composite (Figure 5). This composite image shows excellent color contrast between lithologic types (Figure 6 shows the corresponding 734=BGR false-color combination, for comparison); and all of the lithologies represented on a geologic map of a portion of the image can be discriminated and traced into regions that are unmapped. The interpretation of this image is still progressing, but the potential that it indicates for application of the difference technique, here and elsewhere, is promising.
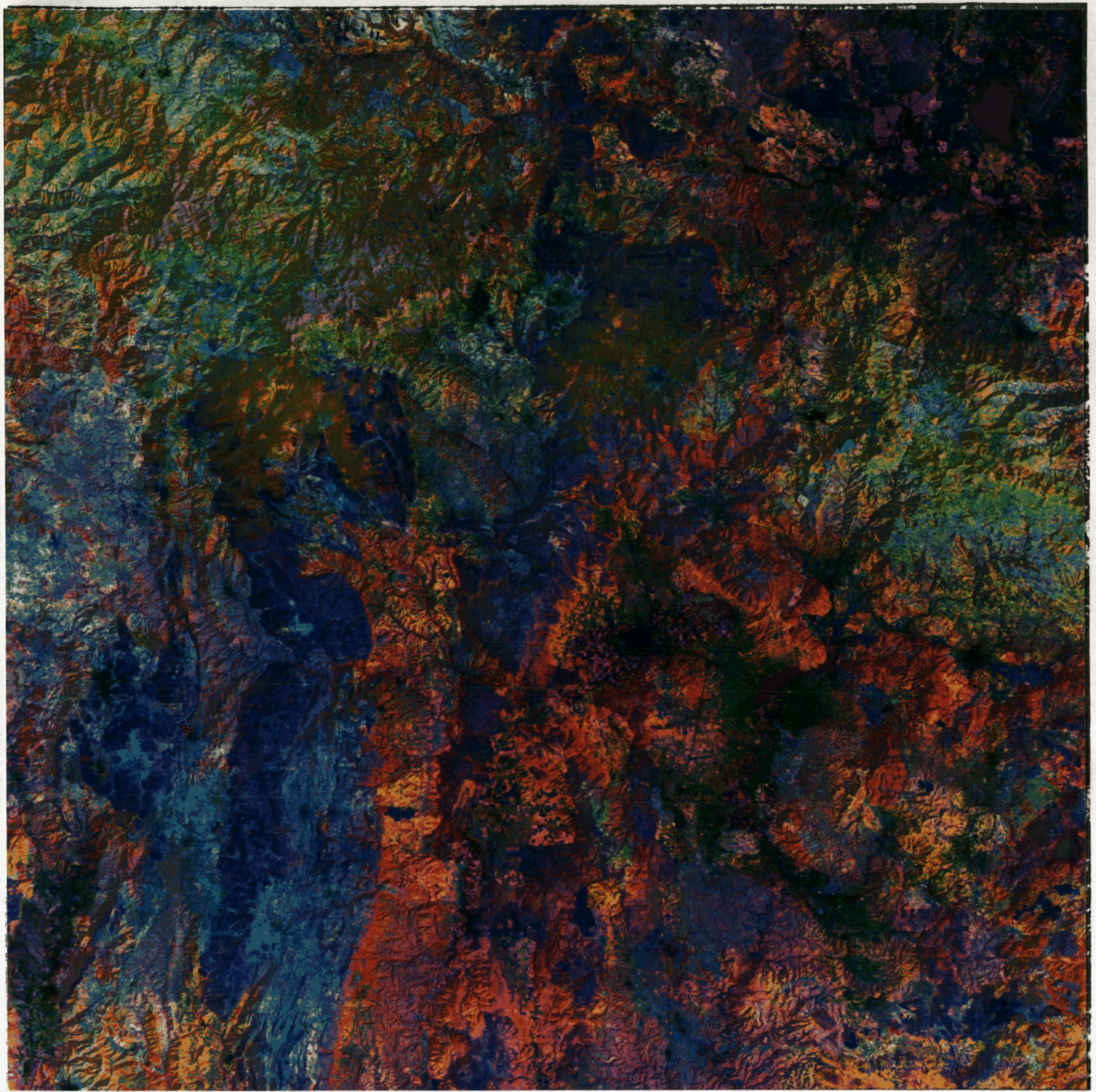
Figure 5: A portion of the Mexico City scene covering the region around Taxco. The image is 2500 by 2500 pixels on a side or about 75 km on each side.
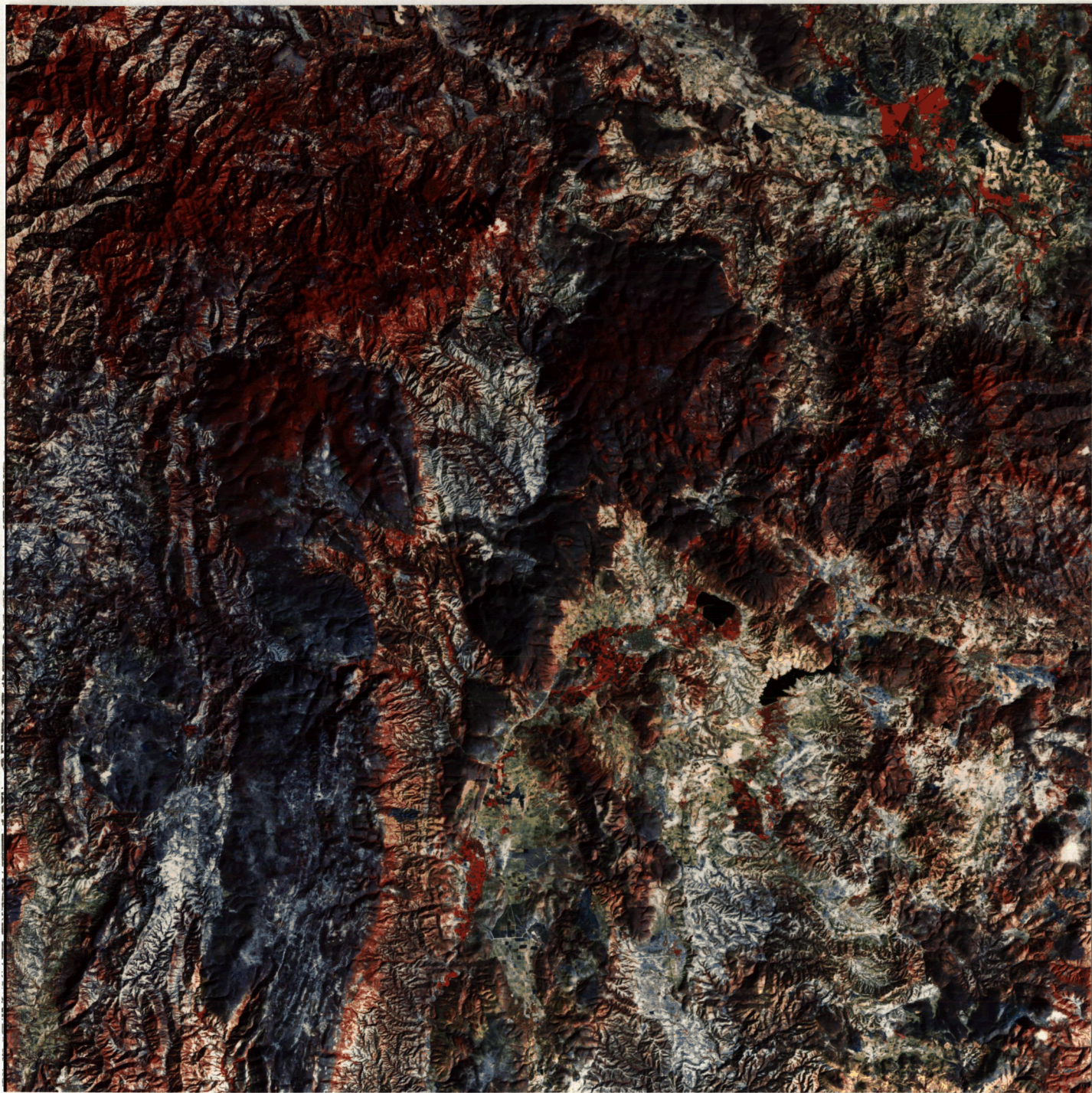
Figure 6: Same area as in Figure 5, but showing the false-color band combination of bands 734=BGR. The separability of units is much more difficult here than on the difference image in Figure 5.

3   Image Interpretation

During the course of the image analysis, the photointerpreter must draw upon knowledge of the character and evolution of landforms based on their geological and structural relationships, and on the geomorphological processes that continuously modify the surface of the earth. Of particular importance when mapping neotectonics is a thorough understanding of the differences between a *fault scarp* and a *fault-line scarp.* Davis (1913) was among the first to define these features. According to his definition, a *fault scarp* is a scarp *originated* by faulting, while a *fault-line scarp* originates through erosion along a fault line. This seems like a trivial point, but it is actually a fundamental difference related to the age and history of movement on the fault in question. A fault scarp begins with a fault at or near its base, and evolves by erosional processes through mature and old stages as the scarp retreats. This older scarp, though it be a mere remnant, is still technically a fault scarp. In contrast, a fault-line scarp is produced by differential erosion of rocks on either side of the fault. This occurs when the fault brings rocks of contrasting erosional resistance together at the surface. Depending on which side of the fault lies the most resistant rock, the fault-line scarp may even face in the opposite direction of the original fault. The most significant aspect of the distinction between fault scarps and fault-line scarps is that the latter are most often related to earlier episodes of deformation, while the former are nearly always related to the most recent movements. Thornbury (1969) discusses these relationships in more detail.

3.1   Interpretation Criteria

Various criteria were used in this study to distinguish young fault scarps from numerous other forms of linear features that are invariably present on satellite images. The list of criteria that follows has been modified from Thornbury (1969), and most of the items are directly applicable to central Mexico.

Items found along both fault scarps and fault-line scarps

1. A front that is both abrupt and imposing. Regardless of whether this type of feature is related to a fault scarp or a fault-line scarp, it usually implies that the *scarp* is young. If it is a fault scarp, then the associated faulting must be young; if a fault-line scarp, then only the erosion need be recent, and faulting may still be quite old.

2. The presence of faulting as documented by evidence such as: exposure of the fault surface and/or slickensides; presence of fault breccia, mylonites, or crushed zones with excessive jointing and fracturing; truncation of geologic strata or structures, and/or associated displacement of same. All of these items together do not determine if a scarp originated through faulting or differential erosion along a fault. They are, however, conclusive evidence for the presence of a fault. Many of these items are difficult or impossible to detect with remote sensing alone, so for this study other evidence for faulting was much more important.

3. Truncation of mountain spurs by triangular facets. Although these are more frequently found along fault scarps, they may also develop along a fault-line scarp. In the case where they are found along a fault scarp, their slopes must be steep (> 30°) to imply very recent faulting.

4. Scarp having a linear base. Faults are usually slightly sinuous and do not extend in straight lines over long distances. Over short distances, however, they may approximate linearity.

5. Deep V-shaped canyons extending from the fault line up into the upthrown block. These are normally more common in association with fault scarps where the streams have cut down into their beds during

uplift. They may also be found along fault-line scarps in areas of regional uplift.

6. Springs at the base of the scarp. These are sometimes associated with zones of faulting, but they do not necessarily indicate active or recently active faulting.

7. Volcanism along a fault trace. This does not necessarily demonstrate recent faulting because it may merely represent renewed volcanism along a zone of weakness marked by an inactive fault. On the other hand, if the recent volcanics are faulted themselves, or if the faulted surface beneath the volcanics is only slightly older, then recent faulting is conclusively demonstrated.

These items were only considered if they were found in combination with others implying recent faulting. These are listed below.

Features indicative of recent or renewed faulting (fault scarps)

1. Relative displacement of Quaternary deposits. As Thornbury (1969) notes, opportunities to make this test are rare. For this reason the MVB is an excellent area to study recent faulting because of its youthful volcanic cover. The generally smooth surface of these deposits (or predictably rough surfaces such as the cones of volcanoes) clearly display any disruption caused by faulting. As a subset of these features we might include young, displaced erosional surfaces.

2. Frequent landslides. Thornbury (1969) included this item in his list of features of ambiguous affinity (see below). However, it seems incredible to assume that a scarp that is prone to slump or slide could exist for a very long time, especially in a region such as central Mexico where active tectonics and earthquakes are the norm.

3. Abnormally small or absent alluvial fans at the base of a scarp. This situation develops when the fault block at the base of the scarp has recently sunk, lowering alluvium previously derived from above the scarp.

4. The presence of scarps in alluvial deposits. Whenever a scarp is found in unconsolidated deposits it provides positive evidence for recent faulting, since such scarps are rapidly degraded by erosion. Thus, unless displacement is extremely rapid, this type of feature is normally small and not easily detected using only TM imagery.

5. Warped terraces. Where stream terraces exhibit abnormally steep slopes or slope reversal, active faulting associated with nearby scarps may be indicated.

6. Earthquakes. Frequent earthquakes are obvious evidence for continued deformation, and shallow earthquakes may be related to recent or active faults exposed at the surface. Unfortunately, no local seismic network has been established yet in central Mexico, so this form of evidence is nearly completely lacking. Large earthquakes produced by subduction of the Cocos plate along the Middle America Trench are fairly common. First motion studies of some of these have been used to constrain relative motion directions for plates in the vicinity of the study area. This is discussed in more detail later.

7. Ponded drainage. This situation develops when a scarp faces upstream and cuts across a stream valley. This is very rare in cases of fault-line scarps.

8. The presence of "rift" features near or along a scarp. These include smaller scarps, sag ponds or basins, ramps, and wedge-shaped hills, often having complex relationships to one another.

9. Poor or anomalous correlation between rock resistance and topographic expression. A fault-line scarp will always have a strong correlation between resistance and topography, i.e. the most resistant rock is *always* found on the scarp side of the fault. The reverse of this relationship always indicates that the scarp is a fault scarp.

10. For faults where there is no significant difference in rock strength on either side, two additional features are strong indicators of recent faulting. The first is an increasing stream gradient as the fault line is approached. These "wine-glass" or "hour-glass" valleys, as they are called, result from rejuvenation of the stream near the fault when movement on the fault is renewed. If this movement is rapid enough, the stream bed may actually be separated vertically by the fault scarp, resulting in the second indicative feature, called a "hanging valley".

Features specifically excluded from the neotectonic interpretation

In the absence of other evidence for recent faulting. the following items may imply the existence of a fault but do not suggest whether it is recent or ancient in origin. They are most common in older, uplifted and eroded terranes that have experienced several overprinted tectonic episodes. As such their locations and trends are more useful in correlating various crustal blocks that may have been displaced relative to each other, but not as indications of neotectonic activity.

- Alignment of notches, cols, and jogs along ridges, with no apparent lithologic control.

- Long, linear, parallel, or *en echelon* stream courses and valleys that cut across or oblique to the regional structural trend.

- Tonal or vegetation alignments.

The actual interpretation of the 1:1,000,000 scale images proceeded in the following way. First, faults were traced from each image separately on a mylar sheet. This was accomplished by scratching the trace of the fault in the surface of the mylar. This was considered to be slightly more accurate than tracing the faults with a pen, which left a line that was too thick to be precise, and it had the additional advantage of leaving the fault visible for later checks of the interpretation. After the interpretations of all the images had been completed, they were fitted together using the mosaic as a base. To make the fault tracings more visible before transferring them to the final diagram, ink was rubbed into the scratches, producing very fine dark lines.

At a scale of 1:1 million, many of the standard photogeological techniques used for detailed interpretations of larger scale aerial photographs remain applicable. However, at such a small scale, only those techniques involving interpretation of larger geologic and/or geomorphologic features and relationships are useful in the evaluation of the regional geologic situation. This is partly because the smaller features are less clearly visible and thus are more likely to be misinterpreted, but also because preoccupation with excessive detail can hamper the regional view. This is not to say that details visible at small scales should be ignored; on the contrary, they should be noted and their presence incorporated into the regional interpretation.

Details of the fault pattern in central Mexico are known to varying degrees for different parts of the region, based largely on ground and aerial photographic surveys. In the western part of central Mexico, ground surveys are fairly complete in the region surrounding the R-R-R (rift-rift-rift) triple junction SW of Guadalajara, due largely to efforts by a group out of Washington University, Tulane University and the University of California (Allan *et al.*, 1987). Within each of the rifts involved in the triple junction, mapping

is still largely in the reconnaissance stage, as is mapping of faults farther to the east. To my knowledge, no detailed mapping within the MVB has been accomplished from the Michoacan-Guanajuato volcanic field eastward. Exceptions to this include works by Sanchez-Rubio (1984), Segstrom (1962), and Urbina and Camacho (1913). Certainly no regional mapping has been accomplished on any scale approaching that which is possible using the TM imagery.

The faulting that gives form to the modern rift structures of central Mexico is generally recognized to be of Plio-Quaternary age (Allan *et al.*, 1987). The faults are therefore usually sharply defined topographically, and this means that they are clearly visible on the Landsat TM imagery. This is particularly true for faults that face away from the sun's illumination, for south- or east-upthrown faults with scarps facing north or west. Faults with fresh scarps facing south or east are often visible through the illumination of their scarps, which produces a sharp bright strip on the image, but if a scarp is eroded then its trace can be hidden in background brightness variations. It is therefore very likely that there is a bias in the interpretations favoring faults on the eastern or southern margins of grabens and on the western or northern margins of horsts. This bias is represented on the maps by a preponderance of faults of this description. Mohr (1974) noticed the same problem during his ERTS survey of rift faulting in east Africa. In many cases this bias could be partly compensated for by examination of enlargements of problematic areas.

The throw direction on normal faults can also be determined through other means such as identification of the drainage pattern (Mohr, 1974). In some parts of the study area this is less help because of the arid conditions and therefore the lack of a prominent surface drainage pattern. On the other hand, in the oldest terrains where the drainage pattern is best developed, young fault scarps can be hidden, especially if they are relatively minor. The drainage in older areas tends to develop along joints and bedding, to the point that young faults disturb the surface pattern too little to be detected. In forested areas, faults are generally harder to detect because of the very dark tones of the vegetation on TM band 5. Vegetation, however, is often denser along the base of a fault scarp, where there is a concentration of near-surface ground water. This can be a reliable guide to the trace of a fault in the arid parts of central Mexico, particularly within the valleys and at the lower altitudes of the plateau in general. In areas that are completely forested, such as the slopes of the strato-volcanoes and other highland areas, it is often necessary to resort to TM band 4, in which vegetation presents a lighter tone, so that faults can be traced using the sun-shadow or illumination of their scarps.

The smallest faults included on the neotectonic maps derived from the interpretation of the 1:1,000,000 scale TM image mosaic are 3 to 4 km long and probably have a maximum vertical displacement of a few tens of meters, the minimum displacement is probably much less, on the order of 5 m. There is some merit to the argument that these smaller faults probably should not be included on a regional map of this type; but their presence on the map is certainly useful for enhancing the visibility of the deformational fabric within the larger zones of deformation.

The advantage of the Landsat TM imagery is that it enables a very detailed survey of the structure and deformation within the entire region of central Mexico for the first time. It must again be emphasized that satellite remote sensing of this type is no substitute for detailed work on the ground, but it does serve as a valuable guide to the most interesting and problematic areas. With respect to what it reveals about already well-studied regions, the satellite imagery enables a solid first interpretation of regional tectonics in more poorly-studied areas. It is also remarkable how much new information can be gained from analysis of the TM images of even well-studied areas.

3.2 An Example of the Interpretation

As an example of image interpretation, Figure 7 shows a portion of the 'Chapala' scene covering the area of the triple junction south-southwest of Guadalajara. The three-armed aspect of the triple junction is easily visible on the image as three basins which converge near the center of the area (TJ). Lake Chapala, the large dark area in the upper right of the image, fills the basin formed by the Chapala Graben. The bright area extending southward from the triple junction is a salina covering the floor of the Colima Graben. Extending to the northwest is the Zacoalco Graben, with smaller lakes filling depressions between small volcanic hills and ridges. Figure 8 shows the corresponding image interpretation.

Tilted fault blocks dominate the spectacular topography in the upper half of the image (blocks marked FB are the best examples). Their relatively smooth tops slope gently to the north or northeast. Small streams are beginning to incise the lacustrine deposits in the upper surfaces of many of the fault blocks. These lacustrine sediments probably correlate with similar sediments in the Sierra Primavera near Guadalajara, which are Pleistocene in age (Mahood, 1980). In contrast, the steep sides of the blocks are rapidly being cut by streams, forming spur ridges and deep v-shaped valleys (V). The ridges are often truncated by triangular facets (f) associated with the faults at the edges of the blocks, and the valleys end along the fault line (FL) which marks the boundary between uplifted and down dropped blocks. On the opposite side of the faults from the valleys (the down-thrown side), the relatively smooth alluvial surface (A) helps to define the faults, which run between the alluvium and the valleys/ridges. All of these features indicate that faulting has occurred recently.

Other examples of faults of probable recent age cut several young volcanic cones (C) within the Citala Graben. Although absolute dating of the faults using only the image interpretation is not possible, it is possible to get relative ages. Since the cones marked (C) in the figure are of Latest Pliocene to Pleistocene in age, based on the similarity of their morphology to dated cones north of Lake Chapala, the faults are of probable Quaternary age, and many are possibly still active. The fault scarps stand out prominently against the smooth surface of the cones. The direction of throw on the faults is determined by whether the scarp is illuminated or in shadow. Examples both illuminated and shaded scarps are shown in the figure.

Figures 7 and 8 also illustrate the differences between scarps interpreted to be associated with Quaternary faulting, and scarps of less certain affiliations, which may be related to older faults and fractures. The southeastern quadrant of the image is dominated by highlands at the northern edge of the Michoacan block, which is bounded in this area by the Colima and Citala Grabens. The highlands are underlain by Mesozoic metamorphic rocks and sediments, which have undergone multiple phases of tectonism in both the Mesozoic and Cenozoic. Many linear valleys can be seen to cross the highland area (dotted lines), and the first impression is that these are faults. Since the surface of the highland is very irregular, it is difficult to determine if these are the result of erosion or recent faulting, so they have not been included on the fault maps. The fault marked (F) in the southeastern corner of the image is an exception to this, because it clearly interrupts alluvial features such as small valleys and ridges that intersect it. Valleys on its eastern side are uplifted and many terminate abruptly against the fault.
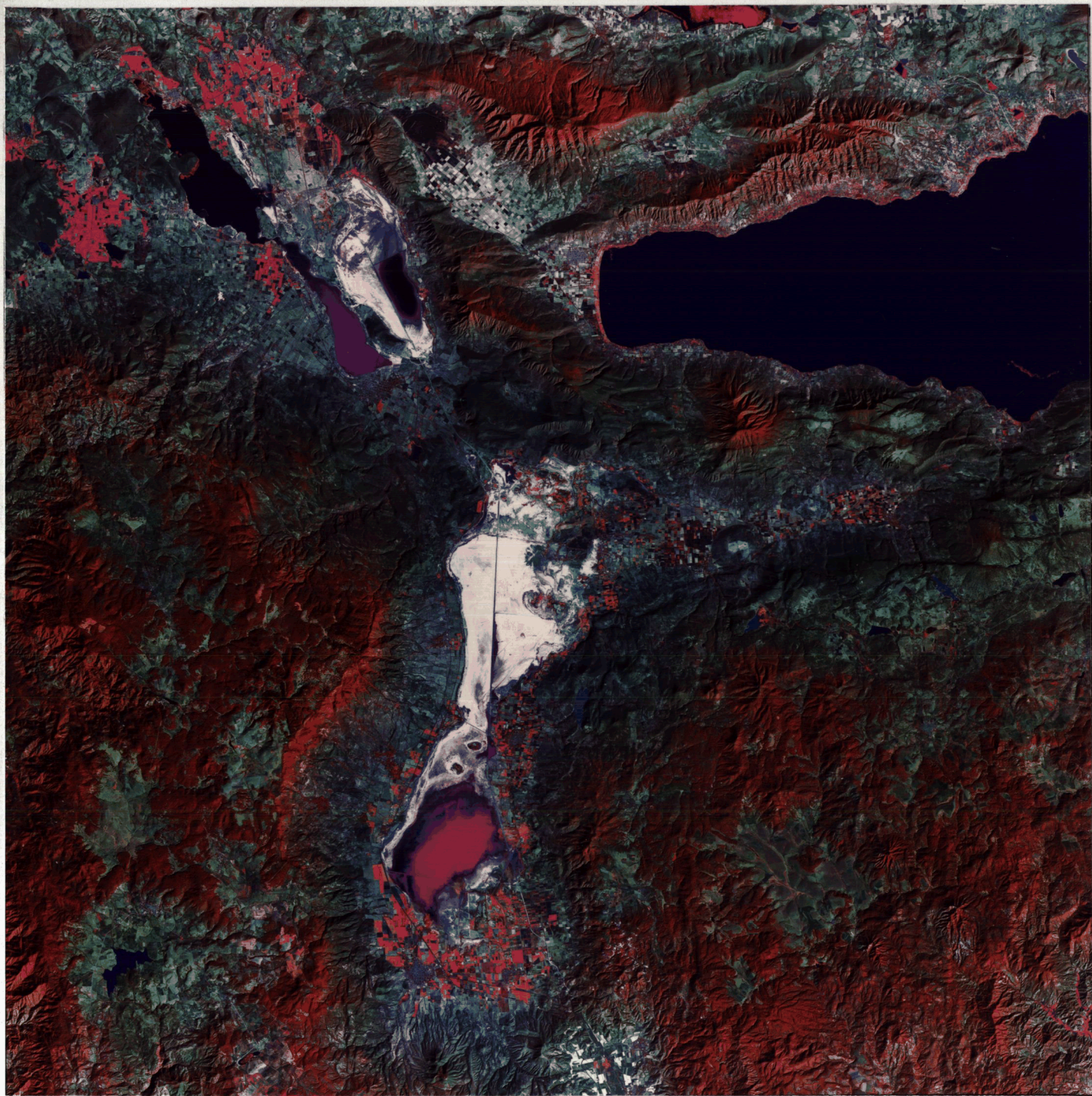
Figure 7: Image of the region surrounding the triple junction SSW of Guadalajara. TM bands 734=BGR on this false-color combination. Compare with Figure 8 for reference.
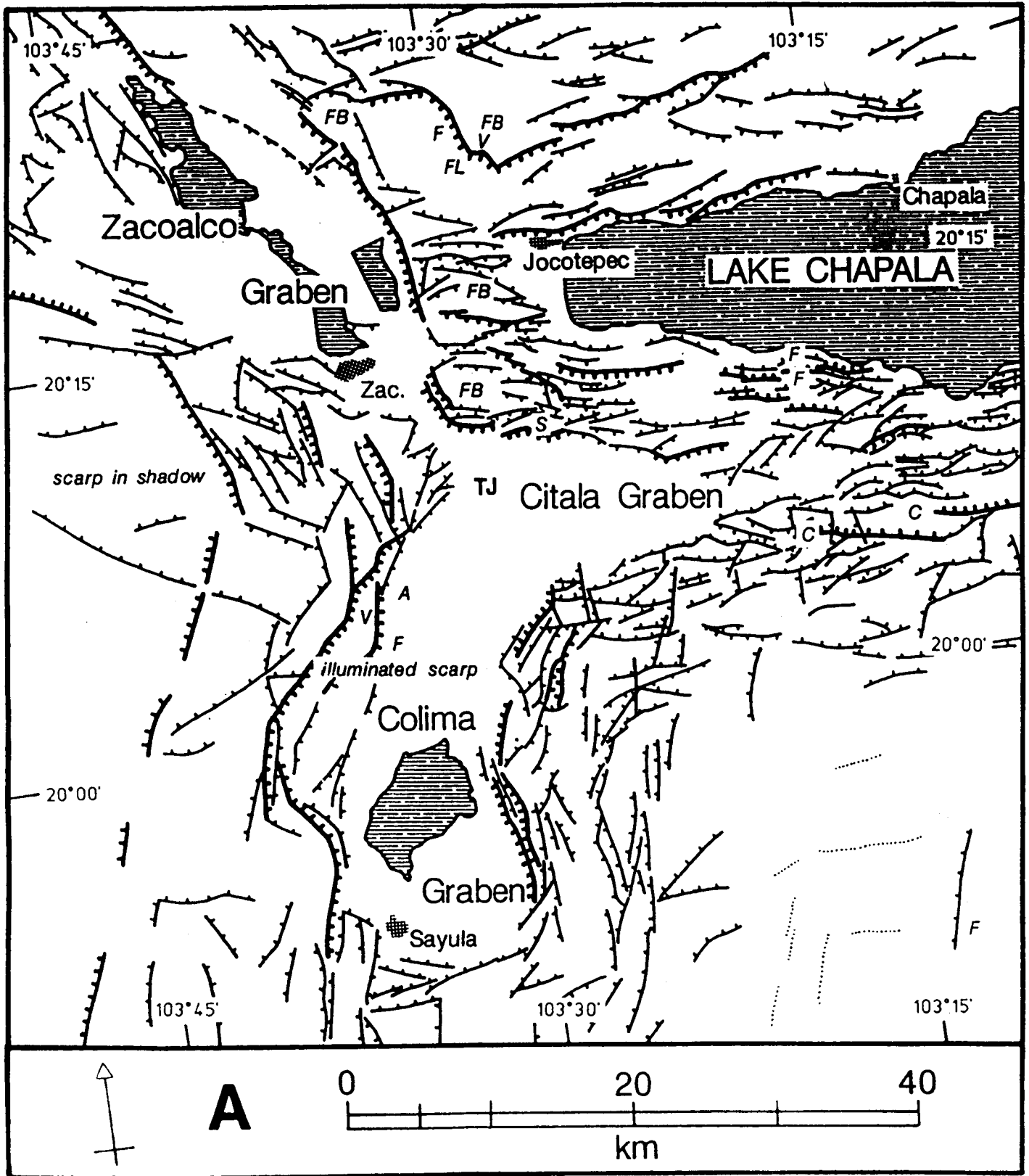
Figure 8: Interpretation of image shown in Figure 7. Labeled features are described in the text.

31

4 Field Efforts

Over the course of our study a total of seven weeks were spent in Mexico, during three seperate trips. Two of these trips, each of approximately three-weeks duration during April-May 1986 and March-April 1988, were for field investigations in and around the Mexican Volcanic Belt; the third trip, one week in October of 1987, was devoted soley to improving our collaborative efforts with our colleagues at UNAM. Figure 9 shows the areas traversed during the two field seasons.

The primary purpose of the field work, as stated in the original proposal, was for gathering of ground-truth information for the interpretations of the TM imagery. During both field seasons, emphasis was placed on:

- reconnaissance covering a maximum amount of ground due to the enormous size of the study area and the limited time available;

- location and documentation (photographs) of Neogene and Quaternary faults and other structures (neotectonic deformation);

- making maximum use of the information on the TM images to plan and execute the field investigation; and

- participation of Mexican researchers and students–at least one (and often more) Mexican was a member of the field party at all times.

These goals were met during both of the field seasons, except that we were not able to visit areas within all of the 11 digital images that we eventually acquired (Figure 9). In general the observations we made on the ground substantiated the image interpretations, and no significant alterations in our interpretations of the neotectonic deformation in the area was necessary.

Field Season, 1986

Only three TM images had been received in Miami at the time of the first field trip. Photographic images for use in the field were produced from our digital data using the Satellite Oceanography Group's VAX11/780 with modified software for display. The areas covered by the three scenes included the area of Guadalajara, and the regions north and south of Mexico City. The goal of the first field season was to cover as much of these regions as possible while gathering information on the exposed lithologies and structures. We planned to use the images to locate recent faults, where we could then evaluate the slip direction and magnitude from the ground. Our regional reconnaissance, combined with information gathered during our discussions with local geologists and our earlier survey of the literature, enabled the formulation of a general framework with which to evaluate the images. The other major goal of this trip was to acquire topographic and geologic maps of the area covered by the TM images, so far as was possible.

Another goal of the field work during this first season was the acquisition of hand-held radiometer measurements for later calibration of the digital TM data. This goal later proved to be impractical. A total of 19 three-band radiometer measurements were taken at localities within all three images (see Figure 9); but during the entire period severe atmospheric haze rendered the measurements all but useless. At times the haze was so dense that visibility was less than two kilometers; and the precise direction of the sun was impossible to determine (without a chronometer and compass). These adverse atmospheric conditions forced us to re-evaluate our plans for calibration of the digital data (we eventually decided that, for our purposes, calibration was of marginal value anyway). We were also prevented from getting very good pictures from the ground of some of the larger fault scarps.
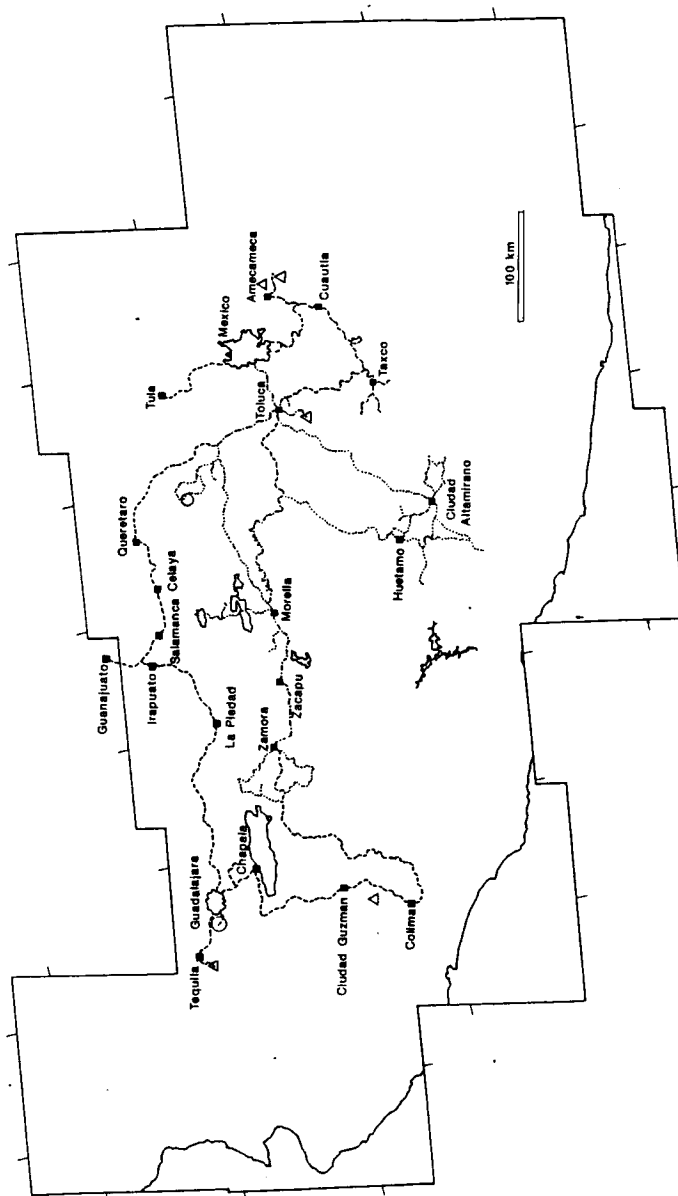
Figure 9: Sketch map of the study area showing the regional coverage of the two field seasons, which were held during the Spring of 1986 (dashes) and 1988 (dots). Reconnaissance geology and Ground-truth data was collected over much of the central and western parts of the volcanic belt, as well as from a large portion of the region south of the MVB. M, Mexico City; G, Guadalajara. Refer to Figure 11 for comparison with the neotectonic deformation in the region.

33

Assisting Mr. Johnson in the field during this trip were Dr. Grenville Draper of Florida International University, a structural geologist with extensive field experience, and Mr. Tony Barros, another graduate student at the University of Miami, and who would later join the research on an associated project funded through NASA.

The first few days were spent in Mexico City, where Mr. Johnson gave a talk at the Institute of Geophysics at UNAM. The subject of the talk was the potential contribution of the TM images to the solution of some of the problems of the geology of central and southern Mexico. Most of this time was occupied by discussions with researchers at UNAM regarding our planned study, and gathering logistical support. We met several representatives of both the Institute of Geology and the Institute of Geophysics at UNAM, most important of whom in relation to our later work were Dr. Ortega (geology) and Dr. Urrutia (geophysics). We also met with Dr. Santiago Charleston, a private consultant of high repute with interests in and around central Mexico.

Dr. Charleston accompainied the group for the first leg of the trip south of Mexico City. He helped familiarize us with the geology of the area between Cuernavaca and Cuautla, where the Mesozoic and Cenozoic sections are fairly well exposed. During the second half of the trip in the area around Guadalajara we were guided by Mr. Jugo Delgado, a graduate student at UNAM working under Dr. Urrutia. He had worked in the area around Lake Chapala, studying Quaternary faulting and graben structures.

Higlights of the trip include (in chronological order):

- reconnaissance of the Quaternary volcanics within the Sierra Chichinautzin, which borders the Valley of Mexico on the south;

- location of a prominent fault situated north of Volcan Popocatepetl and expressed on the ground as a valley cutting transversely through the drainage on the north side of the volcano;

- investigation of the region surrounding Taxco, where we concentrated on the Mesozoic and Cenozoic section;

- a visit to the caves of Cacahuamilpa, where Karst topography in the form of dolines is spectacularly expressed on the TM images within the Albian limestones of the Morelos Fm., northeast of Taxco;

- a reconnaissance visit to Nevado de Toluca;

- in Guanajuato we met with Dr. Juventino Martinez, a professor at that campus of UNAM who is interested in neotectonics;

- documentation of faulting southeast of Guadalajara, as expressed on the TM images and on the ground by large normal fault scarps and tilted fault blocks capped by Pleistocene lacustrine deposits and volcaniclastics;

- observation of faults within the large Sierra La Primavera caldera of Pleistocene age, west of Guadalajara;

- a reconnaissance visit to Volcan Tequila;

- observation of faults in Quaternary volcanics and volcaniclastics south of Ciudad Guzman and east of Colima;

- reconnaissance and radiometric measurements at Tula, the ancient Toltec capitol north of Mexico City.

Field Season, 1988

All but four of the eleven TM images used in this study were in hand before the second field trip in the spring of 1988. Most of these had been digitally enhanced and photographic enlargements produced during earlier visits to the Image Analysis Facility at Goddard Space Flight Center. Also, because we had already interpreted the images, we were in a much better position to plan the trip, and thus we were much more successful in choosing specific localities to visit.

Again, most of the first week was spent in meetings with our Mexican colleagues at UNAM in Mexico City. Mr. Johnson met with Dr. Fernando Ortega, Dr. Jerjes Pantoja, Dr. Max Suter, and Dr. Anna Lillian Martin del Pozzo (all geology), Dr. Jaime Urrutia, and Dr. Harald Bohnel (geophysics), and Dr. Nieto-Obregon (engineering). Mr. Johnson also met with Dr. Charleston, and Dr. Negendank, who had just returned from the field.

Accompanying Mr. Johnson in the field on this trip was Mr. Enrique Cabral, a student at UNAM who is studying under Dr. Urrutia. Dr. Jerjes Pantoja also accompanied the group for the first half of the trip. He is an acknowleged expert on the geology of the Balsas basin and his assisstance in the field proved invaluable. Also accompanying the group during most of the trip was Mr. Michiel Kupferschmidt, a German student studying under Dr. Negendank.

The primary goal of this trip was to attempt to fill some of the large gaps in ground coverage left by the first trip, due to the significant increase in our TM data base during the interim period. This was largely accomplished. We were able to get ground-truth information for five of the TM scenes, three of which had not been visited at all previously.

Highlights of the trip include (in chronological order):

- documentation of faulting near Teotenango, an ancient Toltec fortress city built on the Holocene Tenango basalt;

- traverse through the Mesozoic and Cenozoic section between Toluca and Ciudad Altamirano (conclusion: current geologic maps represent the western boundary of metamorphic rocks as being too far east);

- investigation of the Tertiary section east of Ciudad Altamirano, which shows multiple angular unconformities within the Oligo-Miocene Balsas red beds and overlying volcanics;

- documentation of 2.5 to 3 km of right-lateral offset on a fault cutting a porphyritic dike of probable Oligocene age, east of Ciudad Altamirano;

- reconnaissance southwest of Ciudad Altamirano along road to Zihuatenango (Mesozic section);

- collection of paleomagnetic samples from upper Cretaceous/Tertiary red beds at three separate localities (these are being analized by Mr. Cabral at UNAM);

- first documentation of Late Cretaceous (probably Maastrichtian) thrusting of the Mesozoic sequence between Ciudad Altamirano and Huetamo (structural relationships traditionally had been ascribed to normal faulting by Dr. Pantoja and later workers, and we are currently working on a paper describing the thrusts);

- documentation of intense fault brecciation and deformation of Tertiary rocks, and faulting that cuts Quaternary alluvium and colluvium in the Balsas river basin east of Presa de Infiernillo;

- documentation of faulting that cuts Quaternary deposits north of Morelia;

- observations of faults offsetting pavement on roads between lakes Cuitzeo and Yuriria, in an area where the faults that cut the Quaternary volcanics appear very fresh and sharp on the TM images (we visited this area on a tip from Dr. Max Suter, of the Institute of Geology at UNAM);

- observations of faults cutting Quaternary cones west of Morelia;

- documentation of faults with offsets exceeding 200-300 m occurring on the northern wall of the Quaternary San Juanico graben, located southeast of Lake Chapala;

- documentation of the large Quaternary offset on the Pajacuaran fault, located east of Lake Chapala;

- documentation of the large Quaternary offset on the Pastores fault, southeast of the Amealco caldera;

- reconnaissance visit to the Amealco caldera.

5   Neotectonics: Rifting

The following sections describe faulting of Plio-Quaternary age in central Mexcio as observed on TM images. The maps presented in Figures 10 and 11 show regional compilations of this deformation. Many of the following sections contain figures that are enlargements of areas within these maps, but the reader will often be referred to Figures 10 and 11 in order to show regional relationships.

The western part of the study area can be subdivided into four principal structural elements in which recent deformation has taken place: 1) the Tepic-Chapala Rift; 2) the Colima Rift; 3) the Chapala Rift; and 4) the area SW of Guadalajara where the first three structures intersect, forming a R-R-R triple junction. The region encompassing these four features is covered by the four westernmost TM images of the mosaic, the 'Tepic', 'Jalisco', 'Guadalajara', and 'Colima' scenes (see Figure 2).

5.1   The Tepic-Chapala Rift

The western end of the MVB lies within a linear topographic depression known as the Tepic-Chapala Rift (Allan *et al.*, 1987), shown in Figure 12. This rift consists of a NW-trending series of grabens, half grabens, and pull-apart basins that together extend some 240 km from Guadalajara to the Pacific coast west of Tepic. Taken as a whole, the rift varies in width from 40 to 70 km, although the widths of the individual basins that form it rarely exceed 30 km. These down-faulted basins are generally floored by Plio-Quaternary volcanics, mostly lavas and pyroclastics, along with larger calc-alkaline volcanoes such as San Juan, Sanganguey, Ceboruco, and Tequila. Previous work in the area has concentrated primarily on the geology, petrology, and geochemistry of these volcanics (Thorpe and Francis, 1975; Gastil *et al.*, 1978; Nelson, 1980; Nelson and Carmichael, 1984; Dremer and Nelson, 1985), particularly those associated with the major andesitic centers. Few published works on the area involve detailed tectonic studies, although Nieto-Obregon *et al.* (1985) provide a structural analysis of part of the area, located north and west of the Santa Rosa dam. Analysis of the neotectonic map of the Tepic-Chapala Rift derived from the TM data has yielded some interesting and unexpected results, which are described later in this section.

5.1.1   Pre-Pliocene Geology and Structure

The region is underlain by a deformed Mesozoic volcanic and sedimentary sequence that is metamorphosed where it is found in contact with widespread granitic intrusives of Late Cretaceous age. These rocks are best exposed north of the Bahia de Banderas, and display a complex fold and fault pattern (Gastil *et al.*, 1978).

The Tertiary chronology of events in this part of the MVB can be best understood when one considers the tectonic evolution of the Pacific margin of Mexico. Gastil *et al.* (1978) recognized two periods of volcanic activity in the Tepic region prior to the Pliocene. The first involves a volcanic sequence of Early Miocene age (21-16 Ma), consisting of rhyolites and associated andesites and basalts. These rocks are younger than the volcanics of the Sierra Madre Occidental, which are mainly Oligocene ignimbrites (McDowell and Keizer, 1977); and Nixon *et al.* (1987) has recently concluded that the younger volcanics indicate a shift in the locus of magmatic activity westward, from the eastern part of the Sierra Madre Occidental to the Pacific coastal region by the Early Miocene. The second period of volcanic activity noted by Gastil *et al.* (1978) resulted in a Late Miocene sequence of lavas, mostly basalts. These rocks are primarily exposed near the coast west of Tepic; and Nixon *et al.* (1987) associate this activity with the incipient rifting of

NEOTECTONIC MAP OF CENTRAL MEXICO

Fault Scarps and Fractures interpreted from a

Landsat Thematic Mapper Image Mosaic

Key:

Fault Scarp
marked on down-thrown side

Fracture

□ Cities

▲ Volcanic Features

Cities
A - Ameca
C - Colima
Cr - Colima
CG - Ciudad Guzman
G - Ciudad Guzman
I - Irapuato
M - Morelia
Ma - Manzanillo
P - Patzcuaro
PV - Puerto Vallarta
S - Salamanca
T - Toluca
Te - Tecoman
U - Uruapan

Volcanic Features
1. Volcan de Colima
2. Nevado de Colima
3. Volcan San Juan
4. Volcan Sangangan
5. Volcan Tecitic
6. Volcan Cantaro
7. Volcan de Tequila
8. La Primavera Caldera
9. Amealco
10. Nevado de Toluca
11. Popocatepetl
12. Iztaccihuatl
13. Patzcuaro Caldera
14. Amealco Caldera
15. Cerro Urechuela

Jalisco Block

Michoacan Block

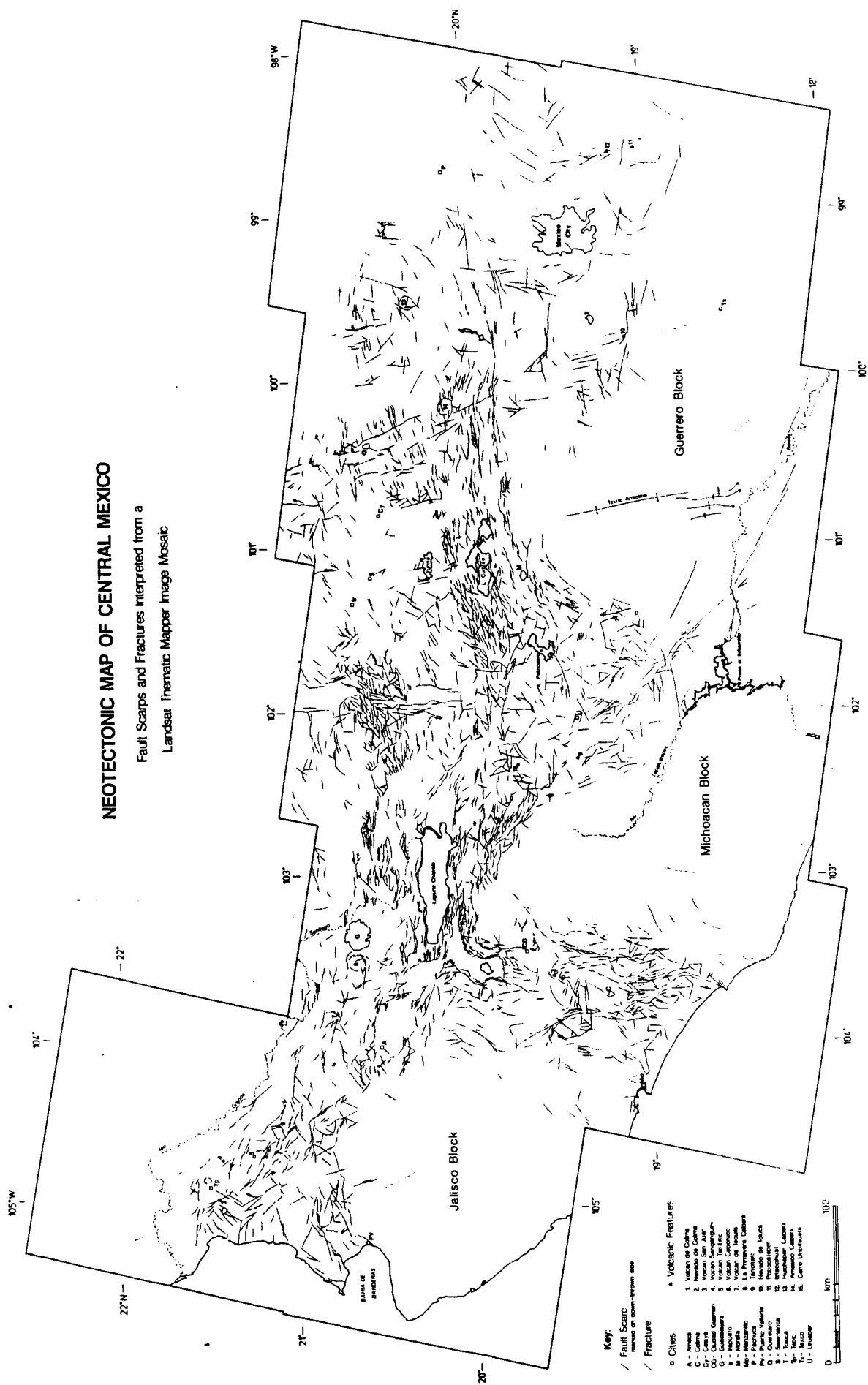Guerrero Block

BAHIA DE BANDERAS

Laguna Chapala

0 | km | 100

Figure 10: Neotectonic map of central Mexico derived from the interpretation of Landsat Thematic Mapper imagery at a scale of 1:1 million. The locations of major cities and volcanic features are marked on the map for help in location.

38

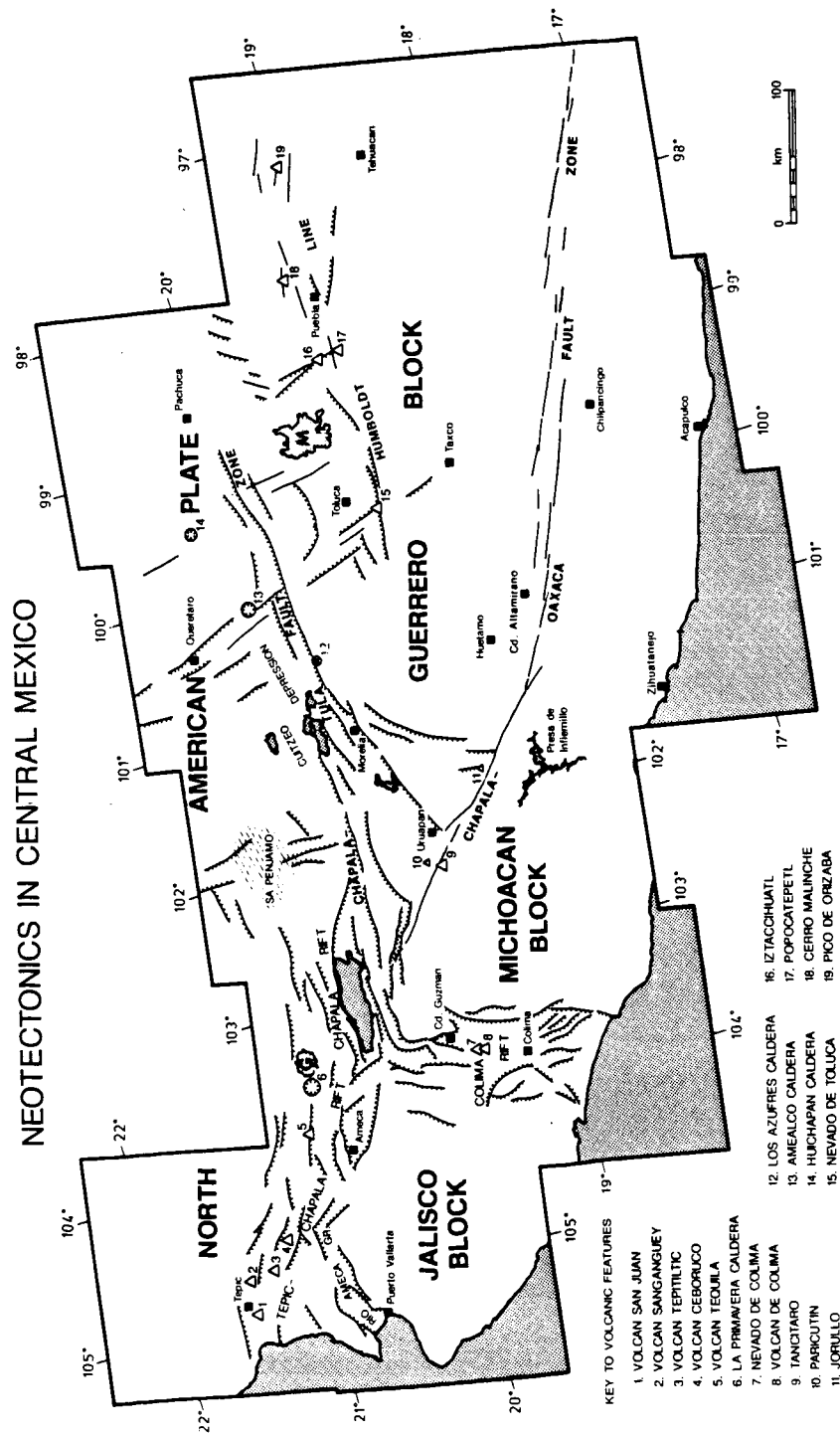# NEOTECTONICS IN CENTRAL MEXICO

Figure 11: Sketch map showing neotectonic deformation in central Mexico, simplified from Figure 10. Also shown are interpretations of four images not included in Figure 10, continuing the trace of the Chapala-Oaxaca fault zone to the southeast.
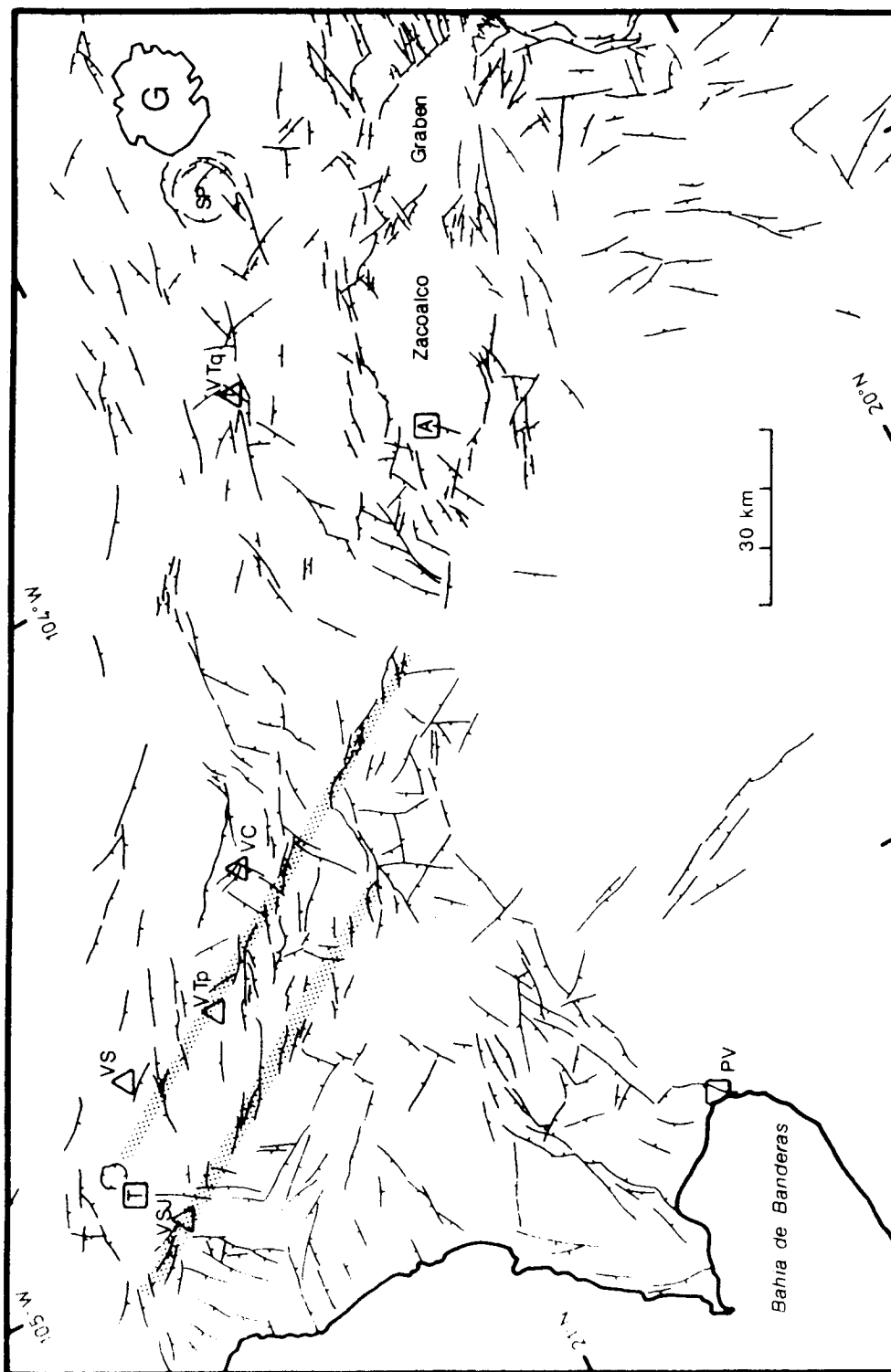
39

Figure 12: Fault map of the Tepic-Chapala Rift derived from image interpretation of TM images at 1:1 million scale. Tick marks are on inferred down-thrown side of faults. SP = Sierra la Primavera; VSJ = Volcan San Juan; VS = Volcan Sanganguey; VTp = Volcan Tepitiltic; VC = Volcan Ceboruco; VTq = Volcan Tequila; PV = Puerto Vallarta; A = Ameca; T = Tepic; G = Guadalajara. The stippled lines are inferred left-lateral basement fractures (see Figure 13).

the Gulf of California. Further inland, Nieto-Obregon *et al.* (1985) have noted an assemblage of mixed pyroclastic products with ages spanning the same period (10-5 Ma). They interpret these deposits as either the last phase of volcanic activity in the southern Sierra Madre Occidental, or as evidence for the existence of a "proto-Mexican Volcanic Belt". Whatever their association, volcanics of this age and type seem to be restricted in western Mexico to the southernmost part of the Sierra Madre Occidental, and represent a transitional episode.

In the Tepic region Gastil *et al.* (1978) noticed that the pre-Pliocene volcanic strata are tilted to the northeast in a series of fault blocks. The western margins of these blocks are uplifted by NW-SE trending faults. These structures may be related to Late Miocene back-arc extension in the Sierra Madre Occidental (Nixon *et al.*, 1987), or they may result from the extensional episode that led to the formation of the Gulf of California. These faults will be discussed in more detail later in relation to the tectonic interpretation of the region from the TM data.

5.1.2 Plio-Quaternary Volcanism

Since the Early Pliocene, alkaline, peralkaline, and calc-alkaline volcanics have been erupted contemporaneously within the Tepic-Chapala Rift (Allan *et al.*, 1987). The six largest volcanoes in this part of the MVB are all relatively small in volume (< 70 km^3) compared to those further east. They generally display complex eruptive histories involving rapid growth of the calc-alkaline central volcano followed by caldera formation and the eruption of alkalic cinder cones and lavas on the flanks of the main edifice (Nixon *et al.*, 1987). Volcan Sanganguey began its most intense episode of calc-alkaline activity since 0.3 Ma ago (Nelson and Liveries, 1986), which atests to its relative youth. The other major eruptive centers have slightly more eroded slopes, indicating that they may be only slightly older. Some, such as Volcan Ceboruco, are partially obscured by clouds on the TM image.

Although much smaller in total volume, the alkalic eruptions have been active for a much longer period, and the valleys below the volcanoes are usually floored by older alkalic cinder cones and flows, which extend beneath the larger and more youthful calc-alkaline centers (Allan *et al.*, 1987). The alkaline volcanic activity extends back to the Pliocene, as indicated by a date of 4.3 ± 0.17 Ma obtained by Gastil *et al.* (1978) from a hawaiite.

Gastil *et al.* (1978) noted several subparallel chains of young cinder cones and craters located southeast of Volcan Sanganguey, trending about N315°. Similar chains were noted west of Volcan Ceboruco and northwest of Tepic. Luhr *et al.* (1985) described alignments of cinder cones crossing Volcan Las Navajas. The TM image of the Volcan Tequila area also shows a similar alignment of eruptive centers on the western flank of the volcano. Presumably, these alignments coincide with deep fractures in the underlying basement rock. This form of tectonic control on the spatial distribution of eruptive centers seems fairly common in the western part of the MVB, and its relationship to the tectonic situation in the region is discussed later.

5.1.3 Plio-Quaternary Structure visible on the TM Imagery

The grabens and pull-apart basins that compose the Tepic-Chapala Rift are generally confined between two major NW trending faults, the Pochotitan fault system on the north, and the Mazatan fault system on the south (Allan *et al.*, 1987). Parts of the Pochotitan system are visible on the TM imagery northeast of Volcan Ceboruco, where a series of SW-down faults parallel the Rio Grande de Santiago; but it is difficult to identify faults on the images that can be clearly related to the Mazatan fault system. Also,

a major graben structure has been discovered breaking off of the main trend of the Tepic-Chapala Rift and extending to the Bahia de Banderas. These facts may indicate that the Mazatan fault system is less important as a bounding fault system on the south of the Tepic-Chapala Rift than previously thought, or that it is probably an older feature that has not undergone much recent displacement.

The Zacoalco graben is the southeasternmost of the grabens that together form the Tepic-Chapala Rift, and from this TM survey it also appears to be the largest and to have the most well-defined form; it will be described in more detail in the section covering the triple junction. Other grabens appear less prominently on the images. Exceptions to this are the NW-SE trending graben containing Volcan Ceboruco, and another southwest of Volcan Tepitiltic.

Allan *et al.* (1987) state that the majority of the faults in the rift have a NW trend, and this is confirmed by the fault pattern visible on the TM images. The most recent episode of faulting in the region appears to have been initiated near the end of the Miocene or the beginning of the Pliocene, and evidence for continued deformation until recent time is widespread throughout the area (Nieto-Obregon *et al.*, 1985; Allan *et al.*, 1987). A major NW trending fault is associated with Volcan Tequila, along with several faults and fractures of other trends. On enlargements of that area the dominant NW-SE faulting can be seen to localize the eruptive centers of lava cones and flows, particularly on the western flank of the volcano.

Several fault trends that are not oriented NW are also present. Northwest of Tepic is an alignment of several E-W trending faults with S-down throw. Few structures that may be related to the rift system are visible north of this fault system. West of Tepic, south of Volcan Ceboruco, and immediately to the northwest of the Zacoalco graben are concentrations of NE-SW trending faults, the majority of which appear to have a NW-down throw. These faults are likely to be antithetic faults related to shear in the rift system (see below).

5.1.4 Regional Deformation: Left- or Right-Lateral?

Allan *et al.* (1987) have emphasized that the faults bounding the Tepic-Chapala Rift on the north have experienced strike-slip as well as dip-slip displacements. They cite an example north of Volcan Tequila near the Santa Rosa dam where a young (less than 0.2 Ma) lava cone has been offset in a right-lateral sense by about 0.7 km. In addition, Nieto-Obregon *et al.*, (1985) concluded that a large right-lateral fault system exists in that area (line D-D', Figure 13), oriented in a N295° to N290° direction, from orientations of fractures and small faults. They also interpreted triangulation data, gathered from the area around the dam, as an indication of active right-lateral motion at approximately 0.2 cm/year. Luhr *et al.* (1985) and Allan *et al.* (1987) believe that this evidence indicates right-lateral motion, combined with extension, on the Tepic-Chapala Rift as a whole.

Interpretation of the Landsat TM images indicates that the dominant sense of motion across the Tepic-Chapala Rift may not actually be right-lateral; and a significant proportion of the deformation seen in the region is in fact due to left-lateral shear. Before discussing the new evidence in more detail, an important conclusion of Nieto-Obregon *et al.* (1985) must be reviewed. Although they found that motion in the immediate vicinity of their study area was right-lateral, Nieto-Obregon *et al.* (1985) did not believe that this sense of deformation continued very far to the west. Instead, they cited evidence from an earlier survey of Nayarit state (Delgado-Argote *et al.*, 1978) and another paper (Del Rio, 1979), that indicates that a major left-lateral fault system of NW-SE orientation extends from where it follows the valley of the Rio Grande de Santiago southeastward, beyond and to the west of Volcan Tequila (Figure 13). They conclude that their right-lateral fault system is actually a conjugate of the more important left-lateral system. The evidence for this left-lateral fault system includes the orientation of the fracture pattern, right-handed en

echelon riedel shears, and the orientation of fold axes in ignimbrites. The fault map derived from the TM data verifies and amplifies their conclusion.

Figure 13 shows faults of the Tepic-Chapala Rift as interpreted from the TM images, together with this author's tectonic interpretation. The locations of the most prominent volcanic features are also included in the figure. Line A-A' shows the axis of a linear concentration of primarily NW-SE oriented faults, which are mostly aligned 5° to 35° counter-clockwise from the trend of A-A' (N328°). Trend A-A' roughly corresponds to the location of a large fault mentioned by Gastil et al. (1978) that marks the uplifted western margin of a tilted fault block, one of a series of NW-SE oriented blocks in which pre-Pliocene volcanic strata dip to the NE. The summit of Volcan San Juan also lies along trend A-A'.

The pattern of faulting at the surface along line A-A' is consistent with that of wrench faults produced experimentally and observed in the field (Tchalenko, 1970; Wilcox et al., 1973; Harding, 1974); and assuming that line A-A' represents the trace of a deep-seated zone of weakness and deformation, its orientation relative to those of the faults at the surface (see Figure 12) marks it as a major left-lateral wrench fault or fault system.

Trend B-B' is similar to trend A-A', and also includes large volcanic features: the large caldera northeast of Tepic; Volcan Tepitiltic; and Volcans Sanganguey and Ceboruco both lie less than 10 km to the NE of this trend. Both trends A-A' and B-B' are parallel to C-C', which is the approximate trace of a large left-lateral fault system mentioned by Nieto-Obregon et al. (1985). To the east of C-C' is a prominent right-lateral conjugate system (D-D'), which roughly follows the Rio Grande de Santiago canyon (Nieto-Obregon et al., 1985).

5.1.5   The Rio Ameca Graben

The Bahia de Banderas fills the western end of a large, and previously undefined graben structure. This graben will be referred to as the 'Rio Ameca graben' in this report, because the Ameca river occupies the graben for much of its course. The Rio Ameca graben is approximately 90 km long and trends in a E-W to ENE-WSW direction from where it branches off the main trend of the Tepic-Chapala Rift in the region south of Volcan Ceboruco. The graben is between 20 and 30 km wide, and is best defined by bounding faults on its margins at its western end near the bay.

Like the Tepic-Chapala Rift, the Rio Ameca Graben is actually a series of sub-grabens, the largest of which is at its western end. A convenient name for the western sub-graben is the 'Banderas Graben', because of its close association with the Bahia de Banderas. The Banderas Graben measures 45 km along its longest axis, is about 15 km wide, and trends northeastward from the Bahia de Banderas. Faults on both sides of the Banderas Graben separate Mesozoic rocks on its margins from alluvium filling its floor. At the coast, its northern and southern margins extend further to the west and southwest, respectively, to form the corresponding coasts of the Bahia de Banderas. The main faults that form the southern margin of the Banderas Graben leave the coast in the vicinity of Puerto Vallarta and extend inland, first NNE for 10 km, then turning to parallel the general trend of the Rio Ameca Graben. Faults on the northern margin of the Banderas Graben trend northeast, are slightly arcuate, and concave to the south. These faults appear to be slightly older than other ENE-trending faults nearby, based on their geomorphological expression. The younger faults have straight, well-defined scarps trending ENE, and occur almost exclusively within the Mesozoic rocks near the margins of the graben.

The southwestern half of the Banderas Graben forms a basin that is filled with alluvium that appears to have been shed from the margins of the graben, although much of it has probably been transported
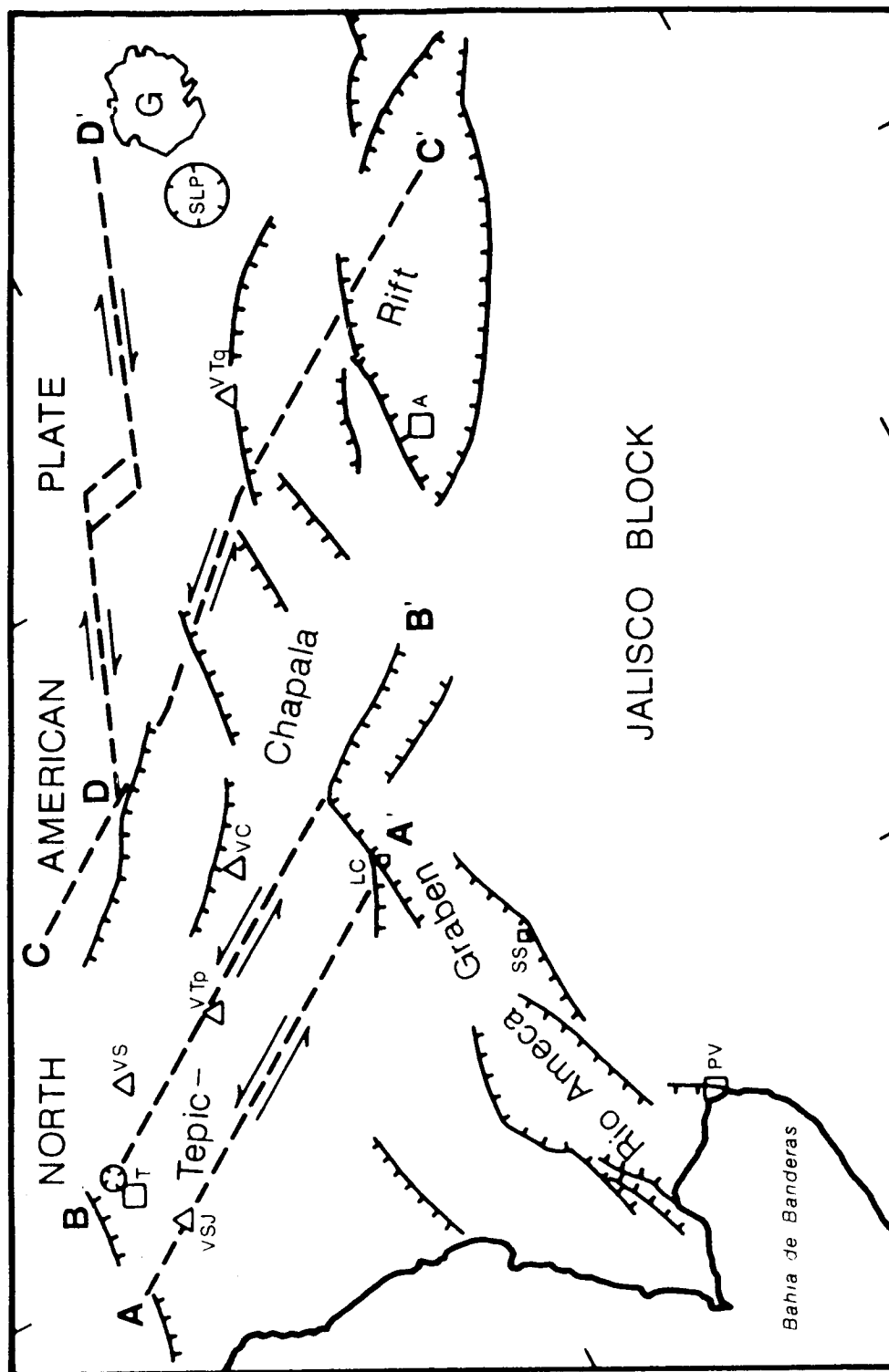
Figure 13: Simplified map of the Tepic-Chapala Rift showing rift structure and inferred basement fractures. Lines A-A', B-B', C-C', and D-D' are inferred basement shear zones and are discussed in the text. VSJ, Volcan San Juan; VS, Volcan Sanganguey; VTp, Volcan Tepitiltic; VC, Volcan Ceboruco; VTq, Volcan Tequila; SLP, Sierra la Primavera; A, Ameca; G, Guadalajara; LC, Los Cerritos; PV, Puerto Vallarta; SS, San Sebastian; T, Tepic.

there by the Ameca river. The northeastern half of the graben does not appear to have subsided nearly as much as the southwestern half, and only its northern part contains alluvium, in the Ameca river valley on the floor of a smaller down-faulted block. The two halves of the Banderas Graben are separated by NW-trending faults that are allowing greater subsidence to their SW.

Fisher (1961) mapped the bathymetry of the Middle America Trench in the vicinity of Mexico. His maps clearly show a deep submarine canyon that cuts across the continental slope and enters the Bahia de Banderas. The canyon is sharply asymmetric, with a very steep scarp along the southern margin of the bay. This scarp extends another 15 to 20 km westward from the mouth of the bay out onto the continental slope. Fisher (1961) states that "depths greater than 100 fathoms lie less than 1000 feet from (the southern) shore (of the bay)". A much more gradual slope extends from the northern shore of the bay down to the base of the canyon near the southern shore. The submarine morphology of the canyon strongly resembles that of a large, asymmetrically down-faulted graben or half-graben, with its surface dipping to the south. It seems reasonable to conclude that the canyon is the submarine extension of the Banderas Graben; and with this taken into account the length of the latter grows to approximately 130 km, and its width stretches to about 40 km at its western, submarine end. Also, the length of the Rio Ameca Graben is also extended to about 180 km.

At the eastern end of the Rio Ameca Graben is another large sub-graben structure. Only faults bounding the northern edge of this structure are clearly defined on the TM image of the area, so it is possibly a strongly asymmetrical half-graben. As this structure contains the town of Los Cerritos, near its northern margin, it is referred to as the 'Los Cerritos Half-Graben'. This half graben is about 40 km long, and though it has no recognizable southern boundary, the width of the zone of deformation associated with it averages about 17 km. A very prominent set of E-W trending normal faults define the northern edge of the half graben, and its northeastern end is truncated by other large normal faults. The latter faults trend NW-SE, and appear to be related to larger structures of the Tepic-Chapala Rift. The faults separate one of the few outcrops of Paleozoic metamorphic rocks in the region outside the half-graben (as shown on the 1:1,000,000 scale geologic map of Mexico published by SPP, Mexico, 1981), from a sedimentary terrace (of probable Neogene age) inside the half-graben. The terrace has been incised by the Ameca river as it winds through the area. Several NE-trending faults also occur within the half-graben, and all appear to have a NW-down throw.

The central section of the Rio Ameca Graben is more difficult to map because of the problem of detecting recent faults within the eroded Mesozoic strata through which it passes. Some faults (with north-down throw) on the southern margin of the graben can be seen extending ENE from the vicinity of San Sebastian. They continue to the ENE and appear to link the southern margin of the Banderas Graben with structures associated with the Los Cerritos Half-Graben. No prominent faults mark the northern side of the Rio Ameca Graben in its central section, probably because of the difficulties mentioned above.

The dominant trend of faults within the Rio Ameca Graben is ENE, paralleling the trend of the graben itself. Other fault trends are present, such as several prominent faults near the eastern end of the Banderas Graben that trend ESE. Extension within the Rio Ameca Graben does not seem to have involved recent volcanism on any scale detectable on the TM images.

At this time the best explanation for the formation of the Rio Ameca Graben is that it represents an extensional boundary between the Jalisco Block and a small portion of continental crust NW of the graben which may be accreting to the Rivera Plate. It trends approximately perpendicular to the direction of subduction of the Rivera plate beneath the Jalisco Block, as derived from the vector diagram discussed later. Also, as the Middle American Trench bends around to the NW, its trend eventually parallels the direction of subduction at a point located approximately at the intersection of the Rio Ameca Graben and

the trench. With this geometrical situation, subduction is not possible along the trench farther to the NW; instead, a tensional regime should dominate. The faults that formed the Rio Ameca Graben may also have taken advantage of an earlier zone of crustal weakness that probably existed in the basement.

5.2 The Colima Rift

A series of fault bounded basins extends about 170 km from the triple junction south of Guadalajara southward to the Pacific coast east of Manzanillo (Figure 14). This structure has been termed the Colima Rift by Allan (1986), and can be divided into three distinct sections, based on structural and morphological considerations. The well defined interior graben of the northernmost part of the Colima Rift has been variously called the "Sayula Graben" (Herrera, 1967), the "Sayula Depression" (Diaz and Mooser, 1972), and the "Northern Colima Graben" (Allan, 1986). This structure joins others from the east and west and opens on its southern end into a much broader basin, the Central Colima Rift, which is mostly filled by volcanic deposits associated with the Colima Volcanoes. Beginning just south of the city of Colima, the Southern Colima Rift begins, displaying a much more complicated pattern of block faulting and extending all the way to the Pacific coast.

5.2.1 Pre-Pliocene Geology and Structure

Since the Colima Rift marks the boundary between the Jalisco and Michoacan blocks, its pre-Pliocene geology shares elements from both blocks. The oldest rocks that outcrop within the rift are Mesozoic in age. The dominant Mesozoic sequence that outcrops within the rift is a thick series of limestones, shales, and sandstones of Late Cretaceous age, primarily in fault blocks within the Southern Colima Rift (Allan et al., 1987). Their deposition may extend into the Paleogene. Allan (1986) mentions a metamorphosed series of limestones, shales, and volcanic sediments of probable Lower Cretaceous age that are exposed at the edges of the Sayula Graben (Northern Colima Graben). He also provides a date (69.43 ± 1.14 m.y.) for a Late Cretaceous granodiorite that is exposed on the western side of the Sayula Graben, but no mention of its relationship to surrounding rocks is made.

The Mesozoic (and possibly Paleogene) rocks are unconformably overlain by Neogene volcanics. These are distributed widely throughout the central and northern parts of the Colima Rift, thickening from a "thin veneer" in the area of the Colima Volcanoes to almost 1 kilometer thickness near the triple junction (Allan et al., 1987). Allan (1986) reports a late Miocene date (approx. 10 m.y.) from an andesite collected near the triple junction. This represents the earliest dated volcanic deposit within the Colima Rift since the Cretaceous/Paleogene. Allan et al. (1987), however, indicate that older volcanics belonging to the Mid-Tertiary suite of the Sierra Madre Occidental may in fact be present near the Colima Rift in the Jalisco Block. Other dates in Allan (1986) show that andesitic volcanism continued in the Late Miocene/Early Pliocene.

5.2.2 Plio-Quaternary Volcanism

The Colima Rift marks the location of a major change in the size of the volcanoes of the MVB and their location relative to the MAT. Northwest of the Colima Rift, volcanoes associated with the Tepic-Chapala Rift are relatively small, generally having volumes less than 50 km^3 (Nelson, 1980). In contrast, the Colima volcanoes are nearly an order of magnitude larger, having a volume of approximately 450 km^3 (Luhr and
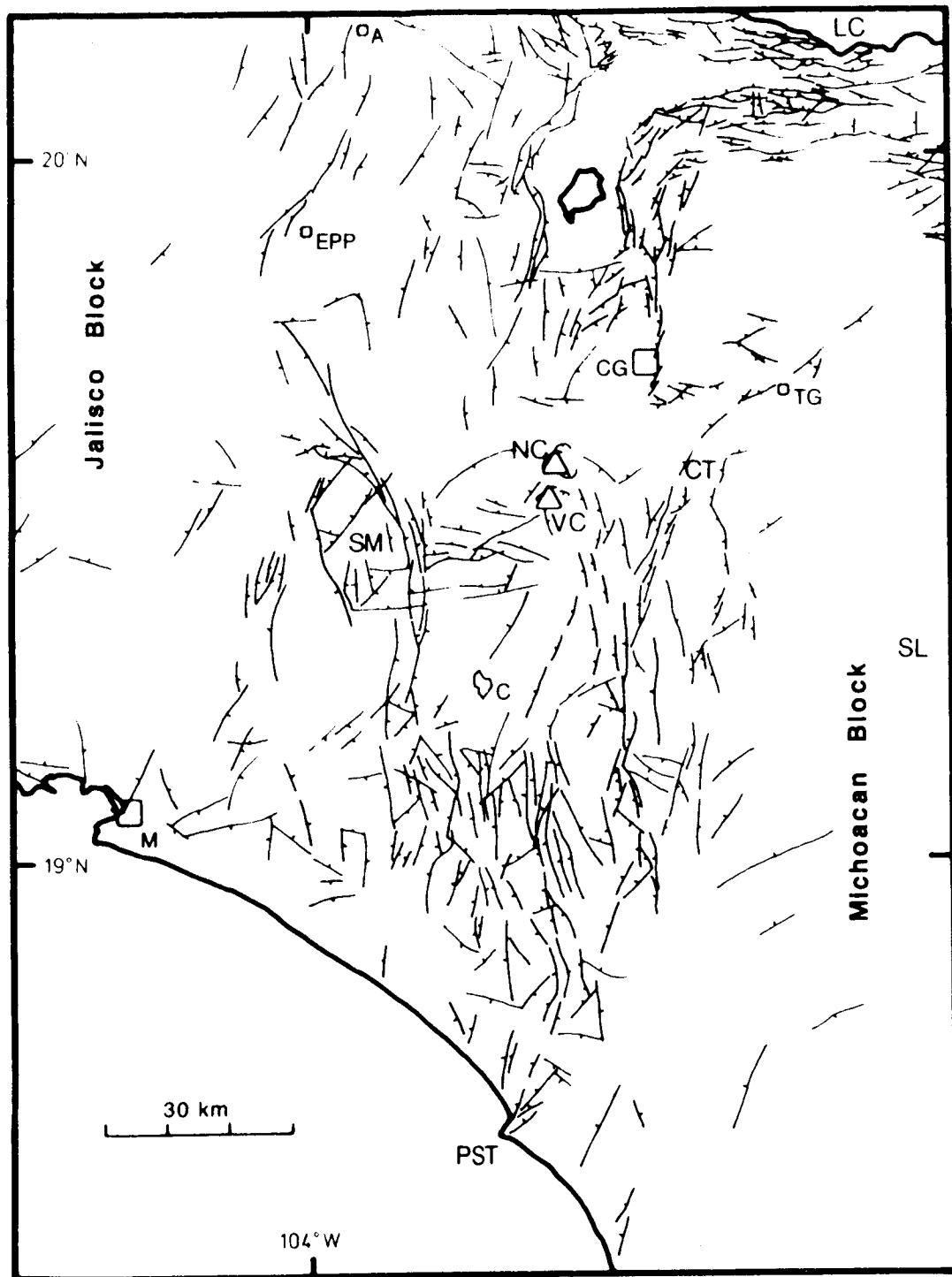
Figure 14: Fault map of the Colima Rift. VC, Volcan Colima; NC, Nevado de Colima; A, Ayotitlan; C, Colima; CG, Ciudad Guzman; CT, Cerro de Tuxpan; EPP, El Palmar de los Pelayo; LC, Lake Chapala; M, Manzanillo; PST, Punto San Telmo; SL, Sierra Lalo; SM, Sierra Manantlan; TG, Tamazula de Gordiano.

Carmichael, 1980). The distance between the Middle America Trench and the volcanic front in the Colima Rift is also 90 km shorter than in the Tepic-Chapala Rift. This contrast in the expression of volcanism in the MVB may be related to variations in the style and rate of subduction between the Cocos and Rivera plates (Nixon, 1982).

Volcanism in the area began with the eruption of andesites in the Late Miocene/Early Pliocene (Allan, 1986), and calc-alkaline volcanism has continued up to the present time. A well documented "pulse" of alkaline volcanism occurred in the Early Pliocene (4.6 to 3.9 m.y. ago), and these rocks have erupted contemporaneously with the more widespread calc-alkaline volcanics up to the Holocene, where there was a new surge in alkaline activity (Allan *et al.*, 1987). The alkaline rocks amount to less than 5 percent of the volume of volcanics in the Colima Rift, but Luhr *et al.* (1985) have cited their presence as evidence for "active" rifting in SW Mexico.

The three sections of the Colima Rift may be delineated on the basis of volcanic as well as structural characteristics. Volcanism within the northern rift is characterized by very small eruptions of alkalic or calc-alkaline rocks, normally from cinder or lava cones and flows. The dominant form of volcanism in the central rift contrasts sharply with that farther north, as evidenced by the very prominent calc-alkaline strato-volcanoes that have been erupted within it: Nevado de Colima and Volcan de Colima. Despite the more severely block-faulted terrain south of the city of Colima, Quaternary volcanism is notably absent within the southern rift (see the next section).

5.2.3   Plio-Quaternary Structure Visible on the TM Imagery

The Colima Rift is a very prominent feature on the TM image mosaic, particularly north of the Colima Volcanoes, which have erupted near the center of the rift. It extends from the triple junction at its northern end southward more than 170 km to the Pacific coast. The basins that define its interior parts average about 40 to 50 km in width; and the rift appears to grow wider closer to the coast. The relatively smooth basin floors contrast sharply with the eroded highlands on either side. In places the alluvium filling the basins is interrupted by tilted fault blocks and Quaternary volcanoes. The contrasting structural style and morphology of the three parts of the rift show up especially well on the TM image mosaic.

The Northern Colima Rift

The structure of the Northern Colima Rift, and particularly its interior graben, has been studied in more detail than other parts of the rift (Allan, 1986). The Northern Colima Rift consists of two well defined fault basins oriented in a more or less en echelon fashion and separated by a narrow horst. Both of these grabens are 15 to 20 km wide and are bounded on both sides by steeply inward-dipping normal faults. The northern graben is 35 to 40 km long with roughly symmetrical sides in plan view; the southern graben widens to the south and is about 25 km long from its narrow northern end to where it joins the much larger graben associated with the Central Colima Rift and is buried beneath the large volcanic complex of the Colima Volcanoes. The small horst that separates the two grabens is situated NW of Ciudad Guzman and is actually a set of fault bounded hills. These hills emerge from beneath the volcanics of Nevado de Colima and Volcan Cantaro, crossing the Northern Colima Graben in a northeasterly direction.

Analysis of the TM images reveals several fault scarps 30 to 40 km west of the main graben of the Northern Colima Rift. Most of these faults have NNE trends, paralleling the direction of the Colima Rift. These faults cut rocks that probably correlate with the Mesozoic/Paleogene sequences of the Jalisco Block. One scarp in particular stands out very well on the imagery, since it is down-to-the-west and much of the scarp is in shadow. It extends NNE from the dammed reservoir NW of El Palmar de los Pelayo to just east of

the town of Ayotitlan, a distance of over 35 km. The dam lies in the valley between the fault scarp and a hill opposite it. The youth of this major fault is demonstrated by the presence of a large landslide near its northern end. Maximum relief on the scarp reaches about 500 m near the landslide.

Allan (1986) estimated that extension across the Northern Colima Rift is 6 to 13 percent of its width, corresponding to approximately 1.5 to 3.3 km extension. A gravity survey by Allan (1985) showed that nearly 1 km of sediments are filling the graben, and combined with the vertical relief of the graben walls (reaching 1.5 km in places) this indicates a total vertical offset of some 2.5 km (Allan, 1986).

The Central Colima Rift

The Central Colima Rift consists of a single wide basin formed by the merging of three smaller graben structures. The Tolima Graben of Herrera (1967) forms the northwestern branch of this basin, while the Northern Colima Graben of Allan (1986) and another graben extend to the north and northeast, respectively. As seen on the TM imagery, the Central Colima Rift is 55 to 60 km long, stretching from the vicinity of the northern flank of Nevado de Colima to just south of the city of Colima. On the south the basin is 45 km wide, widening northward to about 60 km, where the three smaller basins separate.

Faults with up to 1700 m of relief bound the basin on its western side, and form the eastern edge of the Sierra Manantlan, a large horst. The Sierra Manantlan Horst is almond-shaped in plan view, having dimensions of about 30 by 15 km with its long axis oriented NNW. Judging from a brief description in Allan *et al.* (1987) of the rocks that outcrop on the fault scarp at its eastern edge, the horst probably is composed entirely of shallowly dipping Late Cretaceous limestones of the La Madrid Fm. On the TM imagery it is clear that these rocks extend at least 40 km further westward into the Jalisco Block.

Smaller fault scarps mark the eastern flank of the Central Colima Rift in a series of steps leading up to broad, eroded highlands to the east. The Sierra Lalo, within the Michoacan Block, forms the western extremity of the highlands, closest to the Colima Rift. Maximum relief on fault scarps in this area (about 500 m) is found along a series of four fault blocks that together form a gentle curve to the east and northeast of Volcan Colima. These blocks are all severely tilted to the SE. The fault that is common to all four blocks is the most prominent of those on the eastern side of the Central Colima Rift. One of the blocks, Cerro de Tuxpan, has been described by Estela *et al.* (1978) and contains the Encino Fm, a Lower Cretaceous series of clastics and volcaniclastics. These blocks emerge from alluvium in the floor of the basin that forms by the easternmost of the three grabens that converge to form the Central Colima Rift. The line of fault blocks extends down the center of this small graben, which is only 15 km long and about 10 km wide. A series of narrow valleys 2 to 4 km wide and filled with alluvium continue out of the graben NE of the town of Tamazula de Gordiano, cutting deeply into the surrounding hills. These fairly linear valleys may also owe their existence to recent faulting, although this is not so clearly evident on the TM images as it is for the more prominent grabens to the W and SW.

The central part of the Colima Rift is mostly buried beneath the large Quaternary volcanic massifs of Nevado de Colima and Volcan Colima (Luhr and Carmichael, 1980). The volcanic complex of the Colima volcanoes exhibits a very large slump or collapse feature, consisting of a large curvilinear detatchment fault traversing nearly the entire mountain. This fault is concave to the south and outlines a large slump block. The summit of Volcan Colima rides atop the block that appears to have slumped, and a series of E-W trending fractures northwest of Colima seem to be related to deformation of this upper block. About 1.5 km of southward horizontal displacement can be seen on the image.

The Southern Colima Rift

The structure of the Southern Colima Rift is quite different from that further north. As measured between the most prominent faults on either side, the Southern Colima Rift is about 40 km wide at its northern end near the city of Colima. It extends about 55 to 60 km southward to the Pacific coast, where it is about 45 km wide. A series of faults extends between the cities of Colima and Manzanillo, dissecting the hills to the west of the main basin. Thus, this part of the rift actually widens to about 75 km along the coast, if these structures are included. Other faults NE of Manzanillo extend the structures recognized to be related to the rift still further to the west. These appear to form the western boundary of a large N-S trending horst, 20 to 25 km wide, that bounds the main basin of the S. Colima Rift west of the city of Colima. The Manantlan Horst, described above with the Central Colima Rift, forms a smaller, more well defined northern extremity of the larger horst.

Deeply eroded highlands bound the Southern Colima Rift on both the east and west. Very prominent inward-dipping fault scarps mark the edges of the basin. Within several tens of kilometers of the rift on either side, linear structures exist parallel to those within and at the edges of the rift, indicating that deformation associated with the rifting extends well into the blocks on each side. Alternatively, many of these structures (but probably not all of them) may be the result of much earlier deformation events. A discussion of the geology of the highlands surrounding the Colima Rift is left to the sections that describe the Jalisco and Michoacan structural blocks.

The primary difference between the Southern Colima Rift and basins to the north is that it contains a number of very prominent fault blocks. These blocks have been noted previously by Allan *et al.* (1987). These blocks are nearly all oriented almost N-S and tilted to the east. Most appear to be highly fractured and are bounded by normal faults on their western sides, causing in places more than 1 km of relief. They are most likely composed of Cretaceous limestones and volcanic sediments similar to those that outcrop on either side of the rift. The dimensions of the fault blocks varies from 1 to 28 km long and less than 1 to over 10 km wide. They have a slightly *en echelon* trend relative to the S. Colima Rift, which trends more NNE. This fact may indicate some amount of left-lateral shear in combination with the E-W extension in the area.

South of the prominent fault blocks, alluvium fills the basin at the southern end of the S. Colima Rift. The alluvium has been deposited by the Rios Armeria and Coahuayana, two rivers that drain the highlands on the west and east of the rift, respectively. At the coast this sediment is being transported westward by wave action, resulting in a sequence of very large beach ridges that extend all the way to Manzanillo Bay. These ridges are responsible for 4 to 7 km of progradation of the shoreline east of Manzanillo. This westward transport of sediments is probably responsible for the particularly smooth shoreline, which Allan *et al.* (1987) have noted has no protruding delta. Any sediments that would form such a delta are being moved along the coast to the west. The coastline at the southern end of the Colima Rift trends in a NW-SE direction, making the western side of the Southern Colima Rift about 15 km shorter than the eastern side. The smooth shoreline is broken by the San Telmo peninsula (Punta San Telmo), which extends about 5 km into the Pacific ocean. The straight western shore of this peninsula is aligned with faults along the eastern margin of the Colima Rift. Thus subsidence in the southeastern Colima Rift has resulted in about a 5 km retreat of the shoreline (much more if the alluvium filling the graben, the depth of which has not been determined, is considered).

5.2.4 Regional Deformation

Deformation in the Colima Rift appears to be mostly extensional, oriented in a more-or-less E-W direction. This zone of extension marks the boundary between two structural blocks, the Jalisco Block on the west and the Michoacan Block on the east. No major zones of shear are indicated by the pattern of normal faults at the surface, and the direction of extension appears to be approximately perpendicular to the axis of the rift. Since the rift trends about N190°, the extension is probably oriented about N100°. However, in the Southern Colima Rift, fault blocks oriented obliquely to the overall trend of the rift may indicate that extension was somewhat oblique to the trend of the rift, not strictly perpendicular to it.

The time when faulting in the Colima Rift began is difficult to estimate, but Allan *et al.* (1987) conclude on the basis of offset of dated volcanic rocks and the total offset in the Northern Colima Rift that faulting began near the beginning of the Pliocene, 4-5 m.y. ago. This corroborates the conclusion of Diaz and Mooser (1972), who believed faulting in the region of Lake Chapala began in the Pliocene. From the very youthful appearance of many of the fault scarps in the rift, we can conclude that faulting has continued into the Late Pleistocene and very likely into the Holocene (Allan, 1986).

Allan (1986) has noted that the style of faulting is quite different in the Northern Colima Rift than that found in the southeastern graben of the Tepic-Chapala Rift (the Zacoalco Graben). He found that fault blocks in the southeastern Zacoalco Graben have been rotated to the northeast on apparently listric normal faults that dip SW. This is very similar to the kind of deformation found in the Basin and Range Province, a broad area of extensional tectonism (Stewart, 1978). This contrasts sharply with the style of faulting found in the Northern Colima Graben, in which fault blocks are bounded by steeply-dipping normal faults with no evidence for tilting or rotation of blocks. This may indicate that these faults extend to a much greater depth in the crust and also represent less extension than faults in the Zacolalco Graben (Allan, 1986).

The tectonic style varies along the length of the Colima Rift, making it difficult to extend the above conclusions for the Northern Colima Rift to the rest of the rift. Tilted fault blocks within the Colima Rift appear and become more common to the south. This observation implies that listric faulting (Jackson and McKenzie, 1983), and the greater amount of extension that it represents, increases towards the south, reaching a maximum near the coast. This is also illustrated by the more disrupted, random orientation of the fault blocks in the Southern Colima Rift nearer the coast, which Allan *et al.* (1987) conclude is an indication of greater extension. The observed southward widening of the zone of deformation also supports this conclusion.

It has been noted by Nixon (1982) that the Colima Rift overlies the landward extension of the Rivera fracture zone, which intersects the trench at an oblique angle offshore from the southern end of the Colima Rift. This is the section of the Rivera fracture zone east of the East Pacific Rise, marking the left-lateral transform boundary between the Rivera and Cocos Plates. Nixon (1982) postulated that the zone of left-lateral shear extends for some distance beneath the overriding plate, causing a tear or hinge-fault at the surface which is expressed as the Colima Rift. This would mean that the Jalisco and Michoacan structural blocks are actually a single block that has been disrupted internally by relative motion between the plates that have been subducted beneath it. Furthermore, this conclusion would seem to conflict with the theory that the Colima Rift could be an 'active' rift in the sense of Sengor and Burke (1978), and that it is more likely to be a 'passive' form. On the other hand Luhr *et al.* (1985) hypothesized that the Colima Rift corresponds to the landward extension of the northern East Pacific Rise, which they conclude is in the process of translating eastward. This possibility would mean that the rifting in the area is the result of a hot mantle plume that has been subducted, and thus would imply 'active' rifting.

5.3 The Chapala Rift

East-west oriented structures that are recognizably related to the Chapala Rift form a very wide zone extending eastward about 130 km from the western end of Lake Chapala (Figure 15). Faults are more numerous in the vicinity of the lake, and their numbers rapidly dwindle to the east, where they are abruptly truncated by a prominent N-S graben structure south of the Sierra Penjamo (see later section). South of Guadalajara the zone of deformation is about 50 km wide; and it widens rapidly to the east, reaching a maximum of about 100 km wide just to the east of Lake Chapala.

At this time the geology of the Chapala Rift remains somewhat enigmatic, as little work has been published on the area. Diaz and Mooser (1972) and Mooser (1972) provide short summaries of the structure, and more recently Delgado-Granados and Urrutia-Fucugauchi (1985), Nixon et al. (1987), and Allan et al. (1987) summarize additional information on the geology and structure of the area.

5.3.1 Pre-Pliocene Geology

On the basis of limited reconnaissance in the area, Allan et al. (1987) conclude that most of the rocks exposed in the Chapala Rift are volcanic, and that most of these volcanics are Plio-Pleistocene in age. However, a single Late Miocene date reported by Nixon et al. (1987) for a basaltic flow northeast of Lake Chapala, and the similarity of that area to others north and south of the lake as seen on the TM images, indicate that many of the rocks exposed in the rift may in fact be Late Miocene basalts. Rocks of similar age and description are found at the base of the canyon of the Rio Grande de Santiago north of Guadalajara (Gilbert et al., 1985), and as far west as Tepic (Gastil et al., 1978). These basalts represent the only unquestionably pre-Pliocene rocks exposed in the Chapala Rift, and no evidence for older rocks could be seen on the TM images. Few K/Ar dates have been reported in the literature for the area of the Chapala Rift (Watkins et al., 1971; Mahood, 1977; Nixon et al., 1987; Allan et al., 1987), and most of these are concentrated in a small area north of Guadalajara. All of the rocks dated are Late Miocene or younger, and Plio-Quaternary dates predominate.

Beneath the Neogene volcanics in the area, there undoubtably exist rocks similar to pre-Miocene rocks exposed elsewhere in the MVB. These probably include Mesozoic igneous and sedimentary rocks comparable to rocks in the Jalisco and Michoacan Blocks. In addition, the presence of Middle Tertiary volcanics of the Sierra Madre Occidental both north and south of the area (Lopez-Ramos, 1983) suggests that these deposits extend beneath the MVB in the area of the Chapala Rift. The rift is underlain by at least 2300 m of Tertiary volcanics that were drilled in a borehole on the southern margin of Lake Chapala (Pozo Chapala 1-A); remarkably, the hole bottomed at 814 m below sea level without penetrating the volcanic pile (Lopez-Ramos, 1983). No more specific mention is made of the age of these rocks. Less than 50 km to the west Allan (1986) reports a 5.4 Ma andesite flow erupted directly upon a 70 Ma granodiorite stock, which atests to the huge variation in thickness of the Tertiary volcanic pile in the region. Also of note is a comment by Lopez-Ramos (1983) that the rocks in the Chapala 1-A hole do not match the succession of volcanics exposed in fault blocks north of the lake.

5.3.2 Plio-Quaternary Volcanism

No detailed descriptions of rocks of this age have been published, except at the extreme western end of the rift north of the Triple Junction. Plio-Quaternary volcanics are widespread within the Chapala Rift,
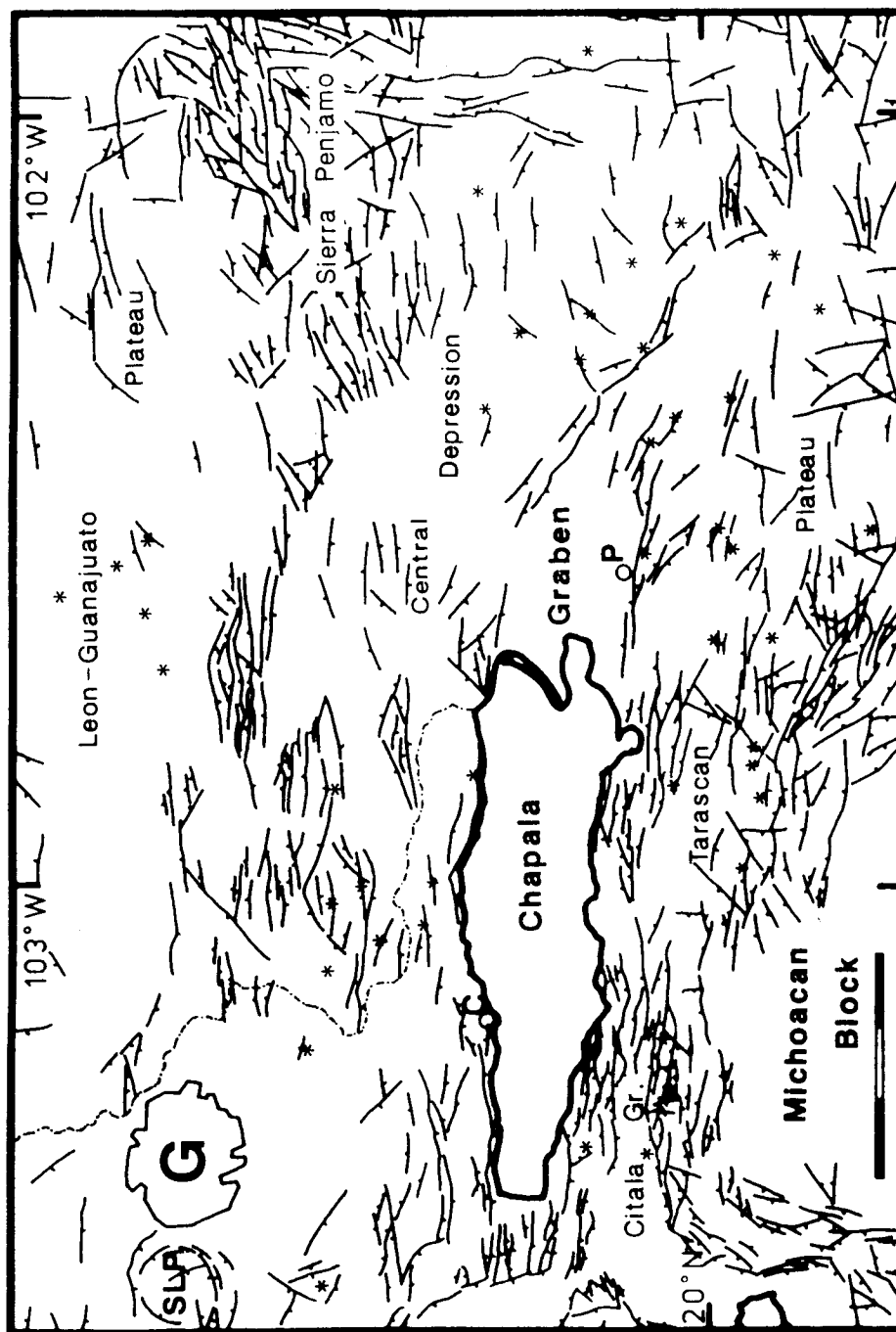
Figure 15: Fault map of the Chapala Rift. Stars show locations of large Plio-Quaternary volcanic cones. C, Chapala; G, Guadalajara; P, Pajacuaran; SICG, San Ignacio Cerro Gordo; SLP, Sierra la Primavera. Scale bar is 30 km long.

and include basalt and andesite flows, tuffs, and volcanogenic sediments (Allan *et al.*, 1987). The most prominent example of these rocks are numerous cones at various stages of erosion. The largest of these form three groups, one centered 20 km NE of the town of Chapala, one immediately west of San Ignacio Cerro Gordo, and another south of Lake Chapala that extends to the east. The cones near Chapala are cut by fractures and large, steep faults trending E-W. The majority of these faults face southward. One of the cones has been nearly cut in half by a very prominent fault with over 300 m of throw. This fault is a very young feature, showing practically no evidence of erosion on the scarp. Cones south of Lake Chapala tend to get larger and more numerous to the east, until they merge with other large cones in the western portion of the Michoacan-Guanajuato Volcanic Field east of Lake Chapala.

On the basis of their morphology, these large cones of the Chapala Rift can be correlated with others to the east in the Michoacan-Guanajuato Volcanic Field (reviewed by Hasenaka and Carmichael, 1985b), and are thus of probable Late Pliocene to Pleistocene in age.

5.3.3 Plio-Quaternary Structure and Morphology

The wide zone of deformation in the Chapala Rift is bounded on the south by an eroded plateau interrupted at intervals by large, deeply dissected cones of Plio-Pleistocene(?) volcanoes. The plateau has been referred to as the Tarascan Plateau (Pasquare *et al.*, 1987) and, like the small volcanic centers that dot its surface, it also extends and widens to the east, encompassing most of the southern Michoacan-Guanajuato Volcanic Field. Based on similarites with dated rocks to the north, the western plateau is probably composed of Late Miocene basalt flows that correlate with similar volcanics as far west as Tepic. The relatively smooth surface of the western Tarascan Plateau is separated from the deeply eroded uplands of the Michoacan Block to the SW by a zone of numerous WNW-ESE trending normal faults, most of which dip to the north. About 250 m of cumulative offset has occurred across this zone of faults, but this contrast in the elevation of the terrains to either side of the faults is greatest near the faults. The elevation of the eroded highland of the Michoacan Block in this area decreases slightly to the SW.

To the north of the Chapala Rift, the Leon-Guanajuato Plateau forms a broad upland, having an average elevation of 1800 to 2000 m and becoming higher to the north and east. The southern margin of this plateau east of Guadalajara is fractured and faulted. These faults become more numerous and appear to have greater offset to the south, forming a sort of gradual transition between the relatively undisturbed plateau and the block-faulted terrain of the Chapala Rift. The Leon-Guanajuato Plateau lies in a zone of transition between N-S trending Basin and Range structures to the north and structures related to deformation in the MVB to the south (Pasquare *et al.*, 1986).

Three basins or grabens form the topographic expression of the Chapala Rift. A short, narrow basin, the Citala Graben (Delgado-Granados and Urrutia-Fucugauchi, 1985), extends eastward out of the Triple Junction SW of Lake Chapala, but it narrows rapidly within 30 km. It was described by Urrutia-Fucugauchi (1986, pers. comm.) as being the most active structure related to the Chapala Rift, having the freshest evidence of recent faulting. This is corroborated by features seen on the TM images, but since this basin is really more closely associated with the Triple Junction, a more detailed description is left for the next section. This basin is separated from the basin containing Lake Chapala by a range of tilted fault blocks.

Lake Chapala (elev. 1500 m) fills the western two thirds of an elongate depression 115 km long and 10 to 25 km wide. The eastern third of the basin is filled by alluvium. This basin has often been referred to in the past as the Chapala Graben. On its north it is bounded by steeply southward-dipping normal faults that define large fault blocks. These blocks and the faults that define them can be clearly seen on the TM image extending at least 50 km north from the northern shore of the lake. They average 10 to 15 km

in length and 2 to 4 km in width and most dip gently to the north. Many appear to be highly fractured in directions sub-parallel to the general trend of the rift. Displacement on faults in the area ranges from nearly 1 km down to the limits of detectabilty using the TM images (5 to 10 m, depending on the sharpness of the scarp). The longest fault, the Ixtlan fault (Mooser, 1972) extends along the northern shore of Lake Chapala and continues to the east for over 50 km. To the south of the Chapala Graben the picture is reversed: large fault blocks dipping gently to the south, bounded by normal faults that dip steeply to the north. Maximum offset on northward dipping faults here is slightly less, reaching about 800 m on the large scarp just south of the town of Pajacuaran, SE of Lake Chapala (the Pajacuaran fault (Mooser, 1972)). The Chapala Graben narrows to about 10 km wide at its eastern end, where the Ixtlan and Pajacuaran faults converge about 35 km east of the lake.

Northeast of Lake Chapala, and south of the Leon-Guanajuato Plateau, the number of fault blocks that emerge above the alluvium decreases and the country opens into a broad plain, forming the third major basin in the Chapala Rift. This plain is at the western end of the 'Central Depression' morpho-structural division of Pasquare et al. (1987). This division includes most of the Rio Llerma basin and extends all the way to the Queretaro-Taxco Fracture system, 230 km to the east. Its average elevation gradually rises from around 1600 m near Lake Chapala to over 1700 m at its eastern end near the city of Celaya, beyond the limits of Chapala Rift structures (as defined here).

5.3.4 Regional Deformation

The total amount of extension across the Chapala Rift has not been calculated. Nor has the total offset on faults within the rift, nor their age. In general terms, faulting in the region probably began in the Pliocene (Diaz and Mooser, 1972). Allan et al. (1987) conclude on the basis of fault-scarp morphology and cross-cutting relationships with Pleistocene volcanics that Chapala Rift faulting continued into the Late Pleistocene. The very sharp, abrupt truncation of spur ridges with triangular facets and the near lack of alluvial fans at the base of many of the faults, as seen on the TM images in the Chapala Graben, supports this general conclusion.

The regional deformation has clearly been extensional, oriented N-S, since the most recent phase of tectonic activity was initiated in the Pliocene. The axis of the Chapala Rift represents the zone of separation between the North American Plate on the north and the Michoacan Block on the south. This axis is best defined as running E-W through the center of the Chapala Graben section of the Chapala Rift, since this is the section that has subsided the most.

5.4   The Triple Junction

About 55 km south of Guadalajara the three zones of extensional tectonism described in the previous sections of Chapter 5 intersect to form a prominent R-R-R Triple Junction (Figures 7 and 8). This feature stands out prominently on the Guadalajara TM scene. The pre-Pliocene geology of this area has already been discussed separately in the previous sections, so this section will focus entirely on its Plio-Quaternary geology and structure.

5.4.1 Plio-Quaternary Volcanism

Luhr and Lazaar (1985) describe a chain of at least eight small lava and cinder cones south of Guadalajara (the Southern Guadalajara Volcanic Chain). These are aligned in a NW-SE direction, along a trend of about N112°. The cones of this chain extend southeastward to the zone of E-W faulting associated with the Chapala Rift, and the southeasternmost cone is deeply cut by a very prominent normal fault. To the northwest, additional cones may extend beneath the slightly younger deposits of the Sierra la Primavera. Luhr and Lazaar (1985) conclude that the cones are Plio-Pleistocene in age. They point out that the orientation of the chain is important for the establishment of a 'fix' on the NE-SW oriented extensional field that developed in the region sometime since the end of the Miocene.

Many more cones and flows occur in the area north of the Triple Junction and south of the Sierra La Primavera. These are seen on the TM imagery to have very similar morphologies to those described by Luhr and Lazaar (1985), so they are interpreted to be of comparable age (Pleistocene). These cones and flows do not appear to be aligned along a dominant trend. According to Allan (1986), calc-alkaline volcanism has proceeded in this area since at least 10 m.y. ago.

Closer to the Triple Junction, the largest cones and domes have erupted within and on the flanks of the Citala Graben. Allan and Carmichael (1984) describe alkaline volcanic rocks that have been erupted within the Colima Graben. These rocks have erupted contemporaneously with calc-alkaline volcanics of the MVB since the Late Pliocene, though in much smaller volumes (Allan, 1986). Petrologically, these rocks are more closely related to volcanics associated with continental rifts, and are rarely found in active continental margin environments (Allan, 1986).

5.4.2 Structures Visible on the TM Imagery

The Triple Junction consists of a three-pronged basin bounded on two sides by eroded highlands and on the third by a block-faulted volcanic plain. North of the Triple Junction, the area situated between the grabens extending to the northwest (the Zacoalco Graben of Allan (1986)) and the east (the Citala Graben of Delgado-Granados and Urrutia-Fucugauchi (1985)) contains the most striking examples of tilted fault blocks seen within the Guadalajara scene. These large blocks are generally tilted to the NNE, are highly fractured, and are bounded on their southern and southwestern sides by very large fault scarps in various stages of erosion, from very eroded to very youthful in appearance. The faults appear to dip steeply to the south and southwest. Many of the fault scarps show evidence of several episodes of movement, such as truncated spur ridges with triangular facets. Blocks north of the town of Chapala were seen by the author to be capped by weakly consolidated lacustrine deposits of probable Pleistocene age. The generally unconsolidated nature of these sediments is shown by the very extensive erosion displayed by many of the fault scarps located north of Lake Chapala. Despite this rapid erosion of the scarps, the tops of the blocks remain relatively smooth, tilting to the NNE away from the Triple Junction at angles between 11° and 18°. The tilt angle is easily measured using the TM images combined with topographic maps. This angle is generally steeper closer to the Triple Junction, becoming less pronounced farther to the northeast.

The style of deformation on either side of the southern branch of the Triple Junction (the Colima Graben of Allan (1986)), and south of its two northern branches, contrasts sharply with that exhibited in the area to the north. The highlands to the southeast and southwest of the Triple Junction are deeply eroded but seem for the most part to be flat-lying, showing little evidence for tilting. However, uplift is more marked in these areas than to the north of the Triple Junction. The average elevation of the floor of the triple junction is slightly lower than 1500 m, while the highlands to the southeast and southwest average about 2000 m or

more. In contrast, the plains south and southeast of Guadalajara and north of the Triple Junction average about 1650 m, only slightly higher than within the Triple Junction itself. The exception to this is the peaks of the tilted fault blocks, some of which reach elevations that exceed the highest elevations found on either side of the southern branch (Bola del Viejo, 2960 m, north of Lake Chapala, and Cerro Garcia, 2750 m, south of the lake but still north of the main eastern branch of the Triple Junction, are two examples).

A basalt flow exposed at the rim of the canyon of the Rio Grande de Santiago has been dated by Gilbert *et al.* (1985) as having an age of 0.5 Ma. They note that canyon cutting is younger than the flow. This is strong evidence that the regional uplift that led to the erosion of the canyon has occurred since the Late Pleistocene. This fact, combined with the presence of Quaternary grabens oriented in the classic triple-splayed pattern (Quennell, 1985), and Late Pleistocene-Holocene alkaline volcanics (Allan *et al.*, 1987), indicates that the rifting in west-central Mexico is similar to the "active" form of Sengor and Burke (1978).

5.5 Summary

Neotectonic deformation in the crust of the western part of the study area is dominated by rifting. Three active rifts form a triple juncion located south of Guadalajara, forming the normal triple-splayed Rift-Rift-Rift pattern. The Tepic-Chapala Rift is the most complex of the three; it stretches from the triple junction northwestward to the coast west of Tepic. The Chapala Rift extends eastward from the triple junction; its central graben contains Lake Chapala, a large but shallow natural lake. The north-south trending Colima Rift completes the trio and extends from the triple junction to the Pacific coast south of Colima.

This part of Mexico has been the subject of several recent studies. Allan (1986) and Luhr *et al.* (1985) reviewed the structure and geology of the area around the triple junction. Diaz and Mooser (1972) provided an early study of the Chapala Rift. Nieto-Obregon *et al.* (1985), Gastil *et al.* (1978), and Gastil and Jensky (1973) studied structures, volcanism, and tectonics in the Tepic-Chapala Rift. Recent reviews of tectonics and volcanism in the area have been provided by Allan *et al.* (1987) and Nixon *et al.* (1987).

From our work with the TM images, combined with the works listed above, the Neogene tectonic and volcanic history of the area can be summarized as follows:

1. *Miocene.* The waning stage of southern Sierra Madre Occidental volcanism deposited ignimbrites, basalts, and tuffs over a large portion of the region between Guadalajara and Tepic. These rocks are cut and tilted by northwest-trending faults of Late Miocene age, forming tilted fault blocks. The Late Miocene basalts and faulting are related to incipient rifting along the "proto-Gulf of California", which extended southeastward to form a "proto-Tepic-Chapala Rift". A significant amount of right-oblique slip was accommodated along the northwest trend of the proto-Gulf, probably driven by extremely oblique subduction along southwestern Mexico from about 12 to 7 Ma (Schilt *et al.*, 1982).

2. *Pliocene.* A new stress field began to develop after the rifting of Baja California from the Mexican mainland and flooding of the Gulf of California in the Latest Miocene. This is probably related to coincident changes in the configuration of plates in the Eastern Pacific and resulting changes in the convergence direction (Schilt *et al.*, 1982). Normal faulting and block tilting continued in the Tepic-Chapala Rift, and locally thick Pliocene lacustrine deposits were accumulated and later tilted in the basins thus formed. During this period faulting probably began in the Colima and Chapala Rifts, and the triple junction was born. Basalts, ignimbrites, and andesites of this age indicate continued subduction of the Cocos plate.

3. *Quaternary.* During this period the major calc-alkaline strato-volcanoes were erupted in the basins

formed by the rifting. Rifting continued (and is continuing) to form horsts and grabens, cutting the volcanics soon after their deposition. Associated uplift has been significant in places, leading to the excavation of the canyon of the Rio Grande de Santiago north of Guadalajara, for instance.

Important contributions of the TM interpretations to a better understanding of the deformation in the region include:

- the regional distribution of faults and rift structure was mapped in much greater detail than ever before through the use of the TM images. The complexity of the faulting at the margins of the grabens that intersect in the area is clearly apparent in figures 15 and 19 through 22. Many of the fault scarps show evidence of several episodes of movement, such as truncated spur ridges with triangular facets and multiple slope breaks. These features are easily seen on the TM images of the area (as demonstrated for other areas in a later section), and are generally associated with Quaternary faulting, as noted previously by Allan (1986).

- The more detailed fault maps of the area derived from the TM imagery led in turn to the discovery and mapping of the Rio Ameca graben, a small, previously undescribed feature branching away from the main trend of the Tepic-Chapala Rift (Johnson, 1987). The Rio Ameca graben is approximately 90 km long and intersects the coast at the Bahia de Banderas. Faults on the margins of the graben extend farther to the west and form the northern and southern shores of the bay, which is the offshore extension of the graben. The graben appears to have formed between a portion of crust which has accreted to the Rivera plate on the northwest, and the Jalisco block on the southeast. North of where the offshore projection of the graben intersects the trench, subduction has ceased (Johnson, 1987).

6 Neotectonics: Transtension

6.1 The Cuitzeo fault trend

The generally disorganized nature of faulting within the Michoacan Triangle becomes much more regular and intense to the NE in the vicinity of Lake Cuitzeo. The faulting in this area will be referred to here as the Cuitzeo fault trend. Figure 16 shows the region and the faulting within it as mapped from the TM images. It extends ENE to where it is effectively truncated by the Queretaro-Taxco Fracture System. On the west in the vicinity of La Piedad, the area of associated faulting ends near the Penjamillo Graben, a prominent N-S trending feature. Most of the faults of this area are oriented ENE, with their northern side downthrown. They are generally less than 10 km in length, and most have offsets that can be measured in tens of meters. Many are much larger, such as those south and west of Lake Cuitzeo, which have vertical offsets of up to 500 m or more. A strong correlation exists between vertical offset and extent of erosional degradation on these scarps, the largest faults being eroded the most. South of Queretaro the ENE trending normal faults interact with fractures parallel to the Queretaro-Taxco Fracture System, forming numerous short horst and graben segments that are tilted and disorganized. Faulting in the area generally has a very youthful expression in most places, particularly between Lakes Cuitzeo and Yuriria, where the faults are smaller and more numerous (Figures 17 and 18).

As is the case for the Michoacan Triangle, the basement of this region is poorly exposed and has not been extensively studied. Oligo-Miocene volcanics associated with the Sierra Madre Occidental province undoubtably underlie those of Plio-Quaternary age in the area, based on their presence in such a relationship in adjacent areas to the east and west. Older rocks are present in the Guerrero Block, immediately to the south of the area. Rocks that correlate with these are also likely to extend beneath the extensive volcanic cover.

The volcanics of the MGVF also extend to the NE into this area, but in general these are older than those to the SW (Hasenaka and Carmichael, 1985a). These are dominated by small cones and shield volcanoes, where the generally smooth surfaces prominently display the faults that cut across them. Murphy and Carmichael (1984) described 13 maars that have erupted in association with the MGVF volcanics west of Lake Yuriria. The maars are near the northern limit of concentrated Plio-Quaternary volcanism associated with the MGVF, and the more numerous volcanoes are concentrated south of Lake Yuriria.

The topographic depression that contains the Cuitzeo Fault Trend extends eastward out of the Chapala Graben and continues into the region around Queretaro, where it is abruptly truncated by the Queretaro-Taxco Fracture System. The depression has an average elevation of 1800 m, and measures approximately 90 by 250 km, elongated in the E-W direction. Only its eastern two-thirds is occupied by the Cuitzeo Fault Trend. The Penjamillo Graben extends across the depression in a N-S direction near the western end of the faulting associated with the Cuitzeo Fault Trend. To the north and south the depression is flanked by the highlands of the Leon-Guanajuato Plateau and Guerrero Block, respectively.

A striking contrast exists between the northern half of the depression, which is a smooth alluvial surface, and the southern half, where the majority of the more concentrated faulting is located. In part this dichotomy in structural style may be due to the unconsolidated nature of the alluvium, where any recently active faults are likely to be rapidly erased through erosional processes. As noted earlier, the majority of volcanic deposits are located south of Lake Yuriria, and faulting in this area is consequently better preserved.

The Cuitzeo Fault Trend can be interpreted as a tensional boundary between continental Mexico (the
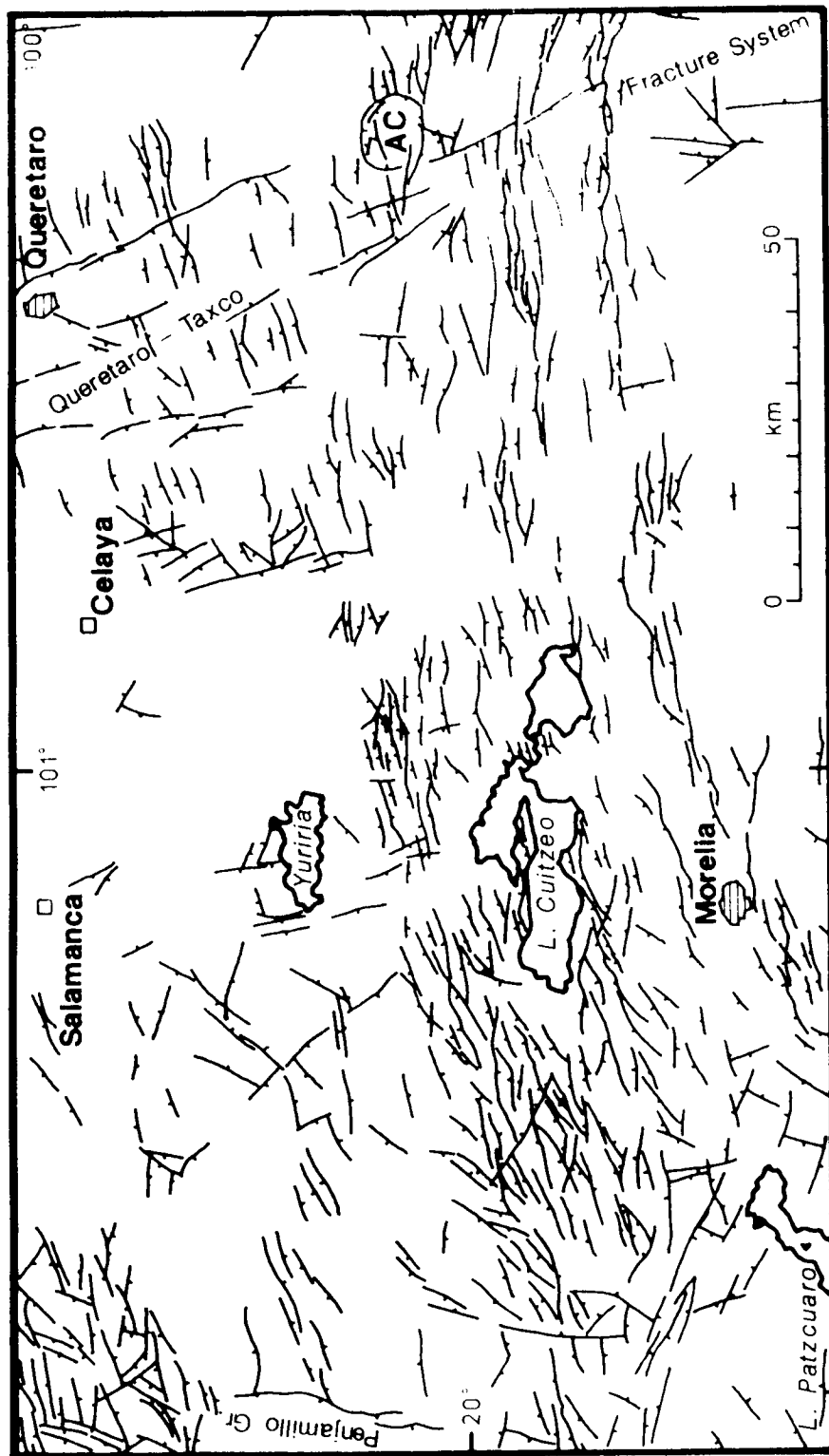
Figure 16: Fault scarps mapped in the region of Lake Cuitzeo, the Cuitzeo fault trend. The most numerous faults have a general trend of about N75°, which has been used to constrain the relative motion between the North American plate and the Guerrero crustal block. The faults in the northwestern corner of the figure are within the Sierra Penjamo. AC, Amealco Caldera.
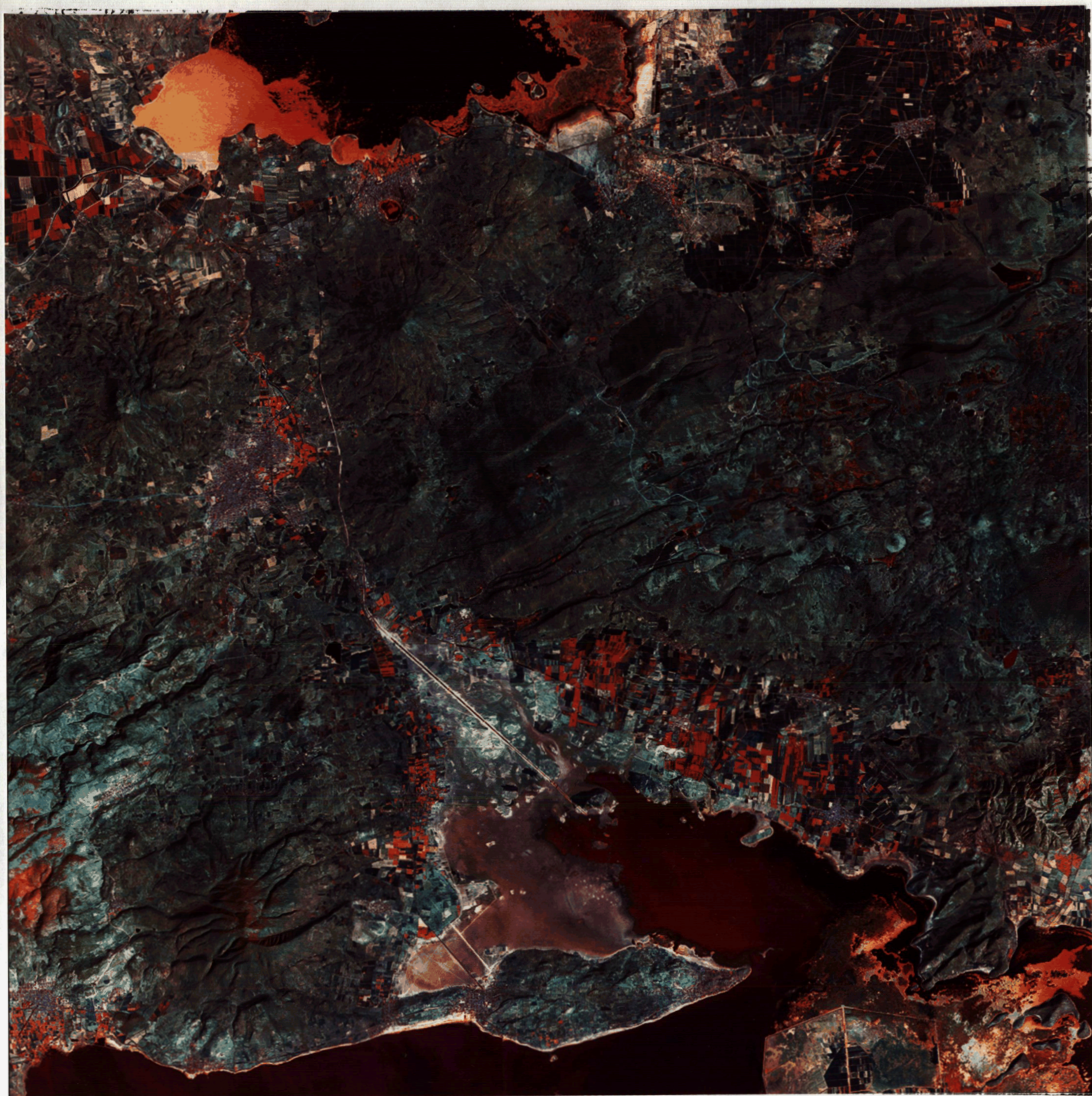
Figure 17: TM image of the region between lakes Yuriria and Cuitzeo. The image shows TM bands 754 as blue, green and red, respectively. Multiple small normal faults with very young morphology cut the volcanics in this area. See text for more details.
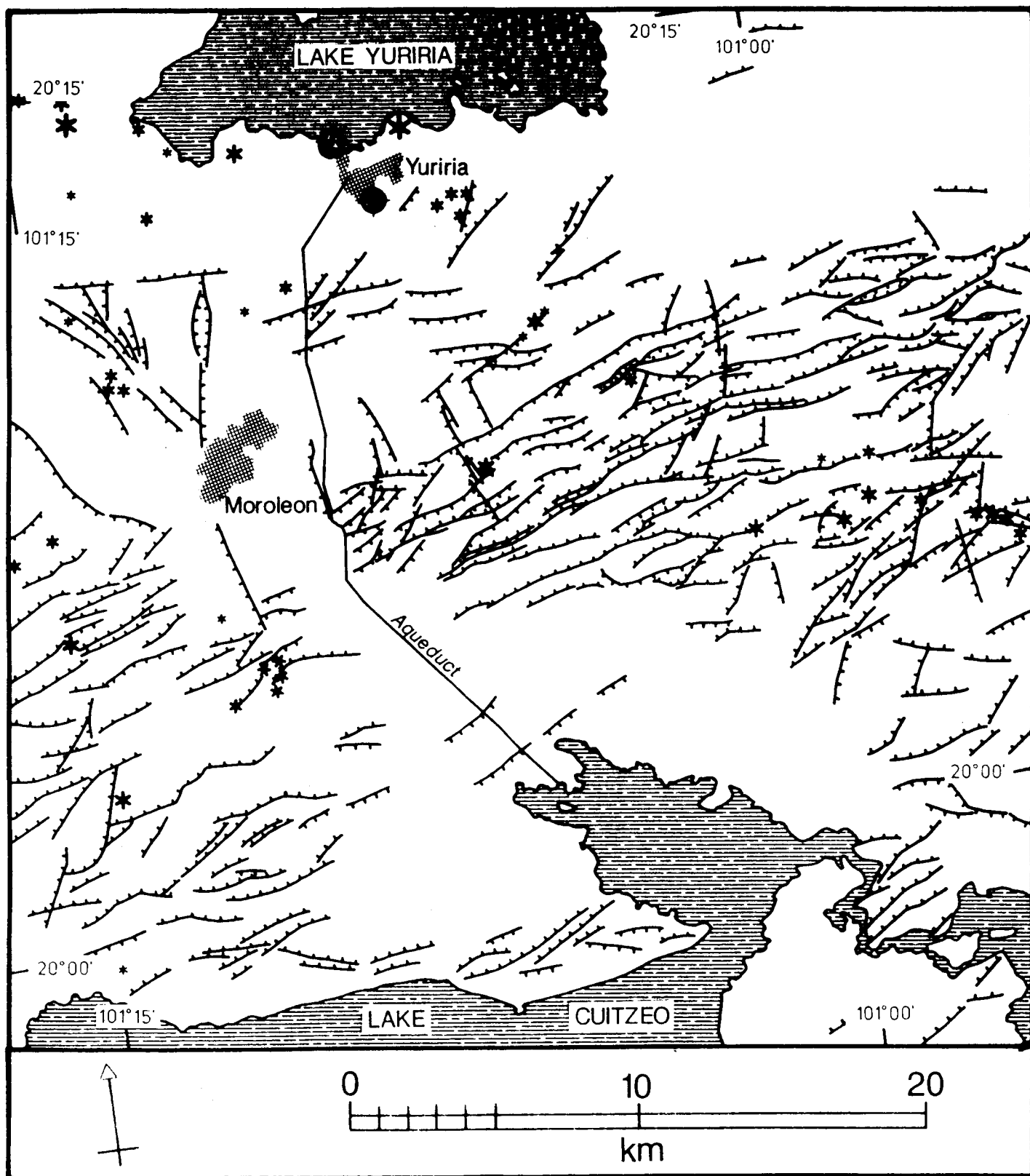
Figure 18: Detail of fault scarps mapped between Lakes Cuitzeo and Yuriria, interpreted from a digitally enhanced enlargement (figure 17). Numerous Quaternary shield volcanoes and cinder cones are dissected here by the ENE trending faults. Stars show the positions of most of these cones.

North American Plate) to the north, and the Guerrero Block to the south. Pasquare *et al.* (1987) conclude that since about 2 Ma the σ_3 direction has been oriented NNW-SSE, on the basis of relationships between dated volcanics and tensional structures. This direction can be more precisely measured from the orientations of young normal faults in the area (N60°-80°) as being oriented N330°-350°. The apparent *en echelon* distribution of these faults in relation to other prominent structures to the south trending E-W (the Chapala-Tula Fault Zone) indicates that extension in the region may actually be transtensional, with a left-lateral component superimposed upon the extension described above.

6.2 Eastern High Plateau

This region of broad high plains interrupted by volcanic ridges extends from about 100°W longitude eastward beyond the eastern edge of the study area at 98°W, a distance of over 250 km. Figure 19 shows the general configuration of the plateau, the structures found within it, and its relationship to surrounding areas. This area roughly corresponds to the Eastern Plateau of Pasquare *et al.* (1987). On the west it is mostly bordered by the Queretaro-Taxco fracture system. The valley of the Rio Moctezuma runs along the northwestern edge of the plateau. To the northeast lies the canyon of the Rio Grande de Tulancingo; beyond that deep valleys cut through the folded Mesozoic rocks of the Sierra Madre Oriental and the elevation drops 2 km to the coastal plain of the Gulf of Mexico. To the east the plateau extends beyond the eastern end of the study area to the N-S volcanic chain of Cofre de Perote-Pico de Orizaba. Finally, on the south the plateau is rimmed by the Quaternary strato-volcanoes and cinder cone fields of the MVB.

In this region the structures seen on the TM images are generally of an older character, and the younger tectonic activity appears to be much less intense than for areas to the west. The large-scale deformation within the area that can be clearly identified as recent (Quaternary) becomes more rare to the east, and the most active zones are largely confined to the area's western sector.

The Eastern High Plateau is almost entirely above 2000 m in elevation. The elevation is greatly increased in areas where Quaternary volcanic activity has been concentrated, reaching over 5000 m southeast of Mexico City in the Sierra Nevada. This area of greatly elevated terrain in the MVB has the greatest crustal thickness outside of the Mexican Altipano. The thickness in this area is at least 40 km and may even reach 50 km in its eastern half (Urrutia-Fucugauchi, 1986). Crustal thickness elsewhere in the MVB averages between 30 and 35 km.

6.2.1 Pre-Pliocene Geology and Structure

Situated beneath the Plio-Quaternary volcanics of the plateau is a thick series of Oligo-Miocene volcanics that form the basement of the region. These rocks are associated with the Sierra Madre Occidental volcanics farther west, and they fill localized tectonic depressions that formed in the area of the plateau at roughly the same time as the volcanism was active. In the area south of Mexico City older rocks of the Sierra Madre Oriental emerge from beneath the volcanic cover. On the TM images these rocks display prominent WNW-ESE trending faults and fractures that may be related to the Oligo-Miocene volcanic activity (Negendank (1974)). Mooser *et al.* (1974) report that a borehole east of Mexico City (Pozo Texcoco) penetrated 2060 m of these mid-Tertiary volcanics before encountering the unconformity above the underlying sedimentary rocks of the Sierra Madre Oriental. These folded and thrusted Mesozoic sediments form the basement of the area.

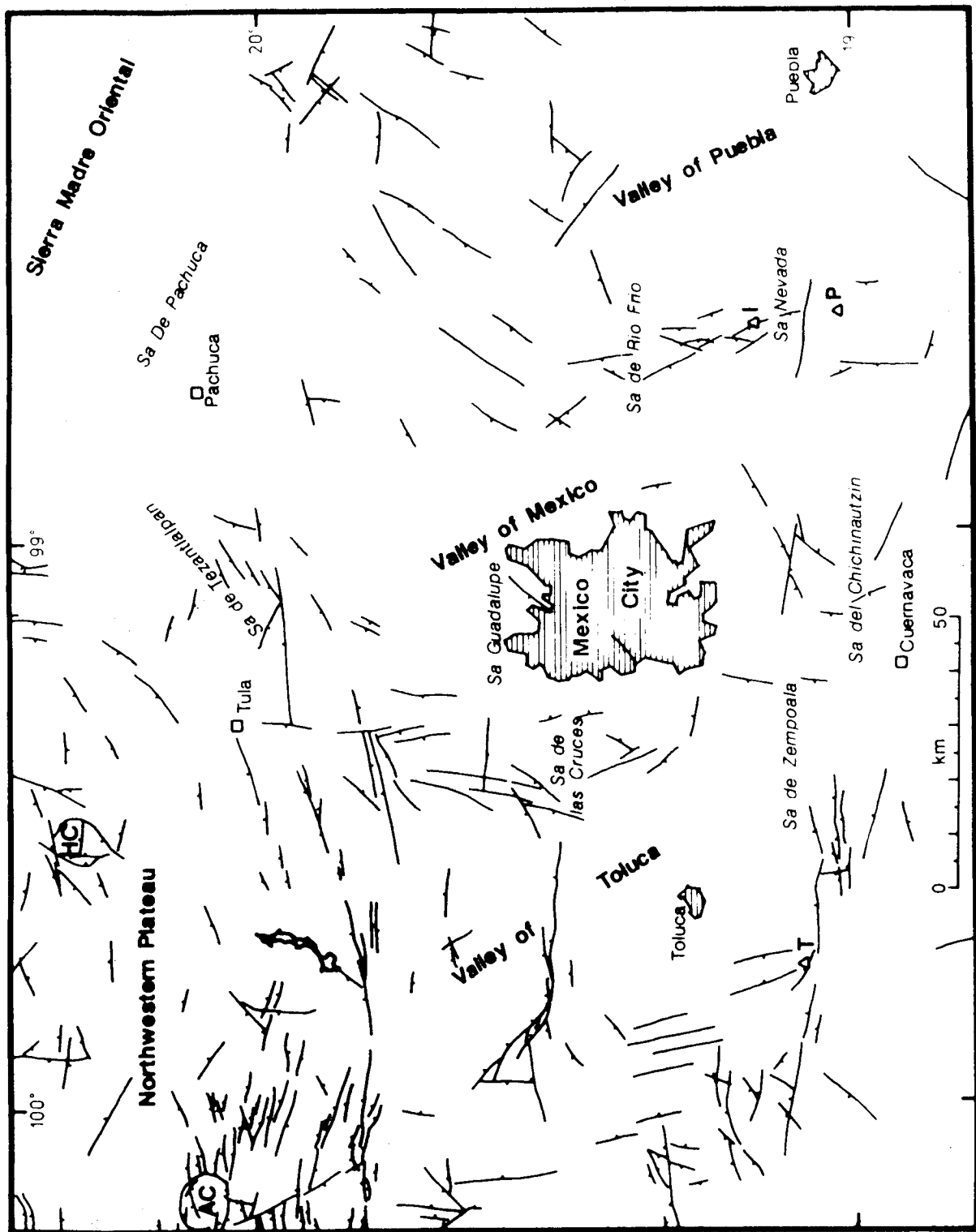The Tertiary volcanic succession on the plateau is interesting because of its apparent close relationship to

Figure 19: The area of the Eastern High Plateau, showing the fault scarps that could be mapped on the TM images. I, Iztaccihuatl; P, Popocatepetl; T, Nevado de Toluca; AC, Amealco Caldera; HC, Huichapan Caldera.

the tectonic development. In the region of the Valley of Mexico, Mooser *et al.* (1974) recognized seven volcanic units, five of which are of Oligocene or Miocene age. The Oligocene Tezontlalpan Group and the Oligo-Miocene Xochitepec Group are both related to WNW-ESE fractures. This pattern of older faults and fractures can still be seen on the TM images in the region south of the volcanic cover, exposed within the Guerrero Block. The volcanics of this period are found in isolated, severely eroded exposures in ridges at the margins of the Valley of Mexico. Other ridges of similar erosional character occur north and northwest of Mexico City, where they are faulted by the Chapala-Tula Fault Zone.

The next three volcanic units are related to NNW-SSE faults, and are primarily exposed within the high volcanic sierras that trend in the same direction, bordering the Valley of Mexico on the east and west (Mooser *et al.*, 1974). The Lower Sierra Group is a basic volcanic complex of Late(?) Miocene age. It forms the base of the succession of volcanics in the Sierra de las Cruces and Sierra de Rio Frio, which are situated on either side of the Valley of Mexico. These NNW-SSE trending ridges of volcanics developed from north to south as a series of stratovolcanoes formed along faults of the same trend (Mooser *et al.*, 1974). This activity, expressed as the Upper Sierra Group, continued into the Early Pliocene. The N-S trending Valleys of Toluca, Mexico, and Puebla began to take on their modern form during this period, as the faults at their margins became active. The surface of the Eastern High Plateau is topographically dominated by these almost evenly sized depressions.

The Sierra Guadalupe, a small ridge immediately north of Mexico City, also developed in the Late Miocene. It began with deposition of andesite and dacite flows, followed by the formation of a small graben and extrusion of additional volcanics (Mooser *et al.* 1974). Such activity in this area ceased before the beginning of the Pliocene.

6.2.2 Plio-Quaternary Volcanism and Structure

The Plio-Quaternary volcanism and structure of the Eastern High Plateau is known primarily from work done by Mooser and Negendank, especially within and around the Valley of Mexico (Mooser, 1963; Mooser *et al.*, 1974; Negendank, 1972; 1974). This work, taken in combination with other work by Martin del Pozzo (1982) and Bloomfield (1975), provide the framework upon which a discussion of the Plio-Quaternary development of the entire plateau can be based.

As mentioned previously, the surface of the plateau is divided into three nearly equally sized depressions. These basins are separated by ridges of Mio-Pliocene volcanics associated with the development of NNW-SSE trending faults on the margins of the basins. From west to east the topographic depressions are the Valleys of Toluca, Mexico, and Puebla. All three of the valleys are named for major cities that lie near their southern ends. The northwestern part of the plateau forms a separate division, making a total of four.

The Valley of Toluca

The Valley of Toluca is the westernmost basin on the plateau. On the south it is bounded by Quaternary cinder cones and Nevado de Toluca, a major Quaternary volcano (Bloomfield and Valastro, 1974). On its other three sides, the basin is ringed by ridges of older volcanics, predominantly of Mio-Pliocene age. The basin is almond-shaped, with a long dimension of 80 km oriented NW-SE, a width of 40 km, and an average elevation of about 2600 m. The elevation within the basin increases to the SE.

The Quaternary volcanics to the south are clearly related to a series of E-W trending faults seen on the TM images. These faults can be seen extending to the east and west of Nevado de Toluca, where they localize

the eruption of numerous cinder cones and viscous lava flows. The trace of these faults is discontinuous because for much of their length they are buried by their associated volcanics. Nevado de Toluca itself lies at the intersection between these E-W trending faults and the NNW-SSE trending Queretaro-Taxco Fracture System. Faults and fractures related to both trends can be seen on the flanks of the volcano and intersect its summit.

Other major E-W trending faults are found near the center of the basin near Ixtlahuaca de Rayon, about 20 km north of Toluca. They effectively divide the Valley of Toluca into northern and southern halves. These faults separate eroded volcanics of the Mio-Pliocene association to the south from alluvium filling the northern half of the basin. Another major zone of E-W faulting associated with the Chapala-Tula Fault Zone cuts the ridges that bound the basin to the north.

The Valley of Mexico

East of the Valley of Toluca is the Valley of Mexico, the largest of the three basins on the Eastern High Plateau. It has an irregular shape and measures roughly 110 km from north to south and 30 to 70 km from east to west (Figure 19). Its southern half is limited on the east and west by the eroded Mio-Pliocene volcanic ridges of the Sierra de Rio Frio and Sierra de las Cruces, respectively. To the south the basin is filled with Quaternary volcanics associated with numerous cinder cones of the Sierra de Chichinautzin. North of Mexico City the basin widens. At its northern end the basin is limited by the eroded volcanic ridges of the Sierra Tezontlalpan and Sierra Pachuca. The elevation of the basin varies between 2200 m and 2400 m, but is generally below 2300 m. The basin is completely surrounded by a watershed, so all drainage is toward the interior, and most of the basin is floored by lacustrine sediments.

As is the case in the Valley of Toluca, the Quaternary volcanics at the southern margin of the Valley of Mexico appear to be strongly associated with E-W trending faults and fractures. The Sierra de Chichinautzin contains most of these small cones and flows. Details of the Quaternary volcanic history of the Sierra de Chichinautzin are discussed by Martin del Pozzo (1982). Monogenetic volcanism in the area has been active since about 40,000 y.b.p. and is composed primarily of scoria and lava cones and thick flows. The TM images of the area reveal many E-W alignments of the cones and flows, but fault scarps expressed at the surface are rare. This may be attributed to the extreme youth of the thick series of volcanics, which have probably covered any faults in the area.

The cinder cone alignments are in line with the E-W trending faults at the southern end of the Valley of Toluca. This E-W alignment of features extends to the east where it intersects the southern end of the Sierra Nevada, a ridge of Quaternary strato-volcanoes extending south of the Sierra de Rio Frio (Nixon et al., 1987). The point of intersection is marked by the only active volcano in the Sierra Nevada: Popocatepetl. Together with its northern neighbor, Iztaccihuatl, this volcano has evolved since the Late Pleistocene along the same series of NNW-SSE faults and fractures that controlled the location of the Sierra de Rio Frio in the Mio-Pliocene. On the TM image these fractures are clearly evident as they cut into the Sierras. Another previously undescribed fault associated with the E-W trend cuts just to the north of Popocatepetl.

To the north, the alluvium that fills the Valley of Mexico is relatively undisturbed by faulting. This may be due to the unconsolidated nature of the sediments, which are easily eroded, and not to a lack of tectonic activity in the area. Cinder cones of probable Quaternary age dot the alluvial surface north and northeast of Mexico City. Their distribution suggests a NE-SW alignment of hidden faults. These alignments are arranged in an *en echelon* pattern, indicating possible left-lateral shear extending to the ENE.

Extensive uplift of the northern plateau in the Quaternary is demonstrated along the canyon of the Rio Grande de Tulancingo. This canyon is about 500 m deep and its walls are capped by basic volcanics that

form the surface of the plateau in the area. These volcanics are labeled as Quaternary on the 1:1 million geologic map of Mexico and they are clearly seen on the TM images to extend on both sides of the deep canyon. Therefore the uplift that caused the incisement of the canyon must also be of Quaternary age, slightly younger than the volcanics that ring the canyon along its rim.

The Valley of Puebla

This is the easternmost basin covered by the study area. Only the foothills of its eastern boundary, the large stato-volcano of Cerro Malinche, are covered by the TM images. To the north the basin is rimmed by eroded Pliocene volcanic centers north and west of Apan. Its western edge is formed by the Sierra de Rio Frio and Sierra Nevada. To the south folded Mesozoic rocks of the Sierra Madre Oriental emerge from beneath the volcanic cover, forming elevated ridges. The basin is about 80 by 50 km in extent, and its elevation averages 2500 m in its northern half and 2200 m in its southern half.

Much of the southern part of the Valley of Puebla is covered by clouds on the TM images acquired for this study. However several prominent faults are seen in the northern part of the basin. These trend primarily NE-SW in a zone extending ENE out of the Valley of Mexico. They are also oriented in an *en echelon* pattern that indicates left-lateral shear. Their age is difficult to estimate and may be Plio-Pleistocene, based on the degradation of their scarps. Several smaller faults are found in the same area trending E-W. These are younger features because they cut the more recent volcanics in the area.

The Northwestern Plateau

This area is characterized by calderas, volcanic mountains and ranges that interrupt the surface of the plateau. On its northwest it is bounded by the valley of the Rio Moctezuma, which crosses an area of linear ridges and faults extending out of the Cuitzeo Fault Trend. To the north and east its edge is formed by mountains of the Sierra Madre Oriental. To the south it is rimmed by ridges of Mio-Pliocene volcanics. It covers an area 70 by 120 km with the long dimension oriented NE-SW, and has an average elevation of about 2000 m.

Extensive Quaternary volcanism in the area is absent. Instead most of the latest volcanism is associated with two prominent Pliocene caldera complexes. These calderas and their associated volcanics have not been studied in great detail, but Ferriz and Mahood (1986) provide a general outline of their geology.

The Amealco Caldera is a silicic volcanic center located at the western extremity of the area along the Queretaro-Taxco Fracture System, about 100 km northwest of Toluca. The age of the caldera forming event is not known precisely, but it was associated with eruptions of rhyolitic ignimbrites that cover lavas dated to 5 Ma (Ferriz and Mahood, 1986). A lava dome fills most of the interior of the caldera. The Huichapan Caldera is the second major complex of that type within the area, located about 100 km northwest of Mexico City. Ignimbrites associated with the formation of the caldera have been dated to 4.2 ± 0.3 Ma (Ferriz and Mahood, 1986). Following the collapse of the caldera, lacustrine sediments filled it and a small rhyolitic dome erupted near its southern end. Although the age of these calderas is slightly older, Ferriz and Mahood (1986) relate them to younger rhyolitic complexes occurring behind the main andesitic arc of the MVB to the east and west.

Other ridges on this part of the plateau are composed of eroded volcanics of probable Mio-Pliocene association. Of particular interest is a long linear ridge, of which the Mesa Rincon los Caballos forms the western extremity, extending for over 40 km west of Pachuca in an E-W direction. It appears to have been formed along a prominent fault or fracture. Its deeply eroded character indicates that the volcanics are probably of Early Pliocene age or older.

6.3 The Chapala-Tula Fault Zone

The Chapala-Tula fault zone (CTFZ) stretches for nearly 400 km along the twentieth parallel (Figure 2). Its western end is marked by the Rift-Rift-Rift triple junction south of Guadalajara; at its eastern end it dissipates in unconsolidated alluvium that fills the northern valley of Mexico. It is primarily composed of aligned north-dipping normal faults that cut the Plio-Quaternary volcanic deposits of the MVB. Many of the faults are arranged in a right-stepping *en echelon* pattern, indicating transtension with a sinistral component accross the CTFZ, particularly in the area west of Morelia. The largest faults associated with the CTFZ are described briefly in the next section. Some short alignments of cinder cones occur along the CTFZ, and the Los Azufres hydrothermal field is located along it 50-km east of Morelia.

Another east-west fault zone can be seen extending along the nineteenth parallel, beginning in an area west of Nevado de Toluca and extending beyond the eastern boundary of the study area (Figures 17 and 18). This fault zone, known as the Humboldt Line, continues the general east-west trend of the CTFZ farther to the east. Along most of its length it is much obscured by recent volcanics, consisting mostly of monogenetic cinder cones and flows. The volcanics are concentrated along an east-west zone that is colinear with the trace of the fault zone. The Sierra de Chichinautzin forms part of this line south of Mexico City. At several locations along this zone, east-west cinder cone alignments can be found either alone or in association with clearly visible fault scarps. Where this fault zone crosses older northwest-southeast trending faults, the large strato-volcanoes of the eastern MVB have erupted, including N. de Toluca and V. Popocatepetl, Cerro la Malinche, and Pico de Orizaba at the eastern end of the study area.

The E-W structural trend of the Chapala Rift can be traced much farther eastward along an aligned series of major normal fault scarps. These scarps generally trend E-W or ENE-WSW and have normal offsets of up to several hundred meters. The fault system that they compose will be referred to in this report as the 'Chapala-Tula Fault Zone'.

South and southeast of Lake Chapala, faults belonging to this trend cut Plio-Pleistocene cones. Most of the faults trend E-W and are high-angle normal faults that drop the block to the north (see Figure 15). These faults converge to the east in an area of complex faulting south of the Sierra Penjamo. This part of the fault zone forms the northern limit of the Michoacan Triangle. The faults in this area have a maximum displacement of 300 m, but most have less. They are mostly oriented within 15° of E-W, and the majority drop the block to the north. This area has a complex pattern of these normal faults that form tilted fault blocks of no consistent orientation.

Figure 20 shows the Pajacuaran fualt southeast of Lake Chapala. This fault forms part of the southern margin of the Chapala graben, the narrow central basin of the Chapala rift, which is also the westernmost end of the CTFZ. In the area shown the fault has a minimum vertical offset of about 550 m, with the floor of the graben downthrown just to the north of the fault. The fault has evidently undergone several episodes of movement, as shown by the prominent break in slope near the base of the main E-W trending scarp (see Figure 21). Several hanging valleys can be seen along the slope break. This sharp break shows that the most recent movement is probably no older than late Pleistocene in age. The rocks cut by the fault are part of a late Pliocene volcanic cone which is in the mature stages of erosion. The rich alluvium surrounding the cone is being extensively used for agriculture. This is a good example of a prominent fault associated with rifting.

Between the area described above and the City of Morelia, the faulting becomes more organized. This area west of Morelia is characterized by very large normal faults in an *en echelon* arrangement. These faults have the same N15° to N20° orientation as the Cuitzeo Fault Trend, and they form its southwestern extremity. Most of the fault scarps have numerous parallel scarplets arranged in a series of steps. This
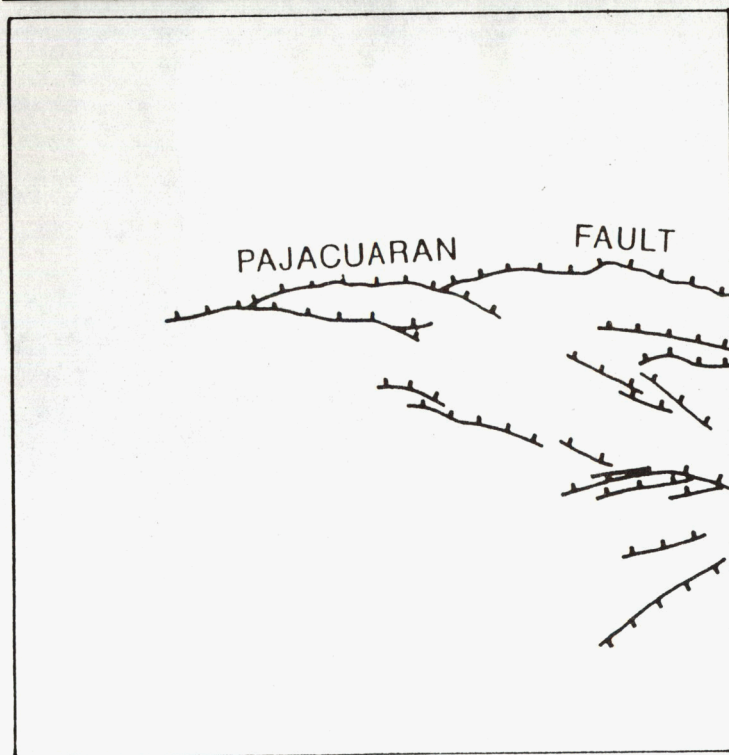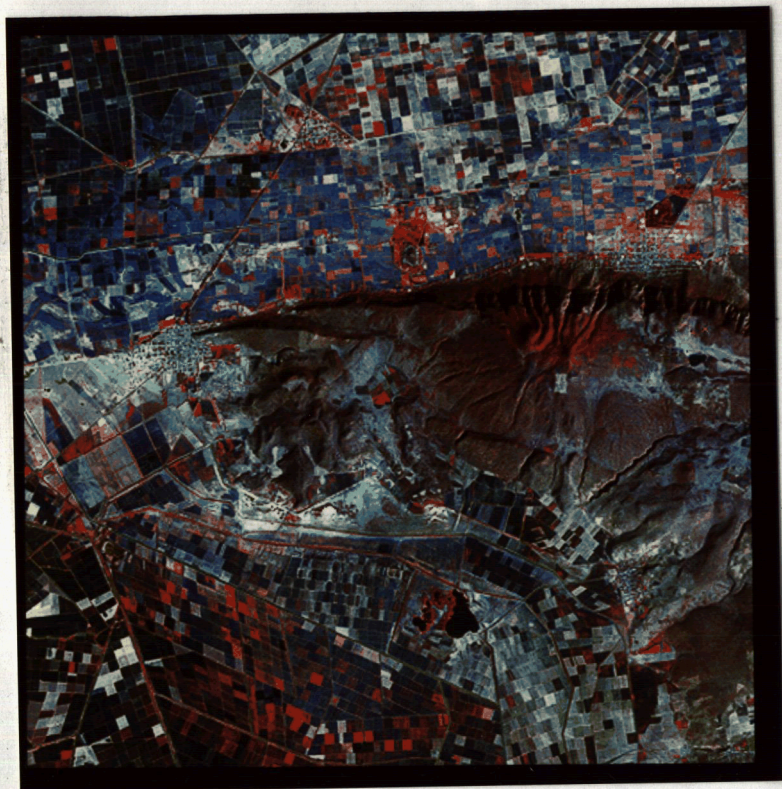
Figure 20: Image of the Pajacuaran fault southeast of Lake Chapala. The image is 500 pixels on a side, or roughly 15 km square. A line drawing of the interpretation of the image is also shown.

Figure 21: The scarp of the Pajacuaran fault as seen in the field from the west. A prominent notch in the scarp (in shadow just above trees in middle distance center) indicates recent offset. See text for discussion.

arrangement is seen best just to the south of Lake Cuitzeo. The faults generally drop the block to the north, forming a series of fault blocks, most of which are tilted to the SE.

Figure 22 is an area of right-stepping *en echelon* normal faults northwest of Morelia. These unnamed fualts cut Pliocene volcanics of the early MVB (Figure 23). Most drop the block to the north, with the result that most of the fault blocks in the area are tilted slightly to the south and southeast. Vertical offset on the faults in this area reaches 350 m. Although young, the faults have an eroded morphology that indicates that they are slightly older than the Pajacuaran fault. They probably belong to a Late Pliocene-Early Pleistocene transtensional phase of faulting in the area documented through extensive field studies by Pasquare *et al.* (1988). This deformation had a sinistral component that is clearly shown by the *en echelon* orientation of the faults. Although these faults appear to be inactive at present, faults to the northeast in the Cuitzeo Depression having the same ENE-WSW trend are among the youngest in the region. Two Holocene lava flows and a small late Pleistocene cone can be seen in the southeast quadrant of the image. These are both associated with the eastern Michoacan-Guanajuato Volcanic Field and its latest phase of volcanic activity.

The faults south of Morelia extend in a nearly continuous series of scarps that stretches all the way to the Valley of Mexico, 200 km to the east. Some of the largest fault scarps belonging to the Chapala-Tula Fault Zone are located in this stretch. Most of the scarps are oriented E-W, and like scarps associated with the trend farther west, they also drop the blocks to the north.

Figure 24 covers the central part of the Los Azufres caldera, located about 50 km east of Morelia along the east-west trace of the CTFZ. (Figure 11). Volcanic products associated with the caldera are Pleistocene rhyolites and dacites erupted upon Mio-Pliocene andesites (Ferriz and Mahood, 1986). As shown by the deep red colors in Plate 2c, the Sierra de Los Azufres is heavily forested. This vegetative cover, however, does not mask the prominent normal faults that cut the volcanics. These faults create an east-west trending pattern of small horsts and grabens, with the largest graben located in the very center of the caldera. Vertical offsets of 150 to 250 m are seen on these faults. The erosional morphology of the faults displays a broad spectrum, from youthful to very mature. This demonstrates that active faulting continued throughout the Pleistocene deposition of the volcanics. An active hydrothermal system exists within the caldera; and it is currently being used as a source of hydrothermal energy. Between Morelia and Los Azufres caldera are several strings of young cones and flows erupted along east-west trending fualts associated with the CTFZ. Similar alignments of volcanic eruptive centers occur east of the caldera. The faults and associated volcanic alignments in the area reveal a major zone of active, east-west trending deformation that corresponds to the CTFZ. The CTFZ in this area forms the southern margin of the Cuitzeo Depression. Farther to the south is the northern interior of the Guerrero Block, which is relatively undeformed recently.

Figure 25 shows the main scarp of the Pastores fault, located about 40 km southeast of the Amealco caldera. Maximum relief on the fault scarp is about 250 m (Figure 26). The dotted line in the figure is the Rio Lerma, flowing from southeast to northwest accross the fault. As the river crosses the fault it cuts a deep canyon in the southern, upthrown block and drops more than 40 m to the small basin north of the scarp. Locally, the river has changed its course several times, as demonstrated by several abandoned valleys that cut across the upthrown block and intersect with its crest. The upper surface of the block south of the fault is now tilted slightly to the south, so the flow direction in these blind valleys has reversed since the formation of the fault. These disturbances of the local fluvial system, combined with an eroded break in slope at the base of the scarp, indicate that faulting was active as recently as the Late Pleistocene and possibly the Holocene. Several older, more eroded faults can be seen cutting Pliocene volcanoes north of the Pastores fault. Only 15 km to the north is the seismically active Acambay fault (Astiz, 1986), which is not shown in Figure 4d. The Acambay fault is a major south-facing normal fault with maximum scarp
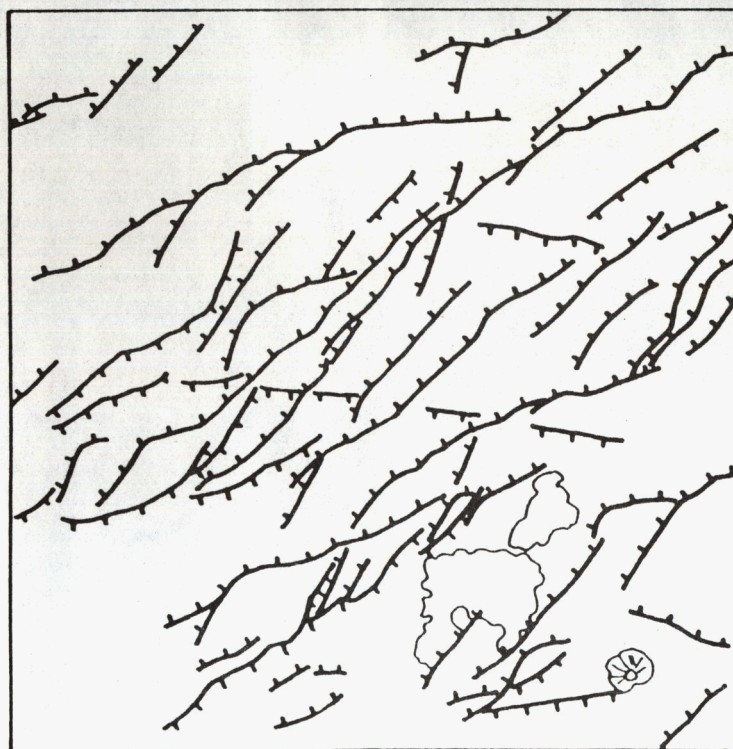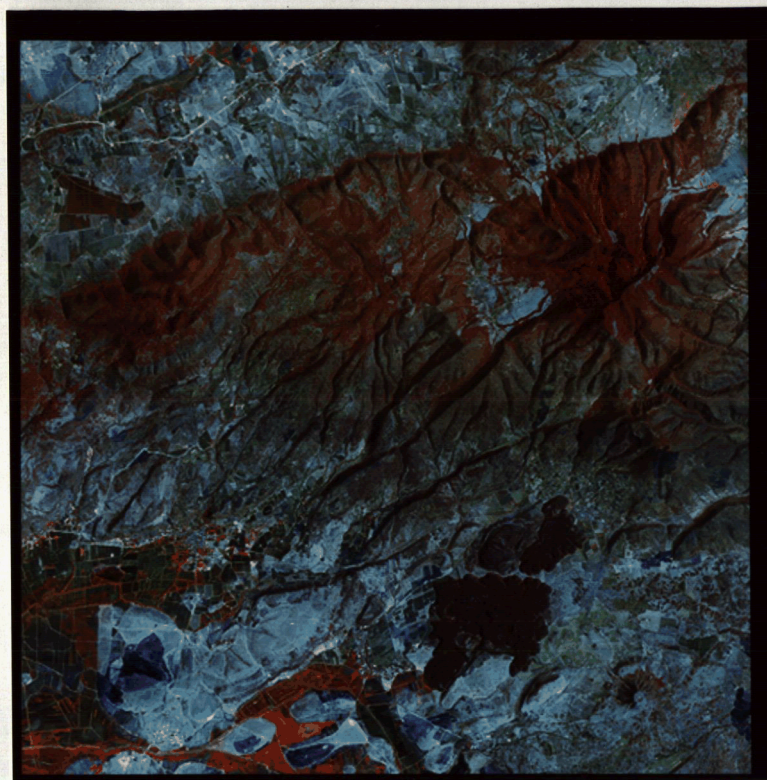
Figure 22: Image of an area of *en echelon* normal faults northwest of Morelia. A line drawing of the interpretation of the image is also shown. See text for explanation.

Figure 23: Photo of 120 m offset in volcanics northwest of Morelia. This is one of the faults illustrated in Figure 22. The view is to the east, showing that the northern block is downthrown.
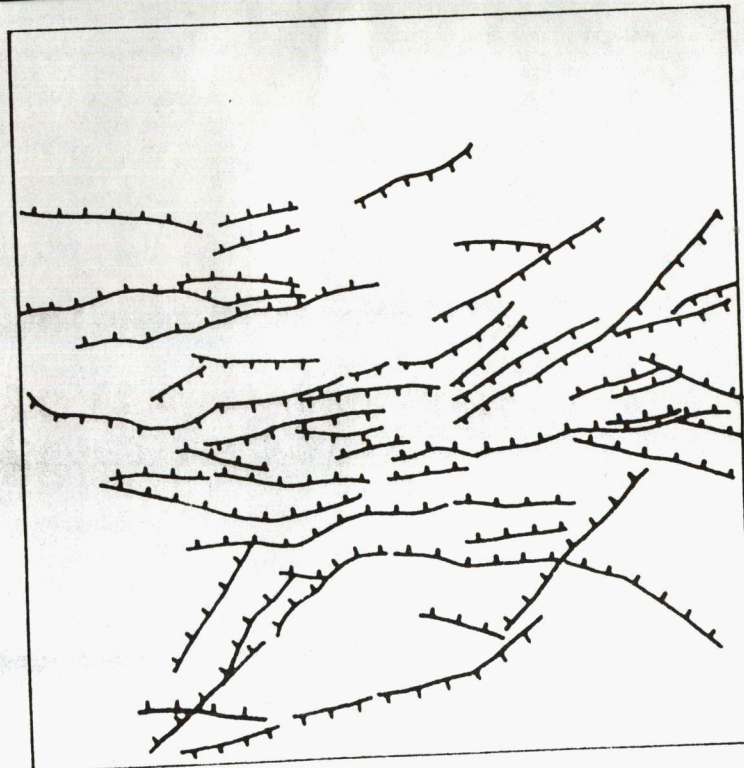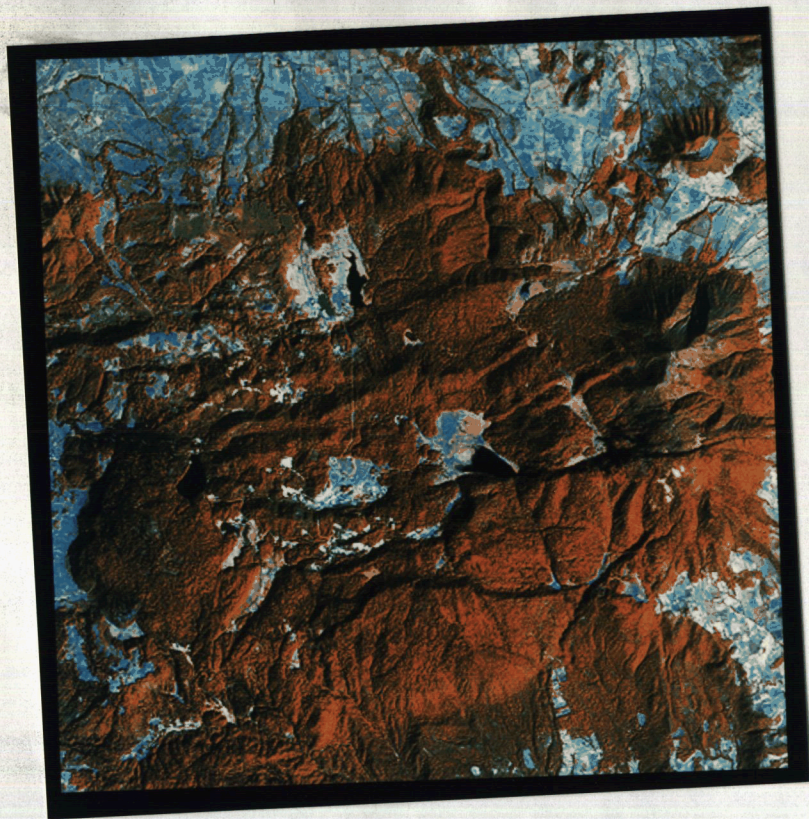
Figure 24: Image showing the area around the Los Azufres Caldera. The image is 500 pixels on a side or roughly 15 km across. A line drawing of the interpretation of the image is also shown. See text for explanation.

relief of over 350 m. Although the Acambay fault is currently active, it appears to have been reactivated only recently because of its very eroded morphology. It is so eroded, in fact, that it is not easily seen on the standard image products used in this study. On nighttime thermal IR (TM band 6) images of the area, however, the warmer, south-facing scarp of the Acambay fault is very prominent. The erosion of its scarp indicates that most of the vertical offset on the fault probably occurred in the Early Pleistocene or earlier. The two faults, Acambay and Pastores, together form an east-west trending graben that is aligned along the CTFZ.

The Chapala-Tula Fault Zone has few major Quaternary volcanics associated with it directly. Small alignments of cinder cones are seen on the images along the fault zone, and the Los Azufres hydrothermal field is also located along it 50 km east of Morelia. On the other hand, the Humboldt line is associated with the major strato-volcanoes in the Mexico City area, as well as the cinder cone fields south and southeast of Mexico City.

6.4   The Queretaro-Taxco Fracture System

The volcanics of the Michoacan-Guanajuato Volcanic Field (MGVF) are limited on the northeast by a series of NNW-SSE trending fractures termed the Queretaro-Taxco fracture system by Demant *et al.* (1976) (see Figure 18). This zone of faults and fractures stretches from north of Queretaro to the vicinity of Taxco, a distance of roughly 250 km. The zone of fractures varies in width from about 20 km to over 40 km.

The faults and fractures associated with the trend reach a maximum offset of about 200 m at Cerro Tres, 10 km southeast of Queretaro. They are best seen in this region and become much more difficult to detect farther to the southeast. The region around Queretaro is a maze of fault blocks because of the interference of faults belonging to the Cuitzeo Fault Trend and those of the Queretaro-Taxco fracture zone. Most of the blocks are 10 to 20 km in length and vary in width, averaging about 3 km. Most are tilted either to the NW or SE. The generally more eroded nature of the Queretaro-Taxco fracture zone mark it as an older feature, perhaps as old as Plio-Pleistocene. The fact that it cuts volcanics of Pliocene age indicates that the most recent deformation along the zone cannot be older than Pliocene. Two major volcanic edifices lie along the trend of the Queretaro-Taxco fracture system: the Amealco Caldera and the large volcano Nevado de Toluca.

Volcanics associated with the formation of the Amealco Caldera lie upon earlier lavas dated at 5 Ma (Ferriz and Mahood, 1986). Volcanism in the area has continued into the Quaternary, as shown by the eruption of a young cinder cone along the trace of a large fault that truncates and breaches the southern margin of the caldera (Ortega-Gutierrez, 1987, pers. comm.). The central stratovolcano of Nevado de Toluca was formed during the Pleistocene (Bloomfield and Valastro, 1974). It lies at the intersection of the Queretaro-Taxco fracture system and an E-W trending series of fault scarps (the western end of the Humboldt Line) which forms the southern end of the Valley of Toluca.
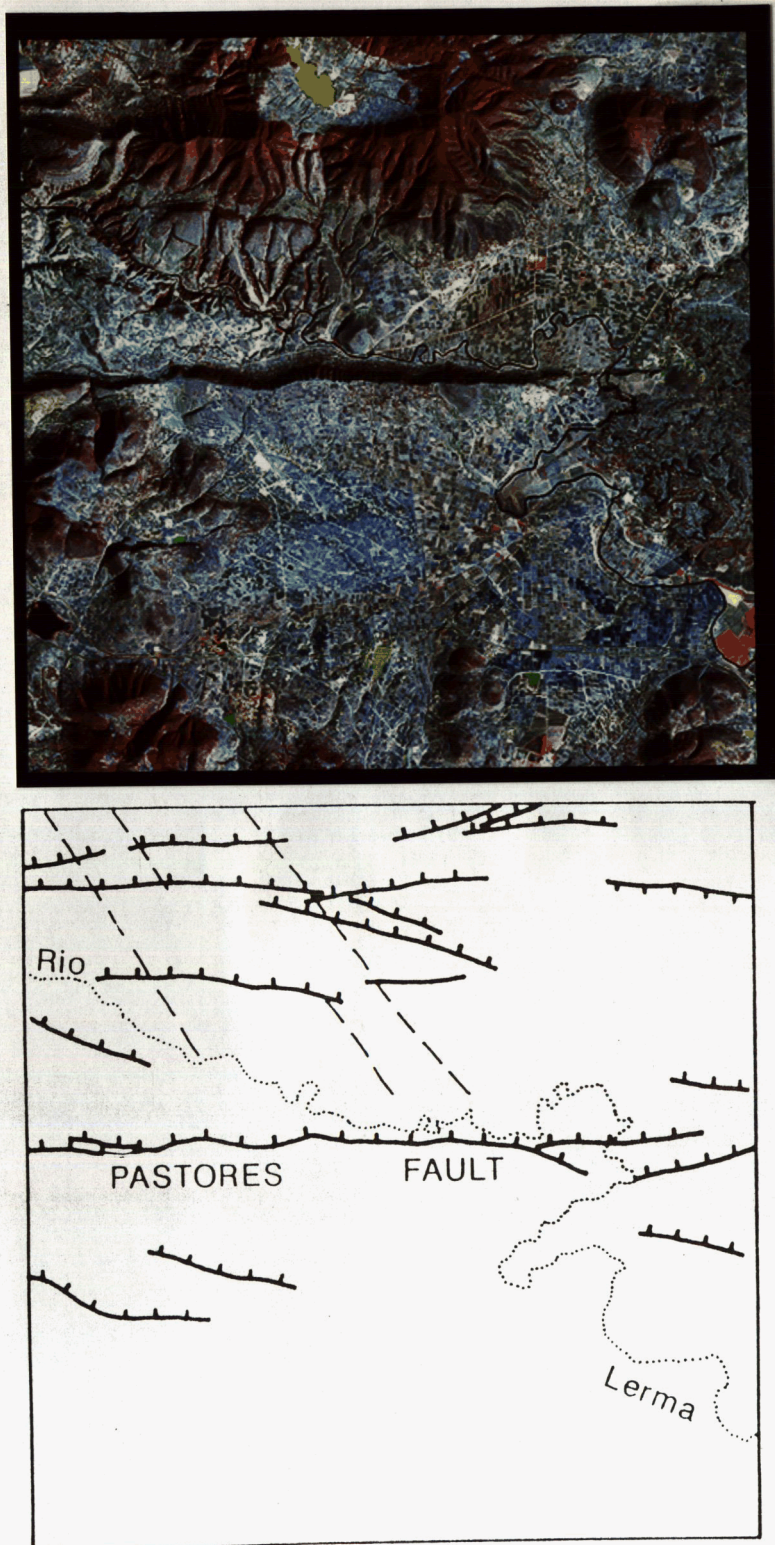
Figure 25: Image of the Pastores fault. The image is 500 pixels on a side or roughly 15 km across. A line drawing of the interpretation of the image is also shown. See text for explanation.

Figure 26: Photo of the Pastores fault as seen from the east. The basin north of the fault is the Acambay graben.

7 Shear: The Chapala-Oaxaca fault zone

The Chapala-Oaxaca fault zone (COFZ) is a major system of trench-parallel faults and fractures located about 180 to 200-km from the Acapulco trench (Fig. 18). It can be traced on the TM imagery for more than 700 km. At its western end southeast of Lake Chapala it is marked by the San Juanico Graben, a narrow Quaternary feature oriented obliquely to the trend of the fault zone. The orientation of this graben indicates sinistral motion along the COFZ as the graben developed. The COFZ continues to the southeast, passing through the southern portion of the Quaternary Michoacan-Guanajuato volcanic field (MGVF). The two youngest cones in the MGVF, Paricutin and Jorullo, lie along the COFZ. Southeast of Jorullo the COFZ is defined by a very prominent linear fault valley. This valley intersects the Balsas River about 40-km east of Presa de Infiernillo, where the main trace of the COFZ bends slightly to the east (see Fig. 18). In the vicinity of the bend faults can be seen cutting alluvium and colluvium of the Balsas River. East of about 101°W, the COFZ appears to be less active recently; and it is not so well defined. However, faults associated with the COFZ can be seen cutting Mesozoic and Tertiary rocks as far east as Oaxaca State.

7.1 The Western COFZ

The western portion of the COFZ appears to be an active sinistral wrench fault, although the COFZ as a whole has probably undergone multple phases of motion, both sinistral and dextral. This is suggested by evidence for several hundred kilometers of dextral offset during the Mesozoic and Early Tertiary along a NW-SE trend in the western part of the MVB (Gastil and Jensky, 1973). This trend is aligned with the COFZ to the southeast, and with the Pacific coast of Mexico to the northwest. Together they form a major trench-parallel tectonic lineament over 2000-km long. We call this the California-Oaxaca lineament or line (COL). Intermittent dextral motions probably dominated the activity along this zone until the mid-Tertiary. Along the portion occupied by the COFZ, sinistral motions probably dominated at its southeastern end during the Oligo-Miocene sinistral translation of the Chortis block (now in Central America) away from the Pacific coast of southern Mexico. Between 10 and 5 Ma, dextral motion prevailed again as Baja California prepared to separate from the Mexican mainland along the northwestern portion of the COL. Since this separation at around 5 Ma, the situation has become more complex. West of Guadalajara the Tepic-Chapala Rift continues to develop, separating the Jalisco crustal block from the rest of North America. The R-R-R triple junction south of Guadalajara divides the rifting from a renewed sinistral wrench fault (the western portion of the COFZ), which separates the Michoacan and Guerrero crustal blocks. In addition, a second major fault zone in the area, the Chapala-Tula fault zone, has developed, severing the Michoacan and Guerrero blocks from the North American plate.

Figure 27 shows the San Juanico Graben, a Quaternary down-faulted basin located at the western end of the COFZ. The normal faults at the margins of the graben cut Plio-Pleistocene andesites and small volcanoes. Fault blocks within the graben (A's in Figure 28) are tilted to the southwest on other high-angle faults. Faulting has continued in the area through the Late Pleistocene and probably the Holocene, as indicated by the break in slope near the base of the north wall of the graben (Figure 29), and scarps that cut alluvial fans at its base. The oblique orientation of this graben relative to the general trend of the COFZ points to sinistral motion on the latter as the graben developed. The graben is thus a good example of a small pull-apart feature developing along an active zone of shear.

Figure 30 shows a section of the COFZ southeast of Jorullo volcano. The fault zone in this area is composed of a number of individual faults that cross the area from northwest to southeast in a narrow zone less than 10 km wide. The light-colored area in the northwestern part of the image is mainly Plio-Quaternary clastics
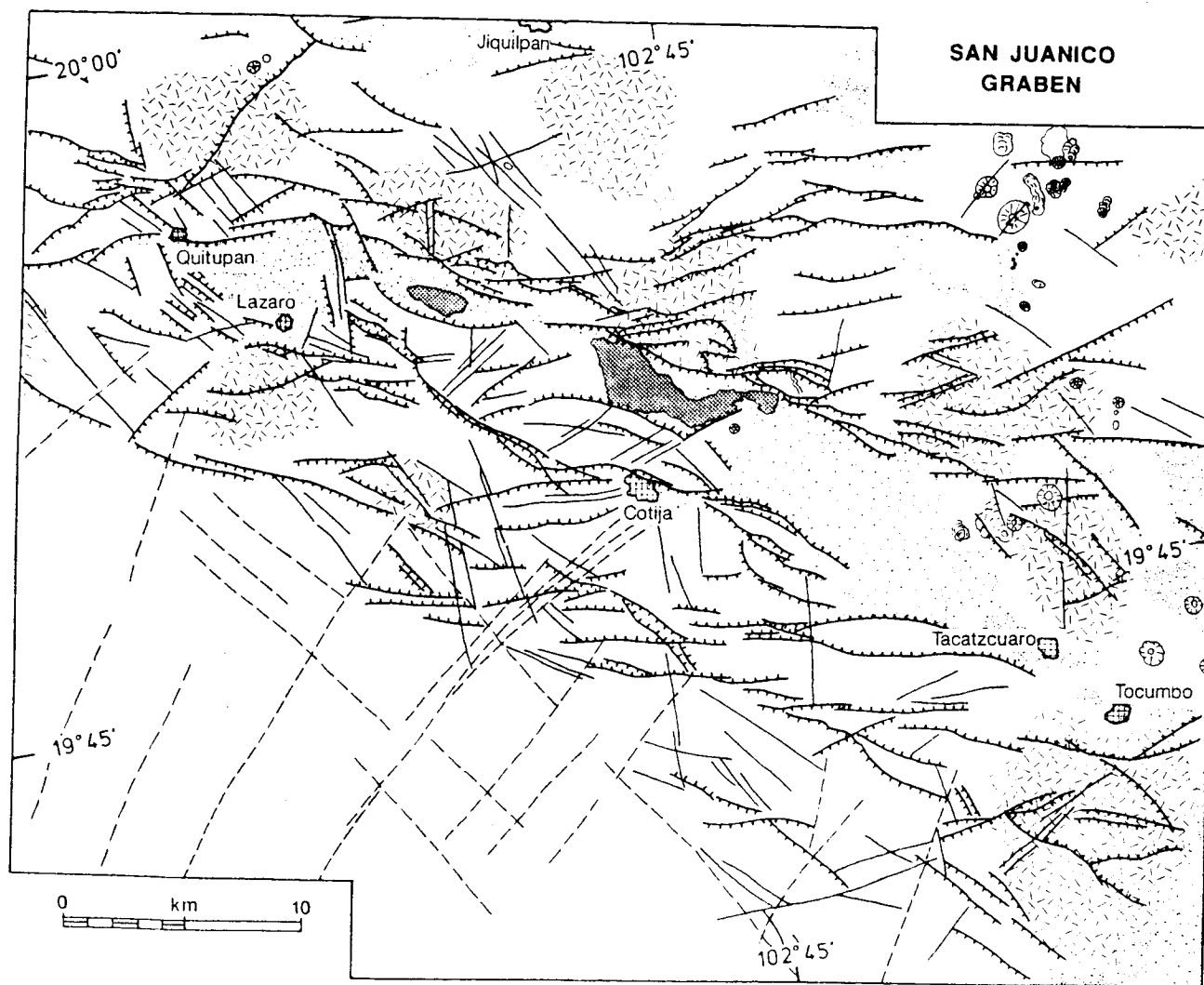
Figure 27: The San Juanico Graben. Stippled pattern shows basins where Quaternary alluvium has accumulated. Dash pattern corresponds to Plio-Pleistocene andesitic centers. Faults are shown with hatchures on downthrown side. Most Late Pleistocene and Holocene cinder cones and small lava flows are also shown. Faulting was interpreted from Landsat TM images.
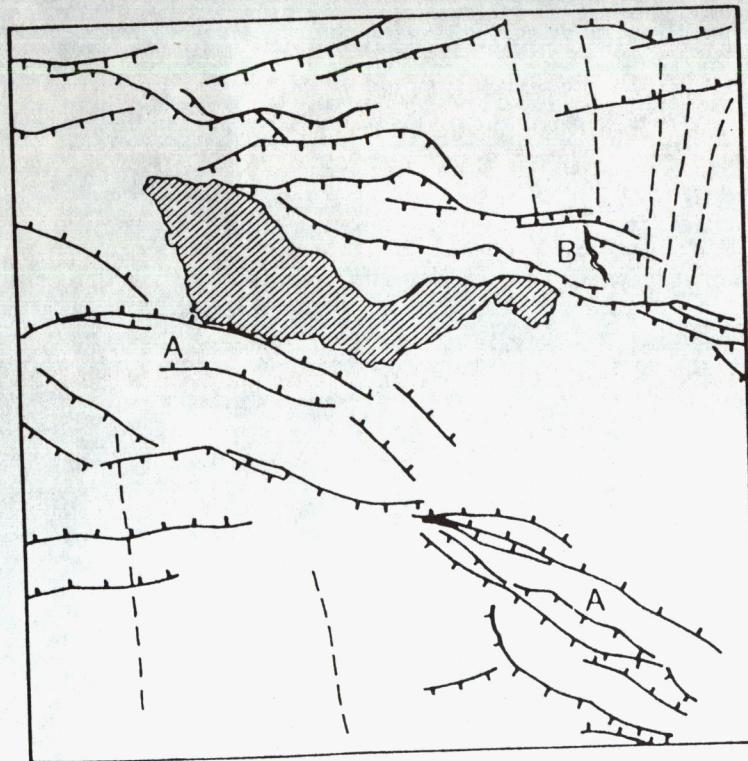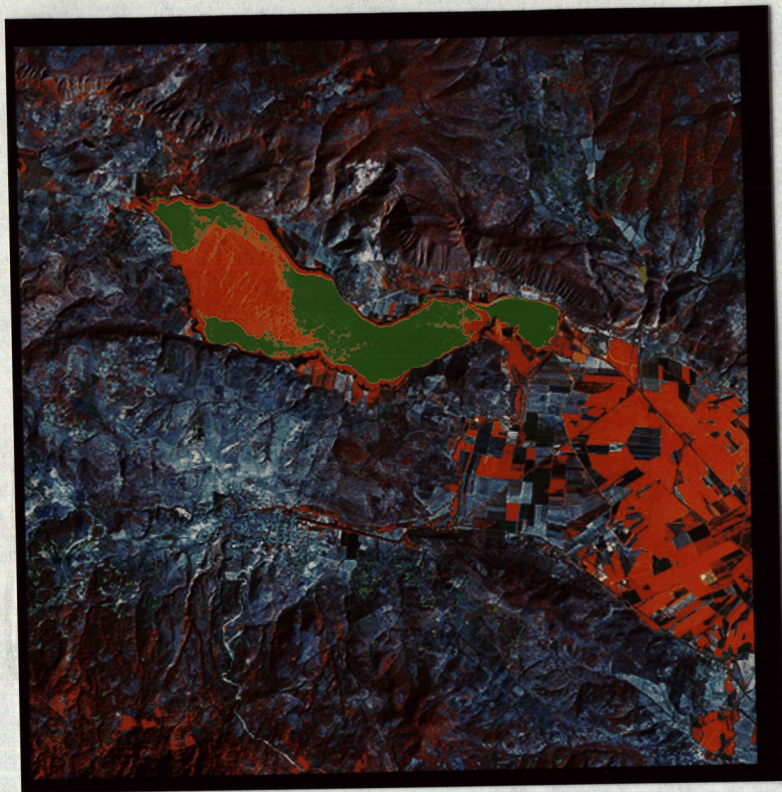
Figure 28: Image of a portion of the San Juanico Graben. The image is 500 pixels or roughly 15 km across. A line drawing of the interpretation is also shown. Compare with Figure 27 for location.

Figure 29: Photo of the central portion of the San Juanico Graben, looking northwest. The northern wall of the graben is on the right, and displays a sharp break in slope, indicating recent activity on the fault. Presa San Juanico is in the distance, center.

that fill a small basin that is colinear with the fault zone. The basin is bounded by faults associated with the COFZ and can be described best as a small pull-apart feature. Many of the faults show evidence on the images of recent left-lateral offsets. For instance, a large stream that flows from A to A' in the figure is offset left-laterally, with the now abandoned paleo-valley marked in black in the figure. The stream flows through an area of clastic ridges of probable Neogene age (stippled pattern between A and A'in the figure), and these are also offset (see Figure 4f and compare with Plate 2f). Just to the northwest at 'B' are somewhat older Tertiary clastics (also stippled) that are also offset left-laterally. The total lateral offset accross the fault zone here is at least 4 km. Most of this motion is of Quaternary age, as shown by its effect on fluvial features. The lava flow in the northwestern corner of the image is Mesa El Malpais, which is derived from a small unnamed cone just to the north. This cone and another close by (Buenavista) are the southeasternmost volcanics of the MGVF. The location of this recent volcanism in the area, including Jorullo and Cerro La Pilita 15 km to the northwest, seems to be influenced by the zone of crustal weakness represented by the recent faulting along the COFZ. The alkalic nature of Cerro La Pilita (Luhr and Carmichael, 1985) can be explained by the local tensional-transtensional regime associated with the small pull-apart feature along the COFZ.

7.2   The Eastern COFZ

Figure 31 shows the location of a sharp bend in the main trace of the COFZ. The fault enters the area from the northwest; and the point where the fault zone bends is located near 'A' in the figure. The main trace of the COFZ continues along a more easterly trend, past point 'B' in the figure, where it crosses the Balsas River. At the point where it crosses the river the fault cuts alluvium and colluvim in the valley. Several faults fan outward from the bend and stretch southeastward, but most do not continue for more than a few tens of kiometers. This fanning out of the fault zone may mark the eastern terminus of active faulting along the COFZ. The recent sinistral offsets seen to the northwest may be distributed between the faults fanning out from the bend, effectively absorbing the relative motion. Farther to the east, faults do not appear to have undergone movements in the Quaternary (see below). However, the fault zone also broadens east of the bend, reaching a width of 30 to 40 km. This implies that the faulting, if it were active, would be distributed over a much wider zone. Thus motion along any single fault within the zone may be much less than farther to the west. More work needs to be done with the images and in the field to investigate the possiblity of recent motions on the COFZ east of the bend.

Figure 32 shows a mountain located in the Balsas River basin east of Ciudad Altamirano. The Balsas River can be seen in the lower left. The mountain is composed of a succession of Tertiary red beds several hundred meters thick, composed mostly of coarse red sands and conglomerates, which belong to the Balsas formation. This sequence is capped by Miocene volcanics. Several minor unconformities can be seen on the image and in the field, prominently marked on the western and southern flanks of the mountain by more resistant conglomerate beds (fine lines in Figure 32). These unconformities show that tectonic disturbances were common in the area throughout the Lower and Middle Tertiary. This deformation may have been related to movement along the COFZ. This part of the COFZ is probably not currently active, but east-west and ESE-WNW faults of Miocene and probable Pliocene age can be seen dissecting the mountain. A right-lateral fault with about 3 km of horizontal offset cuts a vertical north-south dike of Oligocene age (Pantoja-Alor, 1988, pers. comm.) at 'A'. This shows that dextral as well as sinistral motions have occurred along the COFZ. This particular fault may have been related to dextral offset of the entire Pacific margin of western Mexico during the Late Miocene, coincident with the earliest phase of activity along the proto-Gulf of California. Other faults, particularly those at the southern end of the mountain, have significant vertical, as well as horizontal, offsets. This is common in zones of wrench faulting, where small blocks may be rotated and tilted depending on the relative orientations of faults on their margins and the
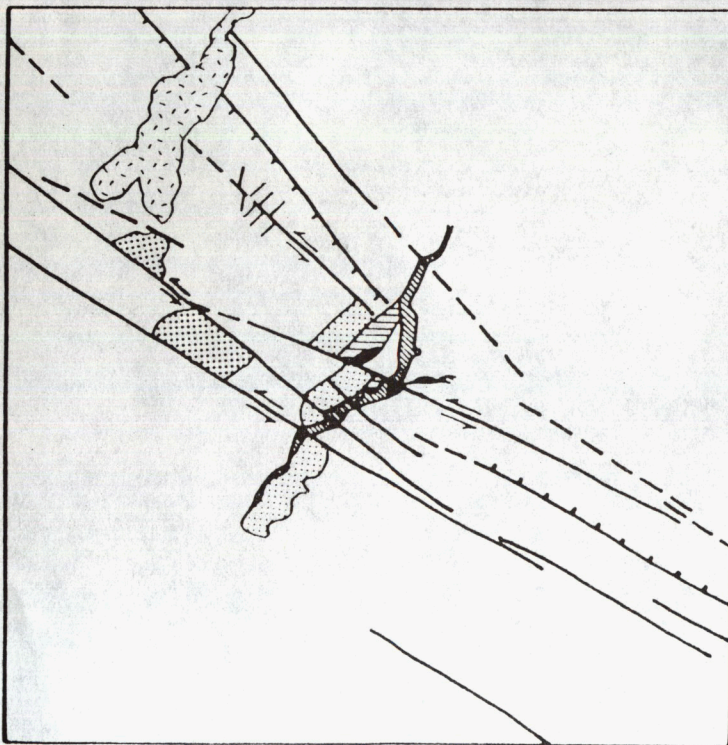
Figure 30: Image of a section of the COFZ southeast of Jorullo volcano. The image is 500 pixels on a side or roughly 15 km across. A line drawing of the interpretation of the image is also shown. See text for explanation.
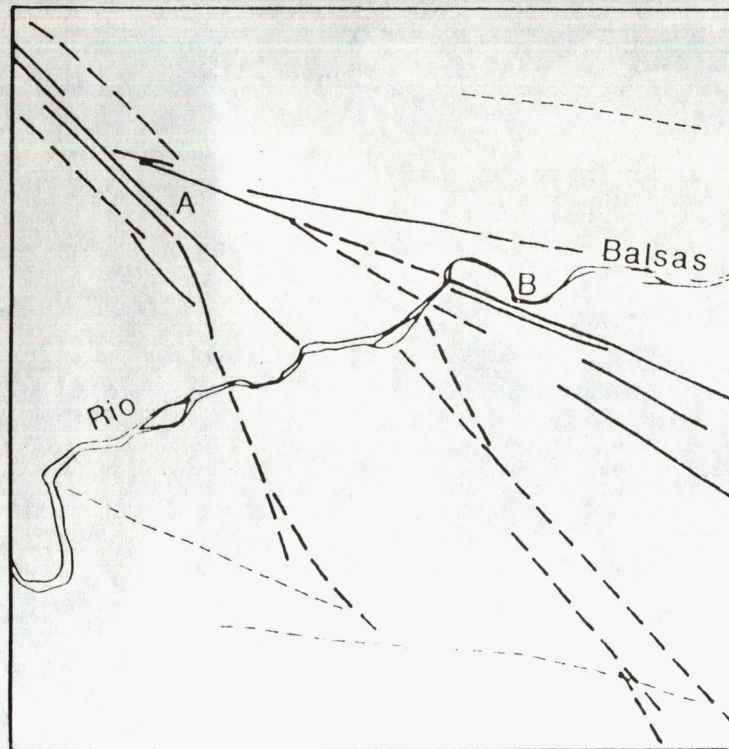
Figure 31: Image showing the region around a bend in the COFZ. The image is 500 pixels on a side or roughly 15 km across. A line drawing of the interpretation of the image is also shown. See text for explanation.
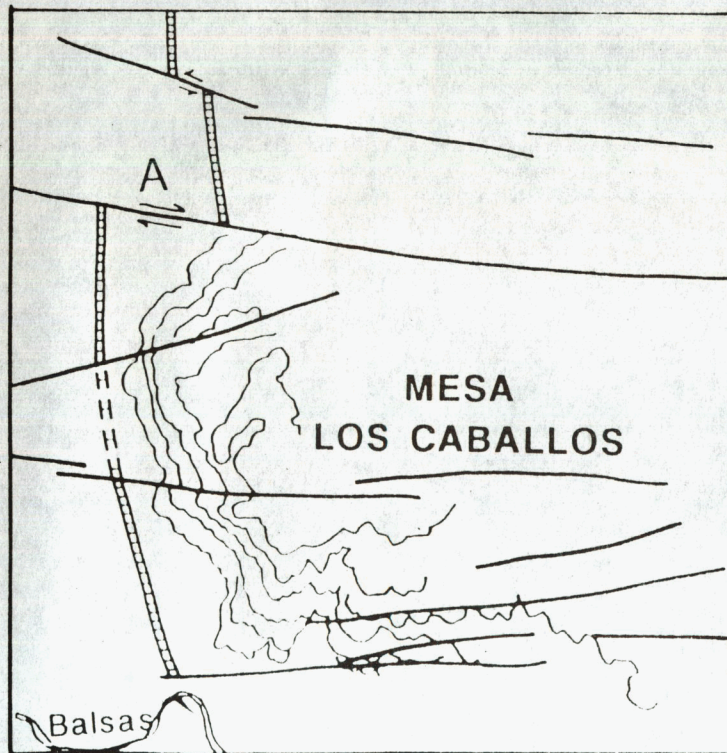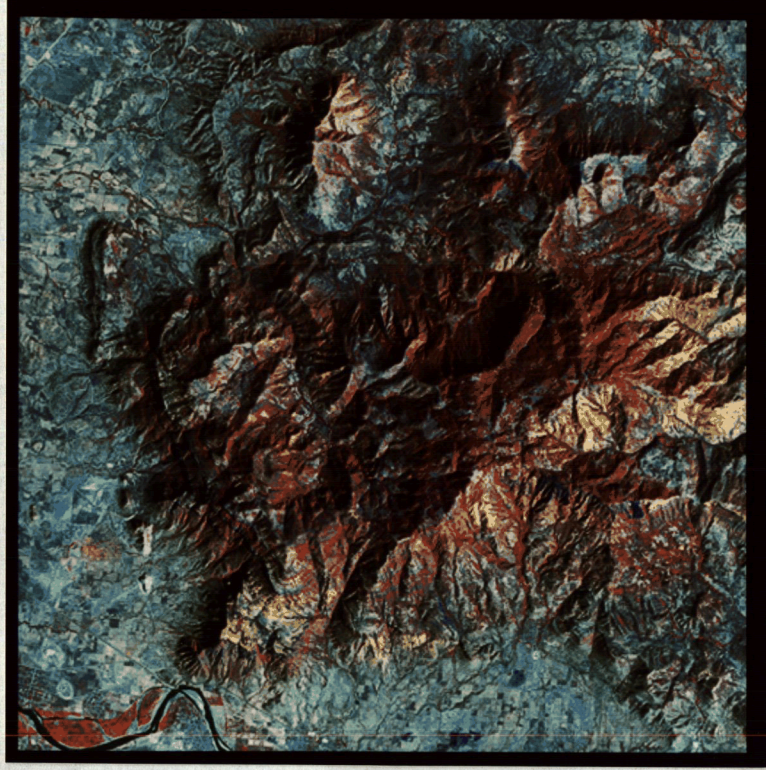
general trend of the wrench fault.

Figure 32: Image showing a large exposure of the Paleogene Balsas formation in the Balsas river basin. The image is 500 pixels on a side or roughly 15 km across. A line drawing of the interpretation of the image is also shown. See text for explanation.

8 Uplift/Extension: The Sierra Penjamo

The Sierra Penjamo is a small range located north of the city of Penjamo. It lies at the eastern end of a region of highlands on the boundary between the Leon-Guanajuato Plateau to the north (average elevation above sea level: 1800-2000 m) and a broad alluvial plain that forms part of the Rio Lerma river basin to the south and east (average elevation: 1800 m). The highland area extends about 70 km westward, where Mesa Negra forms its western extremity, and is approximately 30 km wide. For the purposes of this report, the name 'Sierra Penjamo' will be stretched to refer to this entire area of highlands.

Figure 33 shows the topography of the region surrounding the Sierra Penjamo and Figure 34 shows the faulting there as interpreted from the TM imagery. The Sierra Penjamo is divided into eastern and western halves by a north-south trending graben. The eastern half has a higher average elevation, much of it being above 2300 m; the elevation of the western half averages about 2000 m. The graben that divides the two halves is probably related to similar features further north that cut the Leon-Guanajuato Plateau, forming a southward extension of the Basin and Range Province (Pasquare et al., 1987). This graben, here called the Penjamillo Graben after a town near its southern end, is a prominent feature that both cuts and is cut by other structures in the region, indicating a complex history of motion on the faults that define it. These marginal faults have up to 200 m of vertical offset where they can be seen cutting volcanics of probable Pliocene age.

Previous work on the Sierra Penjamo is nearly non-existent, and few specific references to the area could be found in the literature. Pasquare et al. (1987) classify it as part of a larger area of "dissected structural surfaces", characterized by eroded volcanic sequences of the SMO (Sierra Madre Occidental). The TM images reveal the Sierra Penjamo to be composed of bedded volcanic deposits that appear to be mostly flat-lying or only slightly tilted by faulting. The 1:1 million scale geologic map of Mexico simply labels the area as Tertiary basic and acidic igneous extrusives. However, Nixon et al. (1987, Figure 2) label the area as "Upper Miocene and Plio-Quaternary sequences", implying that they correlate with post SMO volcanic activity or perhaps part of the earliest stage of MVB development. The western portion of the Sierra Penjamo is a plateau composed of Pliocene ignimbrites and Late Miocene basaltic lavas, the latter correlating with similar rocks further west near Tepic and in the canyon of the Rio Grande de Santiago (Nixon et al., 1987, Figure 5). Drainage patterns reveal the presence of several eroded remnants of minor volcanic centers located at the eastern end of the highlands in the Sierra Penjamo proper. Their deeply eroded character suggests that they may be correlatable with the Mio-Pliocene volcanics to the west. Younger volcanic deposits are notably absent from the area, the closest being several large shield volcanoes located within the alluvial plain to the south. These more recent volcanics form the northernmost part of the Michoacan-Guanajuato Volcanic Field, and are of Plio-Quaternary age (a basaltic flow from Cerro Grande, near La Piedad, was dated by Nixon et al. (1987) to 1.60 ± 0.10 Ma). One of these volcanoes south of the city of Penjamo is deeply cut in a spectacular fashion by a very large normal fault; the offset on this fault is so great that the down-thrown (south) side nearly disappears beneath alluvium, corresponding to over 400 m of vertical throw, as determined from topographic maps.

Faulting in the Sierra Penjamo forms a distinctive pattern that correlates remarkably well with patterns created using clay models. Clay experiments conducted by Withjack and Scheiner (1982) show a characteristic fault pattern associated with various types of doming. Figure 35 shows their model of elliptical doming combined with simultaneous extension (extension rate is 1.5 times uplift rate) compared to the faulting in the Sierra Penjamo. This pattern is similar to that of the Sierra Penjamo in several important aspects:

- a zone of concentrated normal faulting within the boundaries of the uplift, striking parallel to the
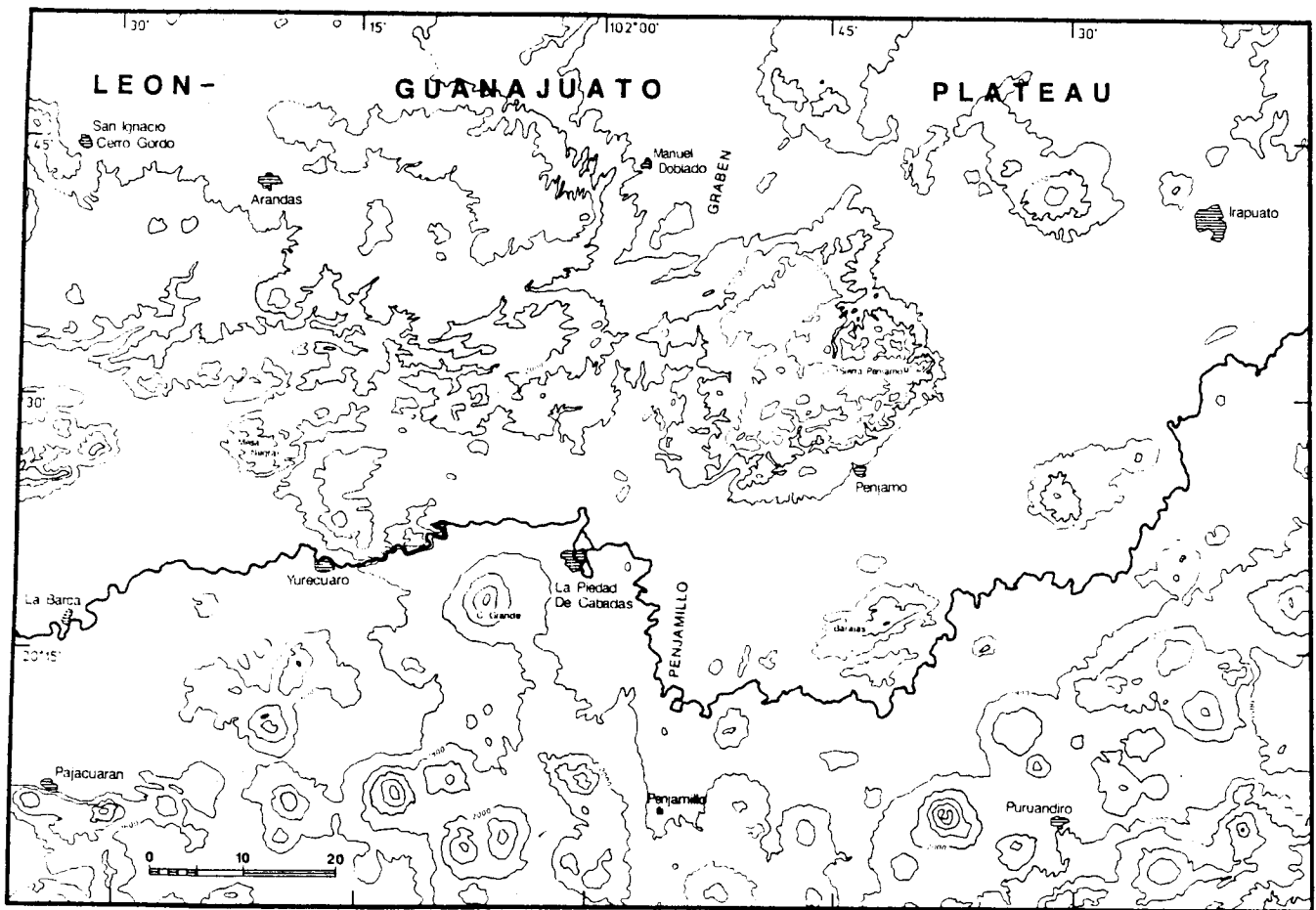
Figure 33: Topography of the region surrounding the Sierra Penjamo. The elevated nature of the Sierra compared to the surrounding Rio Llerma Basin is clearly apparent.
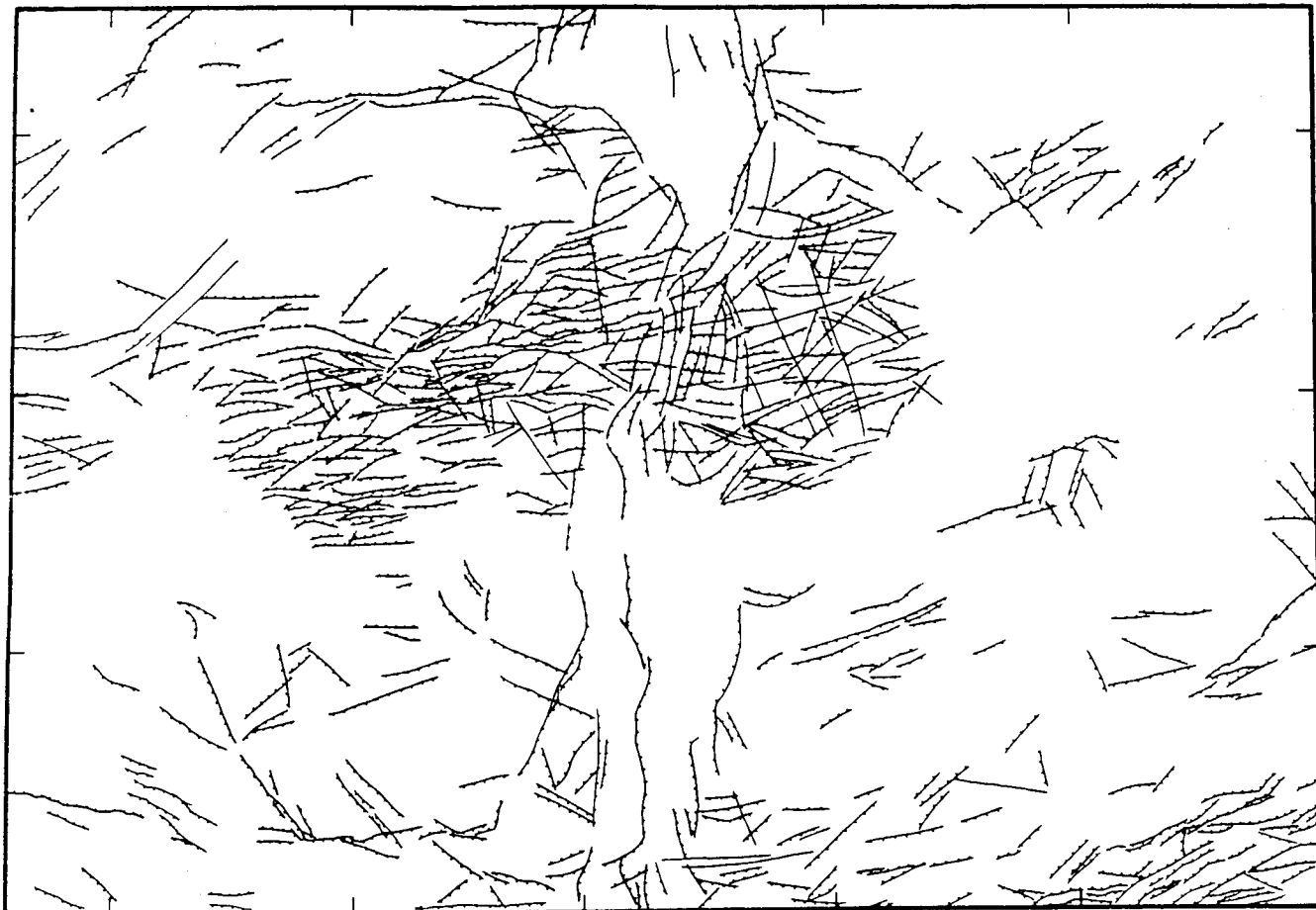
Figure 34: Fault scarps mapped in the region surrounding the Sierra Penjamo. This pattern is very similar to that derived in a clay model of doming combined with uplift by Withjack and Scheiner (1982) (Figure 35). P, Penjamo; MN, Mesa Negra; LP, La Piedad; CG, Cerro Grande; A, eroded volcanic centers; B, large cone cut by fault; *, shield volcanoes. Scale bar is 20 km long.
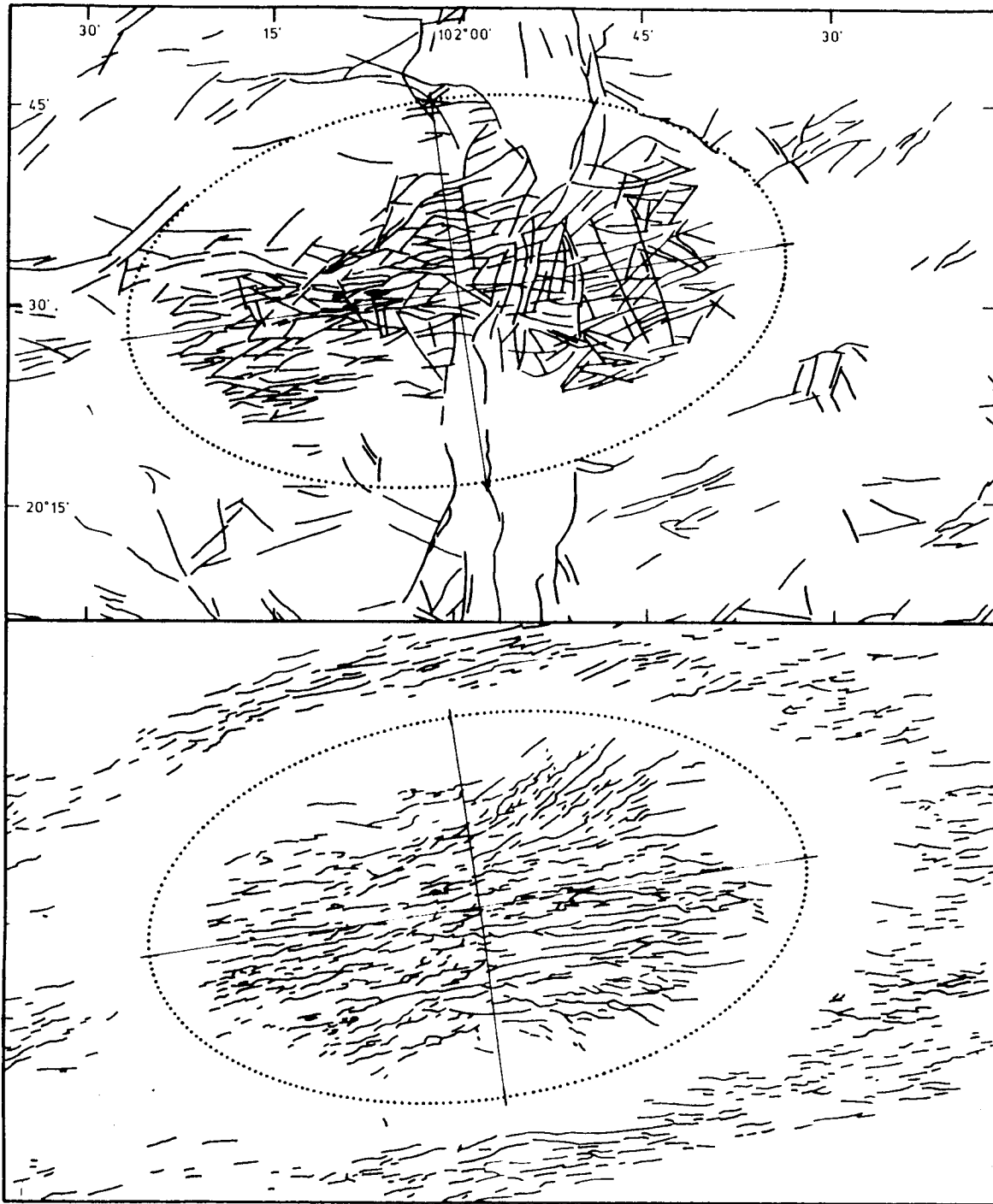
Figure 35: Comparison between modelled deformation during uplift and extension (from Withjack and Scheiner, 1982) with that observed on the TM images of the Sierra Penjamo.

long axis of the dome and splaying outward near its margins;

- a halo of non-deformation at the surface around the periphery of the dome;

- outside of the area of doming, normal faults indicate regional extension.

The above similarities, combined with the elevated topography of the area, lead us to conclude that the Sierra Penjamo has undergone a significant amount of uplift during a period of regional extensional tectonism. The faults cut both Late Miocene and Pliocene deposits, which indicates that uplift began no earlier than the Late Pliocene, about 3 m.y. ago. Geomorphologically, the faults in the area range in appearance from very eroded to very fresh. Thus faulting, and therefore the uplift that caused it, has probably been reactivated several times during the Plio-Quaternary. In fact, this uplift may be continuing today. We believe that the most likely explanation for this repeated uplift is the shallow intrusion of a large magma body, perhaps accomplished in several pulses. This corresponds to stage 1 of the resurgent cauldron cycle outlined by Smith and Bailey (1968), in which intrusion of a silicic magma chamber near the surface is accompanied by swelling and uplift above it. A number of young caldera complexes are found in the northern part of the MVB behind the active andesitic arc (Ferriz and Mahood, 1986), and the Sierra Penjamo is located in a similar position relative to the arc. In one of these caldera complexes, the Sierra Primavera, Mahood (1980) noted a period of uplift prior to caldera formation that may be similar to that observed in the Sierra Penjamo. These similarities support the additional conclusion that the Sierra Penjamo may mark the location of a caldera forming episode sometime in the indeterminant future. The natural disaster that such activity would produce and its accompanying loss of human life are emphasized here, and provide ample incentive for more detailed studies in the area.

9 Inherited Zones of Weakness

Many authors have suggested that lateral crustal movements along major shear zones occurred during the Mesozoic and Early Tertiary tectonic development of Mexico. Urrutia-Fucugauchi (1984) briefly reviewed many of these papers. He relates these movements to plate reorganizations that took place within the Pacific; in addition, rapid motions of the plates in the Pacific, combined with a major change in the direction of convergence with the North American Plate about 40 Ma (from northward to northeastward), may have been the driving force behind the lateral movements in central Mexico. Lower Tertiary paleomagnetic poles from Mexico are rotated counterclockwise relative to the expected directions derived from the rest of North America (Urrutia-Fucugauchi, 1984). This may be caused by rotation of crustal blocks adjacent to large E-W or NW-SE trending left-lateral faults. This interpretation is consistent with recent models of the Mesozoic and Cenozoic development of the southern edge of the North American Plate (such as Pindell and Dewey, 1982). Although such models may be in need of slight revisions, there is an emerging consensus that large-scale motions on zones of sinistral shear in Mexico are a necessity for the reconstruction of Pangea and its subsequent break-up in the Mesozoic.

Figure 36 shows the probable location of two zones of earlier deformation in central Mexico that have been reactivated in the Plio-Quaternary. They follow two major linear zones of neotectonic deformation which have been recognized and mapped using the TM data. This type of reactivation has been documented for portions of the East African Rift (Mohr, 1974).

Trend A-A' follows the trace of the Tepic-Chapala Rift and continues to the southeast along the Chapala-Oaxaca fault zone. Although these segments are aligned and trend N130° to N140°, they display markedly different neotectonic activity. They are separated by the triple junction south of Guadalajara, which may explain their different styles of deformation. Also, because of their colinearity despite this difference in style, they constitute an excellent example of an older zone of weakness that has been recently reactivated. This trend, which is over 900 km in length, has not been described previously in its entirety. Based on examination of large scale images, the fault zone may continue to the SE, where it becomes parallel to the Pacific coast north of Acapulco.

The west coast of mainland Mexico along the Gulf of California continues the line of trend A-A' to the NW; and rifting that led to the development of the gulf may have been localized by this zone of weakness. Gastil and Jensky (1973) place a large fault zone in western Mexico that coincides with A-A'. Their evidence supporting the existence of this fault zone includes offset Mesozoic batholithic and Mexican mineral (silver) belts. Right-lateral faulting along this zone began near the end of the Mesozoic, with additional episodes of activity during the Oligo-Miocene. The latest phase of right-lateral activity in this area began with the opening of the "proto-Gulf of California" about 10 Ma (Gastil et al., 1979), and lasted until about 5 Ma, when Baja California was accreted to the Pacific plate and true oceanic crust began to develop within the gulf. During that 5 million year interval the crustal block southwest of trend A-A' (now the Jalisco and Michoacan blocks) probably moved to the NW along with Baja California, causing much of the observed right-lateral offset. It is possible that over 430 km of total dextral offset has occurred in western Mexico since the Mesozoic (Gastil and Jensky, 1973); but offset along trend A-A' is probably less.

Based on the TM image interpretations, there seems to have been a major reorganization of the stress field within the crust of west-central Mexico after about 5 Ma. Trend A-A', which had been a major right-lateral fault zone, was reactivated as a rift (the Tepic-Chapala Rift) to the NW of a newly forming triple junction. Southeast of the triple junction, trend A-A' was also reactivated, becoming a left-lateral fault zone (the San Chapala-Oaxaca fault zone) separating the Michoacan and Guerrero crustal blocks.
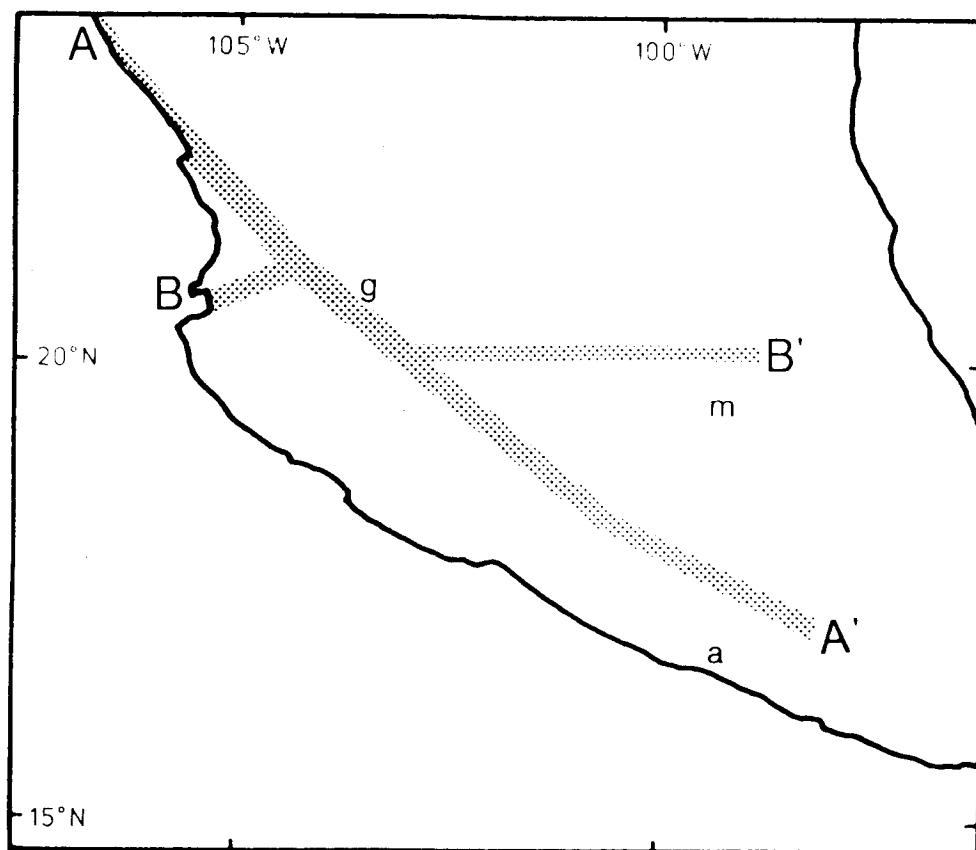
Figure 36: Sketch showing approximate positions of two possible zones along which Mz/Cz motions of blocks in southern Mexico may have been accommodated. '?' marks the location of a prominent branch in the Tepic-Chapala Rift, the Rio Ameca Graben, which may mark the westward extension of B-B'. This would require about 140 km of dextral offset along trend A-A'. Trend A-A' has been recently reactivated, as a rift from A to B, and in a sinistral sense from B to A'. B-B' has also been reactivated, probably as a zone of sinistral transtension. G, Guadalajara; M, Mexico City.

In the vicinity of the triple junction trend B-B′ is truncated by A-A′, indicating that B-B′ is probably an older feature; this may mean that it follows the trace of an older fault. B-B′ may be exposed west of trend A-A′ as the Rio Ameca Graben, which forms a major branch of the Tepic-Chapala Rift. If true, this implies right-lateral offset on A-A′ of at least 140 km.

Trend B-B′ stretches eastward from the vicinity of the triple junction to an area north of Mexico City, a distance of over 420 km. It coincides with the Chapala-Tula fault zone described in section 10.1. It parallels the main axis of the MVB and may exert a strong influence on the orientation of the volcanic belt relative to the trench, providing a convenient conduit by which rising magmas generated by the subduction process can reach the surface. Many workers have suggested that a large fault in this area having this general E-W trend was active in the Mesozoic and Early Tertiary (Urrutia-Fucugauchi, 1984), based primarily on geometrical considerations from plate tectonic reconstructions. Until this study, such indirect evidence had been the only indication that such a fault existed in the area. The extensive linear zone of deformation that B-B′ represents is new and compelling evidence for the existence of a zone of weakness in the crust. So the study of neotectonic deformation in the region can potentially provide an effective window through the volcanic cover, exposing otherwise hidden features within the underlying crust. At this time it is not possible, however, to better constrain the total offset on this feature, which may amount to several hundred kilometers.

10 Relationship of Volcanism to Tectonics

10.1 MVB: General

The results of this study firmly establish a link between deformation in the overriding plate (expressed as neotectonic activity) and the distribution and character of volcanism in the MVB. Volcanism appears to be controlled by tectonics at all scales, from local to regional. This is a significant contribution because it indicates that the oblique orientation of the MVB relative to its trench is not *exclusively* due to variations in subduction geometry and velocity (unless the location of deformation in the overriding plate is controlled in such a way, which seems unlikely).

On a regional scale, the spatial relationship between volcanism and neotectonic activity is clear. Throughout the MVB, volcanism appears to have proceeded in tandem with tectonism. Observations using the TM data show that the tectonic deformation is organized in a coherent manner, forming fault zones that traverse nearly the entire region. The location and orientation of this zone of faulting coincides with those of the volcanic belt. This indicates that the deformation within the crust of the overriding slab plays a significant part in controlling the location and orientation of the volcanic belt relative to the Middle American Trench. In addition, variations in the geometry of subduction along the trench may not be as important as previously suggested. The ultimate control on the location of the Plio-Quaternary volcanism and tectonism within the MVB may be large zones of crustal weakness formed during major Mesozoic and Cenozoic tectonic events. These zones have since been reactivated and are now expressed in the organized zones of faulting that are observed throughout the study area.

10.2 Medium Scale

On the medium scale, between local and regional, two good examples of the relationship between volcanism and tectonics are immediately apparent. The first is the Michoacan Triangle, where the style of volcanism is very different from that in other parts of the MVB. Whereas the volcanic front is normally composed of large central volcanoes, in the Michoacan Triangle it is composed of thousands of cinder cones, which together have erupted at least 9300 km^3 of material (Connor, 1984). This is an order of magnitude greater than volumes erupted from the major central volcanoes of the MVB. The contrast in volcanic style can be explained by the position of the Michoacan Triangle, which is situated in a notch between the North American plate and the Michoacan and Guerrero crustal blocks. This zone of distributed divergence between the surrounding blocks appears to have localized the eruptions of the volcanics, and also influenced the style of the eruptions.

10.2.1 The Michoacan Triangle

Faulting in northern Michoacan State southeast of Lake Chapala is largely confined within a roughly triangular area (Figure 37) bounded on its sides by major fracture zones. Its northern boundary is formed by a prominent E-W alignment of normal fault scarps that extend from Lake Chapala eastward. On the southwest the area is defined by a major system of narrow grabens and fractures (the San Juanico-Buenavista Fault Zone of Johnson (1987), corresponding to the northwestern portion of the Chapala-Oaxaca fault zone), which forms the northeastern edge of the Michoacan Block. Large eroded fault scarps trending NNE-SSW flank the area on its eastern side and form the northwestern edge of the Guerrero Block. Faulting in the area is not completely confined within the triangle defined by these boundaries, particularly

on the southwest; the actual triangle can be defined as the region of extension situated between the North American Plate on its northern side, and the smaller crustal blocks of Michoacan and Guerrero on its southwest and east, respectively. This area is in a state of extension, as shown by the large concentration of normal faults within it. For the purposes of this report, this triangular region will be referred to as the 'Michoacan Triangle'.

Little is known of the basement underlying the volcanics in the Michoacan Triangle. The area is certain to share Pre-Pliocene elements of its geology with areas to the east and west, within the Guerrero and Michoacan crustal blocks.

The Michoacan-Guanajuato Volcanic Field contains nearly 1900 volcanoes, covering an area of about 35,000 km^2, and as such it probably represents the largest cinder cone field on earth (Connor, 1984). Previous work in the area has focused almost exclusively on the volcanics (Williams, 1950; Settle, 1979; Connor, 1984; Hasenaka and Carmichael, 1985a,b; Luhr and Carmichael, 1985); the tectonics of the area have not been studied in detail. This is a unique part of the MVB containing primarily small cinder and lava cones. This form of volcanism contrasts sharply with the rest of the MVB, which is primarily composed of large composite volcanoes (Hasenaka and Carmichael, 1985b). Most of the cones in the area have erupted in the last 3 m.y. (Murphy and Carmichael, 1984). A minimum estimate of the total volume of erupted magma in the field is 9300 km^3 (Connor, 1984). This figure is more than an order of magnitude larger than volumes erupted from large composite volcanoes of the MVB, such as the Colima Volcanoes. Hasenaka and Carmichael (1985a) studied the ages of cinder cones in the field and concluded that all 71 cones younger than 40,000 years are located in the southern part of the field. This area of youngest volcanism in the region is situated within the boundaries of the Michoacan Triangle. Hasenaka and Carmichael (1985b) have recently catalogued the locations and character of over 1,000 of these volcanic centers, which are mostly young cinder or lava cones. The majority of the eruptive vents they catalogued are located within the Michoacan Triangle as defined here, about 250 km from the MAT. Connor (1984) also notes that the volcanoes are concentrated in the southern part of the Michoacan-Guanajuato Volcanic Field.

The faults in the Michoacan Triangle lack a clearly dominant orientation, perhaps indicative of a greater degree of crustal disruption than is expressed elsewhere in the MVB. This conclusion is supported by the absence of large volcanoes in the area. Instead, volcanic activity is characterized by the eruption of hundreds of smaller volcanic centers, which form the densest part of the Michoacan-Guanajuato Volcanic Field (MGVF). As is common further to the west in the Tepic-Chapala Rift some of the cones within the MGVF form short linear segments and appear to be controlled by small fissures or faults; but in general no single fault system controls the majority of the cones. Instead the distribution of cones and surface faulting illustrates a more complex, diffuse pattern of basement fracturing. For this reason it is difficult to determine the orientation of maximum extension within the Triangle.

Although faulting within the Michoacan Triangle has no overall trend, there is evidence for some organization in the pattern. Alignments of fault segments indicate the presence of two more pervasive faults or fault zones in the basement that traverse the triangle in a NE-SW direction. These two fault zones are labeled A and B in Figure 37, and together with the northern and eastern fault boundaries of the Michoacan Triangle, they form a somewhat curvilinear fan emanating from the northeastern corner of the Triangle south of the city of Morelia (see summary diagram, Figure 18). Connor (1984) also noticed a N30-40E trend in the concentration of small volcanoes, which roughly parallels the trend of parts of faults A and B above. A N50-60W trend in the distribution of larger volcanoes (Connor, 1984) is parallel to the northwestern portion of the Chapala-Oaxaca fault zone (the San Juanico-Buenavista fault zone), which marks the southwestern edge of the triangle. The faults trending NE-SW and NW-SE are approximately parallel and perpendicular to the direction of convergence between the Cocos and North American Plates at the MAT.
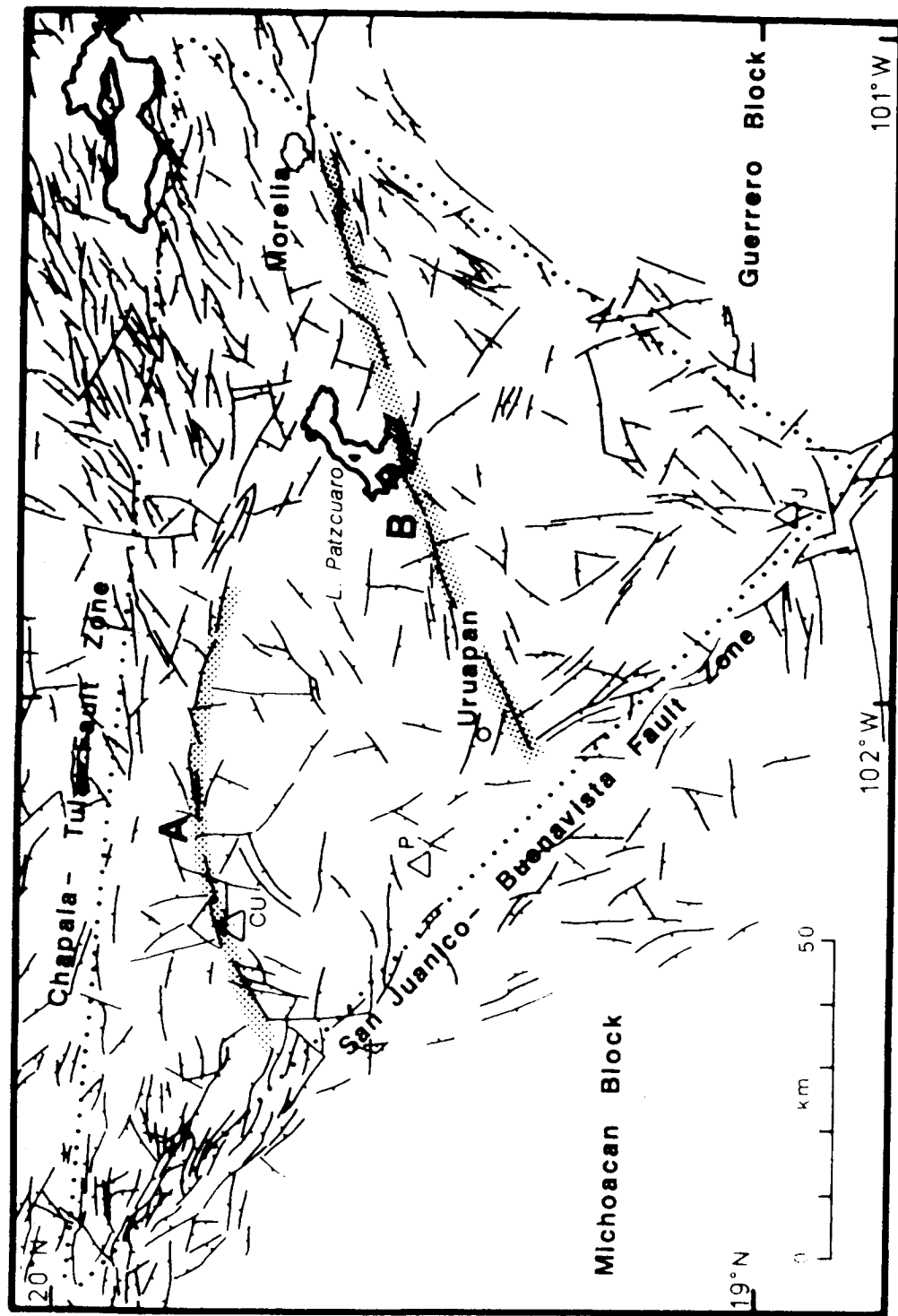
Figure 37: Fault scarps in the region of northern Michoacan State southeast of Lake Chapala. The zone of faulting is confined within a triangular area, termed here the *Michoacan Triangle*, which is situated between the North American Plate and the Michoacan and Guerrero blocks. Dotted lines roughly mark the boundaries of the triangle. Stippled fault zones marked 'A' and 'B' are discussed in the text. CU, Cerro Uripitliuata P, Paracutin; J, Jorullo.

Fault Zone A in Figure 37 extends SW from the north central part of the Michoacan Triangle to the southern end of the San Juanico Graben. Its trace is highly curvilinear, being concave to the south. The individual faults that compose Fault Zone A form prominent scarps cutting deposits associated with Cerro Uripitliuata, the largest volcano in the MGVF with a summit elevation of 3400 m. The highly eroded morphology of this cone marks it as one of the older volcanoes in the area, with deep valleys of possible glacial origin cutting into its crest. Other younger faults of Fault Zone A are associated with strings of small cones.

Fault Zone B begins in the northeastern corner of the triangle and extends to the SW, along the southern shore of Lake Patzcuaro, and intersects the San Juanico-Buenavista Fault Zone at right angles, where it ends abruptly. Like Fault Zone A it is concave to the south, although somewhat less curvilinear. The fault zone is composed of numerous scarps of various morphology, from very sharp to highly eroded. Most have throws that are down to the NW.

10.2.2 Eastern MVB

A second example of medium-scale tectonic control of volcanism in the MVB is in the eastern part of the study area in the region of Mexico City. The surface of the plateau in this area is divided into three depressions of nearly equal size. These basins are divided by ridges of Mio-Pliocene volcanics, which were erupted in association with NNW-SSE trending faults. In the Plio-Quaternary a new set of E-W trending faults and fractures developed, which are very apparent on the TM images. These are associated with volcanics of the same age, mostly cinder and lava cones and flows. Large central volcanoes of the volcanic front have been erupted where the two sets of faults intersect.

10.3 Local

On the local or small scale, individual cinder cones and lava flows are often erupted along the trace of a fault that is visible on the TM images. In other cases, these features are erupted in linear arrangements that imply an unseen fissure or fault is responsible. Individual examples include chains of cones and flows within the Tepic-Chapala Rift, like those on the flanks of Volcan Tequila, which are clearly associated with faults.

11 Crustal Motions

11.1 Crustal Blocks

Based on the TM image interpretation, the area south of the MVB can be divided into at least three separate blocks. From west to east these are named the Jalisco, Michoacan, and Guerrero structural blocks, after similar divisions proposed by Mooser (1972) on tectonostratigraphic grounds (Figure 18). Each block is separated from its neighbors and from the North American Plate by zones of active tectonics associated with the MVB and subduction along the continental margin. Although the primary concern of this study was with these active zones, a general sketch of the characteristics of the blocks that they define is needed for a complete treatment of the region. The purpose of this section is to summarize the geology and internal structure of these blocks.

11.1.1 The Jalisco Block

The Jalisco Block is defined here as the portion of continental crust south of the extreme western end of the MVB. Our knowledge of the geology of this part of southwestern Mexico is very fragmentary, and most of the work done in the area has focused on subjects related to those portions of the MVB that form the northern and eastern boundaries of the block. On the north the Jalisco block is bounded by the Tepic-Chapala Rift, and on its east by the Colima Rift. On its south and west it is bounded by the western end of the Middle America Trench, where active subduction is still taking place in a more subdued, aseismic mode than that farther southeast (Nixon, 1982). About 95 percent of the area of the block (29,000 km^2) is within southwestern Jalisco State. Figure 38 is a sketch map of the portion of the Jalisco Block visible on the TM imagery.

Opinions differ regarding the age of the oldest rocks exposed within the block. Lopez Ramos (1983) shows Paleozoic gneisses and slates exposed in much of the area. These would presumably correlate with upper Paleozoic rocks further east. However, in their work in the western part of the area, Gastil *et al.* (1978) found no evidence for rocks older than Late Jurassic. They describe an andesite-greywacke sequence of Late Jurassic age and an andesite-marble-metasandstone sequence of Early Cretaceous(?) age. This is in rough agreement with the 1:1 million scale geologic map of Mexico, which shows the oldest rocks as Jurassic Metamorphics. Relatively undisturbed Cretaceous (Albian) limestones interbedded with andesites have been described from a borehole in western Jalisco (Pozo Jalisco 1; Lopez Ramos, 1983). These may be correlated with the Morelos Fm. to the east. The metamorphic rocks are intruded by granitic rocks of Middle to Late Cretaceous age. The majority of the Cretaceous intrusives are associated with a large batholith that forms a wide belt of crystalline rock along the coast (Gastil *et al.*, 1978). This extensive terrane is 50 to 60 km wide and extends from the Bahia de Banderas to the area southwest of Colima. These intrusives illustrate that the west coast of Mexico in this area probably has been the site of active subduction since at least the Jurassic. A Late Cretaceous sequence of redbeds and siliceous volcanics overlaps the granites in the west (Gastil *et al.*, 1978). Allan *et al.* (1987) briefly describe a thick (1700 m) series of Late Cretaceous limestones that outcrop in a large fault scarp NW of the city of Colima.

The geologic map of Mexico shows extensive exposures of Tertiary intermediate and acidic extrusives within the Jalisco block. These are probably best correlated with the Oligo-Miocene volcanism of the Sierra Madre Occidental, although Gastil *et al.* (1978) found no volcanics of this age in the region around the Bahia de Banderas and Tepic (which they explained as a consequence of their sampling). These rocks are probably present as far east as the Colima Rift, as noted by Allan *et al.* (1987). In the region of the Tepic-Chapala
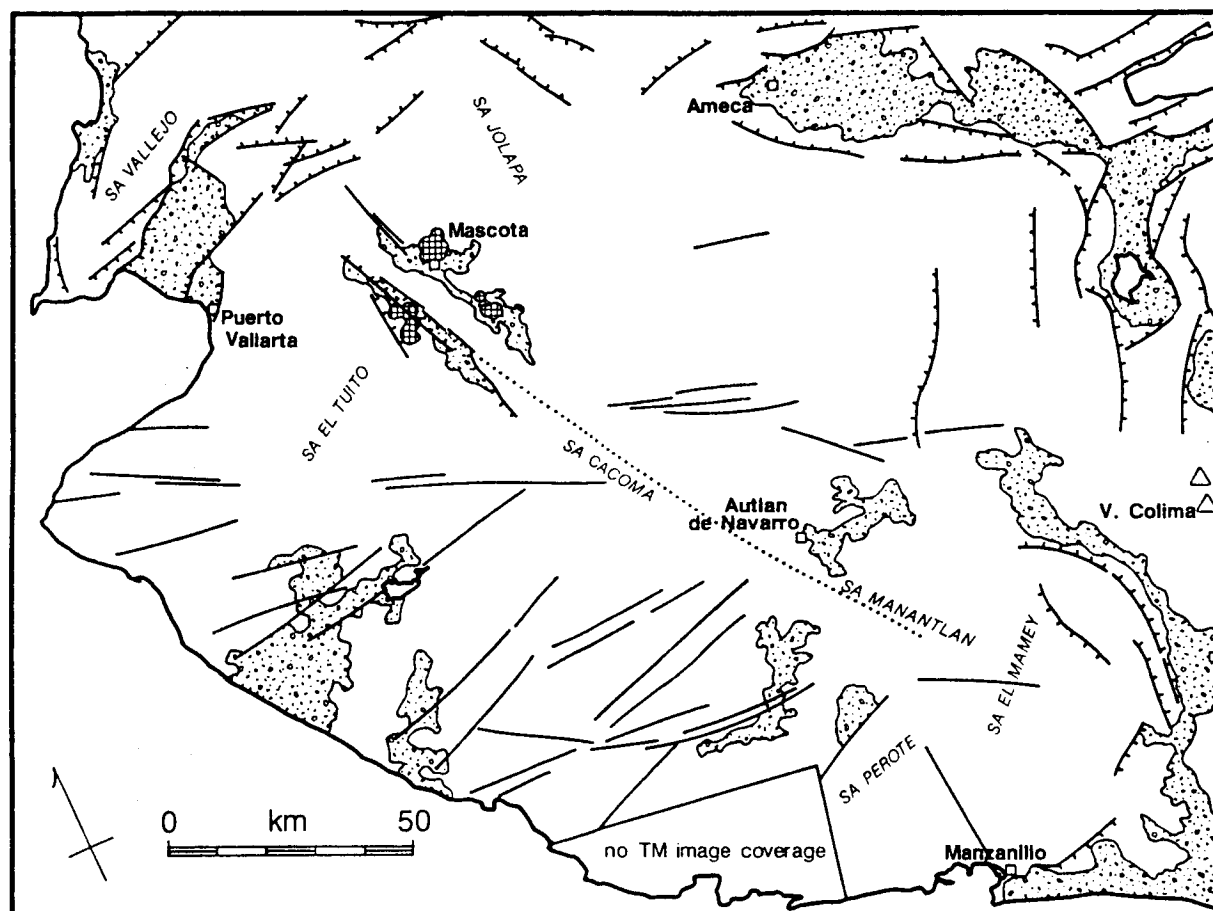
The Jalisco Block

Figure 38: The Jalisco Block. Patterned areas represent Quaternary basins. Orthogonally ruled areas near Mascota are correspond to volcanics of the Mascota volcanic field. A small portion of the Jalisco block is not covered by our TM data, as marked. The most prominent mountain ranges are labeled in small type. See text for additional explanation.

Rift on the northern edge of the Jalisco block, Late Miocene basalts were erupted on the Middle Tertiary volcanics (Gastil *et al.*, 1978). These rocks can best be related to an episode of extension and volcanism in that area coincident with the opening of the Gulf of California.

Figure 38 shows Quaternary basins in and around the Jalisco Block. Most of these are fault controlled and related to extension at the margins of the block. Of particular interest are two subparallel elongate basins in the vicinity of Mascota. These basins contain the only field of Quaternary volcanics discovered to date within the Jalisco Block. Allan *et al.* (1987) briefly describe this field, which consists of cinder and lava cones of various alkaline and calc-alkaline rocks. Other young volcanic fields in the area are either composed of cones that are too small to see clearly with the TM imagery, or they simply do not exist. The very limited extent of Quaternary deposits in the Jalisco block (most are located at its margins) indicates that the block has undergone recent uplift.

The basins near Mascota are bounded by NNW trending normal faults. These faults do not seem to be directly related to any of the more prominent structures on the margins of the Jalisco Block; instead they seem to be an isolated feature like the Mascota cinder cones. Normal faults of very large displacements are located west of the Colima Rift within the Jalisco Block. They seem to be related to the rifting process but are not associated with significant volcanics. Other structures within the Jalisco Block are older features primarily associated with the large Cretaceous batholith. This crystalline terrane is extensively fractured in an E to ESE direction, and the main fractures are easily detected on the TM imagery. The most prominent of these are also shown in Figure 38.

A prominent lineament within the Jalisco block has also been detected on the TM imagery. This feature is shown as a dotted line in Figure 38. It extends approximately 110 km southeastward from the vicinity of the basins around Mascota, with which it is roughly colinear. This feature parallels the coast and is coincident with a linear topographic depression that traverses the central ranges of the Jalisco Block (Sierra Cacoma and Sierra Manantlan).

11.1.2 The Michoacan and Guerrero Blocks

The region south of the Mexican Volcanic Belt is a complex collage of Precambrian, Paleozoic, and Mesozoic rocks, which has been structurally and stratigraphically divided into several tectonostatigraphic terranes (Campa and Coney, 1983; Campa, 1985; Ortega, 1986) (Figure 39). These terranes have reached their present locations through Late Paleozoic collision, Early Mesozoic rifting, Laramide collision and deformation, and possibly several phases of Cenozoic-Holocene tectonics. Examples of Holocene tectonics include the peninsula of Baja California, which has separated from the Mexican mainland and is currently moving northward along the right-lateral San Andreas fault system; and the Tehauntepec ridge, which is an oceanic plateau encountering the Middle America Trench that may eventually be partially accreted to the continental margin of southern Mexico.

In addition to the complexity introduced by the presence of suspect terranes, it has also been suggested that lateral crustal motions along major shear zones occurred during the Mesozoic and Early Tertiary tectonic development of Mexico (Urrutia-Fucugauchi, 1984). The driving force behind these movements remains enigmatic, but may be related to well-documented plate reorganizations within the Pacific (Larson and Chase, 1970; Menard, 1978), combined with rapid and shifting convergence between the North American plate and the plates in the Pacific (Coney, 1978). Cretaceous through Quaternary paleomagnetic poles from central Mexico generally display counterclockwise rotations relative to the directions derived from the rest of North America (Urrutia-Fucugauchi, 1984; Urrutia-Fucugauchi and Bohnel, 1987). This is interpreted to be caused by rotation of crustal blocks adjacent to large E-W or NW-SE trending left-lateral faults. This
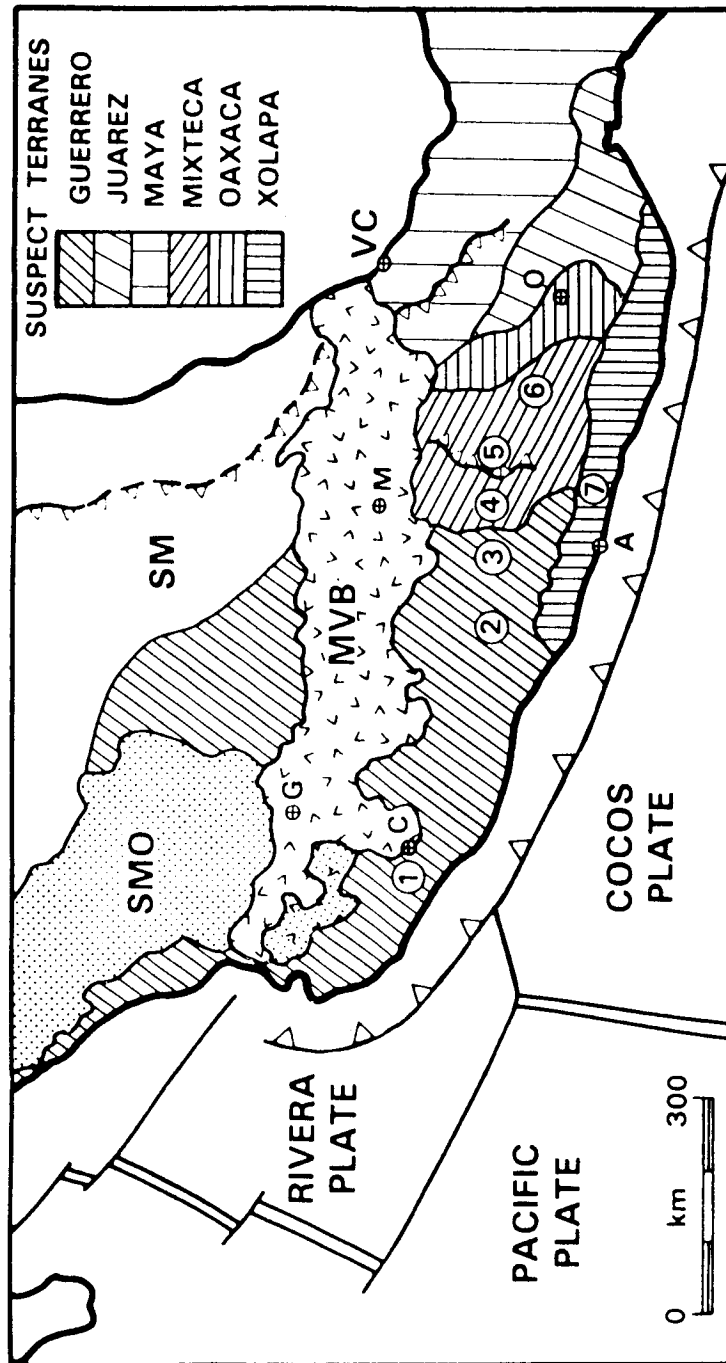
Figure 39: Tectonostratigraphic or "Suspect" Terranes of central and southern Mexico.

interpretation is consistent with recent models of the Mesozoic and Cenozoic development of the southern edge of the North American Plate (e.g. Pindell and Dewey, 1982). Although these interpretations may be in need of revision, there is an emerging consensus that large-scale motions on zones of sinistral shear in Mexico are necessary for the reconstruction of Pangaea and its subsequent break-up in the Mesozoic.

Older tectonic events are recorded in basement rocks (Ruiz et al., 1988). A general division of these rocks has been proposed (Ortega, 1986). Three basement terranes are exposed within the our study area. These are the Guerrero, Mixteca and Xolapa terranes (Campa and Coney, 1983), Figure 2a. Each terrane is characterized by distinct basement types and sedimentary covers; and it has been suggested (but poorly documented) that their boundaries are tectonic (e.g. major faults or zones of mylonitization). Their interpretation as suspect tectonostratigraphic terranes is currently accepted (Howell et al., 1985); but the exact shape, spatial extent, and structural relationships among these terranes are still poorly known. Because of this, the tectonic evolution of the southwestern edge of the North American plate is also poorly known. Although a Laramide (Cretaceous-Tertiary) age for accretion of these terranes has been proposed by Campa and Coney (1983), Campa (1985), and Coney (1987); Moran-Zenteno (1987) and Ruiz et al. (1988) conclude that the provenance and accretionary history of the terranes of southern Mexico is still uncertain. We believe the confusion results from several factors, including: 1) the absence of well-constrained lithostratigraphic correlation from one region to another; 2) the paucity of studies in areas covering the terrane boundaries; and 3) the incomplete and oversimplified interpretation of the Phanerozoic sedimentary record (see Figure 40).

Stratigraphy

Several stratigraphic sequences characterize major terranes south of the MVB (Figures 39 and 40); and in some cases, they distinguish subterranes (Campa and Coney, 1983). Mr. J.A. Barros is currently studying the terranes and their boundaries with funding from a seperate NASA grant (Underrepresented Minorities Initiative). Also, in February 1989 our group in Miami, in association with groups at NASA/JPL and UNAM/Mexico City, will begin a more broadly based study of stratigraphy and tectonics in the region. A short description of the Phanerozoic stratigraphy of the region should be sufficient to demonstrate the potential contribution that remote sensing and image interpretation, combined with topographic data and field mapping, can make toward a better understanding of the geologic history of the area. The best geological maps covering the entire study area are at 1:250,000 scale; and few geological maps at scales up to 1:50,000 exist. A cursory examination of TM images shows that the present maps are inaccurate at the 1:24,000 mapping scale that is possible using TM data (Lang et al, 1987). In fact, in the few areas where 1:50,000 maps exist coverage is spotty, and can be substantially improved using TM data. Each terrane within the Michoacan and Guerrero blocks is described briefly below.

The nature of the basement of the Guerrero terrane is not known, although recent studies by Elias-Herrera (1987) suggest that the meta-volcaniclastic sequence around Tejupilco is underlain by high-grade metamorphic rocks of possible continental basement affinity. However, Elias-Herrera provides no indication of the age of these rocks. The oldest rocks exposed within the Guerrero terrane are Late Jurassic to Early Cretaceous andesitic volcanics and volcaniclastics, interbedded with flysch-like sediments (Figure 40, columns 1-3). Toward the west, volcanics within the Guerrero terrane are more abundant. The entire sequence is slightly metamorphosed along the extreme western margin (Gastil et al., 1978). In contrast, the eastern margin of the Guerrero terrane is occupied by a latitudinal band of more intensely metamorphosed rocks that have been interpreted to be a meta-volcaniclastic sequence of Late Jurassic-Early Cretaceous age (Roca Verde Taxco Viejo and Taxco Schist) (Campa and Coney, 1983). According to Campa (1985), metamorphism of this sequence occurred during the Laramide orogeny (Late Cretaceous-Tertiary). This conclusion will probably need to be reexamined in the light of the fact that the literature and our field work in the area to date have revealed no regionally-metamorphosed rocks younger than late Early Cretaceous

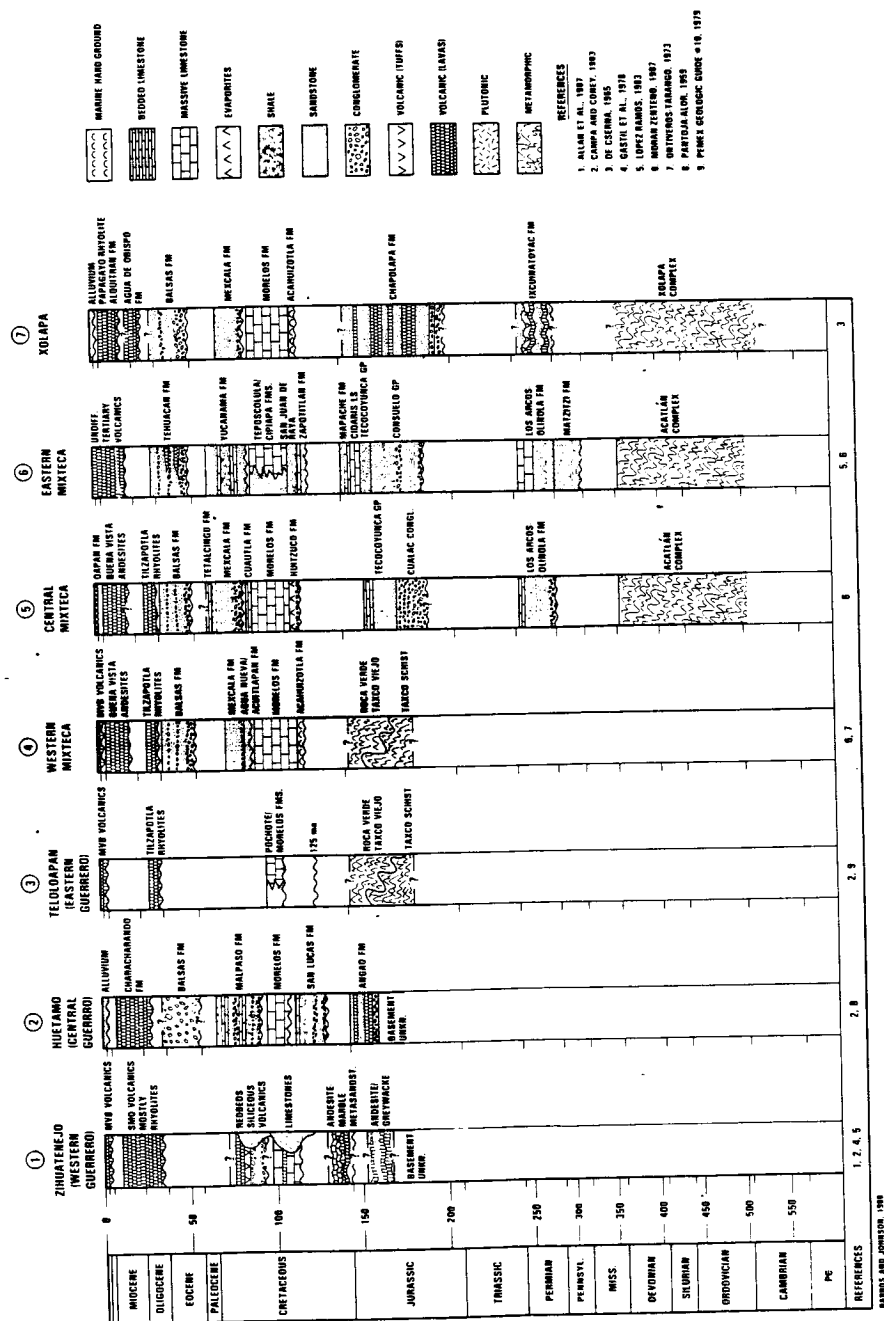# PHANEROZOIC STRATIGRAPHY OF SOUTHWESTERN MEXICO

Figure 40: Phanerozoic stratigraphy south of the MVB.

in age.

The synorogenic sequence described above is separated from similar Late Cretaceous through Cenozoic rocks by Middle Cretaceous platform carbonates of the Morelos Fm. The Morelos limestone (and equivalent strata) is a potentially important stratigraphic marker, because it is expressed throughout most of the proposed study area. Its characteristic geomorphology and color make it easy to distinguish on the TM images. Paleontological evidence shows that the Morelos Fm. is Aptian-Albian in age (Pantoja-Alor, 1959; Fries, 1960).

Immediately to the east of the Guerrero terrane is the western Mixteca terrane (Moran-Zenteno, 1987). The western Mixteca is composed of Late Jurassic-late Early Cretaceous meta-volcaniclastic rocks (Figure 40, column 4), that are the eastern extension of similar rocks found in the eastern Guerrero terrane. These metamorphic rocks are unconformably overlain by the Middle Cretaceous platform carbonates of the Acahuizotla, Morelos, and Cuautla Fms. (Ontiveros-Tarango, 1973). This Mesozoic sequence has many similarities to that of the Guerrero terrane, thus leading to the conclusion that the boundary between the Guerrero and Mixteca terranes (shown in Figure 39) is not well known. Certainly no clear tectonic contact has been mapped that separates the two terranes in that area.

The central lithostratigraphic domain of the Mixteca terrane is characterized by the presence of the Acatlan metamorphics (Figure 40, column 5). The origin of these rocks can probably be linked to the closure of the Iapetus ocean during Late Paleozoic time (Ortega-Gutierrez, 1981). The presence of the unmetamorphosed Upper Paleozoic Matzitzi and Los Arcos-Olinola Fms., in the eastern Mixteca terrane, suggests that the orogeny responsible for metamorphism of the Acatlan complex was not synchronous with the Appalacian-Ouachita-Marathon orogeny, but probably occurred earlier. The Paleozoic Acatlan complex is also unconformably overlain by the Early Jurassic-early Late Jurassic Tecocoyunca Group (Moran-Zenteno, 1987). This sequence appears to represent a marine transgression that began with the accumulation of continental sediments on a passively subsiding cratonic margin. The transgressive sequence is overlain by Middle Cretaceous evaporites and coastal deposits which, in turn, are conformably overlain by the platform limestones of the Morelos and Cuautla Fms. A Late Jurassic and Early Cretaceous unconformity is thus recorded.

The deposition of Jurassic carbonates persisted longer in the eastern Mixteca terrane (Figure 40, column 6) than in the central part. This implies that the Late Jurassic-Early Cretaceous unconformity is diachronous. Lateral changes from shallow water to deeper water basinal facies are also recorded by Middle Cretaceous carbonates.

Following deposition of the Middle Cretaceous carbonate platform sequence, a profound change in sedimentation occurred. Throughout the Guerrero and western and central Mixteca terranes, Late Cretaceous sedimentation was dominated by deposition of typical synorogenic flysch of the Mal Paso and Mexcala Fms. In contrast, marls dominate the eastern Mixteca terrane during Late Cretaceous time. The Mal Paso Fm. is coarser grained and richer in volcanics than the Mexcala Fm. (De Cserna et al., 1978). This evidence suggests that during the Laramide orogeny, the eastern Mixteca terrane was farther away from the area of uplift and volcanic activity than were the western Mixteca and Guerrero terranes.

The Eocene-Oligocene Balsas Fm. is the oldest Cenozoic deposit in most of the study area. No coherent regional pattern of sedimentation for these coarse conglomerates is known; and any tectonic influence on their deposition may be only local. The Balsas and Mexcala Fms. are good candidate marker beds for image interpretation, because they are easily distinguishable on the TM images and have a wide distribution.

Covering much of the area, particularly toward the north, are Miocene through Quaternary volcanic rocks

(Figure 40 (Nelson and Sanchez-Rubio, 1986). These are exposed primarily in the Sierra Madre Occidental and also in the Mexican Volcanic Belt. Although they completely cover older rocks within the volcanic belt, they provide an excellent surface for expression of neotectonic activity (Johnson, 1987). To the south, older rocks and structures are rarely covered by Miocene through Quaternary volcanic rocks.

As shown in Figure 40, column 7, the stratigraphy of the Xolapa terrane is largely unreported. The sequence of formations shown on column 7 is based mainly on the stratigraphic position of units relative to: 1) Middle Cretaceous carbonate strata of the Acahuizotla and Morelos Fms.; and 2) Late Cretaceous flysch of the Mexcala Fm. As shown in the column 7 interpretation, we suggest that the Chapolapa Fm. (De Cserna, 1965) may be a lateral equivalent of the Roca Verde-Taxco Schist. If this is the case, accretion of the Xolapa terrane must have occurred prior to deposition of Middle Cretaceous carbonates that are also present within the terrane (De Cserna, 1965). However, Salinas (1984) suggested a Paleocene age for accretion of the Xolapa terrane. This apparent confusion regarding the Xolapa terrane is a major stratigraphic/tectonic problem that can be addressed directly using mapping results from our proposed TM image analysis.

Tectonics South of the MVB

The tectonic evolution of southern Mexico is still the subject of intense study and controversy. The Mesozoic-Cenozoic igneous rocks that cover much of the country demonstrate that subduction along the Pacific margin of Mexico has been a dominant tectonic factor, probably since at least the Late Jurassic (Atwater, 1970; Urrutia-Fucugauchi, 1986). In addition, most of Mexico was affected by the Late Cretaceous-Early Tertiary Laramide orogeny (Campa, 1985); and Mexican extensions of the Late Paleozoic Appalachian-Ouachita-Marathon orogenic belt (de Cserna, 1960, 1976).

Trench-parallel strike-slip faulting and subsequent along-margin transport of crustal blocks and/or slivers ("Sunda-Style" Tectonics) has been a common phenomenon along the western margin of North America, probably since the late Paleozoic; and southwestern Mexico is no exception. The fitful, episodic nature of this tectonism can be related in time to well-documented variations in the rate and direction of North American convergence with plates in the Pacific. Our recent work with Landsat Thematic Mapper images, combined with field studies, enables an extension of these correlations into southwestern Mexico.

Laramide structures provide the earliest clear example in southern Mexico of the strong correlation of tectonism with Pacific plate motions. Mesozoic sediments were thrusted and folded during the latest Cretaceous-Early Tertiary, with fold axes trending nearly north-south. This event is related to the initiation of high-velocity, east-west convergence with the Farallon plate, beginning between 70 and 60 Ma. Cumulative sinistral motions on numerous ESE trending faults throughout southern Mexico at this time may have significantly altered the shape of the continent. The high rate of convergence continued until about 40 Ma, when it slowed significantly and changed direction, becoming more northeasterly. This is reflected in the lower part of the Balsas formation, which exhibits gentle folds with axes which trend northwest and interfere with the Laramide folds. The 40 Ma event is also coincident with magmatic activity in the Balsas basin, which peaks at about that time. The zone of heated and softened crust that resulted is responsible for the localization of younger strike-slip faulting. Also about this time the main portion of the Chortis block, now in nuclear Central America, began its motion to the east along a major sinistral shear zone. This event can be seen in southwestern Mexico, where Laramide and Early Tertiary structures are offset or interrupted by left-lateral faults. As the new margin gradually became exposed to the effects of subduction it was sequentially uplifted and deformed during the Oligo-Miocene. This is evidenced by numerous angular unconformities and decreasing radiometric ages from northwest to southeast. In the Late Miocene (about 10 Ma) a reversal in the direction of oblique convergence occurred, with right-oblique motion increasing in intensity to the northwest. This resulted in the detachment of a large sliver of crust,

extending along the margin from near Oaxaca state in Mexico, through Baja California and into southern California. The convergence direction became more perpendicular in the latest Miocene, breaking the sliver into several pieces.

Further study of the metamorphic geology of the region should yield answers concerning the history, movement, and accretion of suspect terranes since the Devonian, and also to what extent their boundaries functioned as inherited zones of weakness during later tectonic events.

11.2   Recent Crustal Motions

11.2.1   Movement of the Jalisco Block: Geological Considerations

The major conjugate faults in the Tepic-Chapala Rift (Figure 13) may be used to determine the direction of motion between the Jalisco block and the North American plate. We have shown that a major system of left-lateral shear zones or wrench faults exists within the Tepic-Chapala Rift, having orientations of approximately N148°. Nieto-Obregon *et al.* (1985) determined the orientation of the conjugate right-lateral fault to be between N110° and N115° (N112° will be used for convenience). In this case, the direction of maximum extension should then trend approximately N40°, bisecting the obtuse angle between the conjugate shear zones, while the minor axis should trend N130°, bisecting the acute angle. These conclusions are confirmed by the orientations of cinder cone chains within the rift.

Nakamura (1977) has shown that alignments of volcanic features indicate the orientations of the principle axes of the local stress field. In effect, such alignments are perpendicular to the direction of least compressive stress (maximum tension). The orientation of cinder cone alignments was examined on maps of the area produced by Gastil *et al.* (1978) and Allan *et al.* (1987); these orientations were found to cluster around N130°, which nicely bisects the acute angle between the major fault systems. This is also roughly the orientation of the rift itself, measured from the area of the triple junction northwest to Tepic.

These facts all indicate that the direction of maximum extension for the Tepic-Chapala Rift is oriented at approximately N40°. This means that, on average, the Jalisco block is moving away from the Mexican mainland (North America) along this trend. This conclusion contradicts that of Allan *et al.* (1987) who, after reviewing the latest work on the subject, maintain that the motion between the Jalisco block and North America is oriented more or less parallel to the Tepic-Chapala Rift with a right-lateral sense, approximately 90° away from that derived here. Their conclusion is based largely on the field evidence mentioned previously and on an analysis by Ness *et al.* (1985) which uses plate motions in the eastern Pacific to deduce the Rivera-North American motion. Their assumptions are not stated, but it is clear that they are assuming a minimal or zero amount of relative motion between the Rivera Plate and the Jalisco block of western Mexico, because they state that the Rivera-North American motion "implies that a southern Mexican plate (XMEX) must be moving right-laterally with respect to North America". This is not necessarily true if a significant amount of motion is allowed between the Rivera Plate and the Jalisco block. Right-lateral motion between North America and the Rivera Plate does not have to extend into western Mexico. If subduction of the Rivera Plate is taking place, then an accommodation is made for extensional motion between North America and the Jalisco block. Nixon (1982) concludes that the Rivera Plate may in fact be subducting aseismically at a rate of about 2 cm./year. If subduction is in a generally northward direction, then the convergence rate perpendicular to the trench between the Rivera Plate and the Jalisco block will decrease westward, from a maximum near the Rivera/Cocos boundary to zero near the Tamayo fracture zone. Convergence rates and directions for that portion of the Middle America Trench are notoriously difficult to calculate by means of earthquake focal mechanisms and slip vectors, because of

the paucity of large earthquakes (Nixon, 1982).

A cautionary statement must be made at this point. Further work is needed to confirm the above conclusions, both in the field, and with the TM imagery. Additional lineament statistics for the whole of the Tepic-Chapala Rift system would be helpful, as would confirmation of the left-lateral motion from the ground. A clearer set of images of the area is necessary for a more detailed analysis, because in the images presently available, the contrast is too low and both clouds and cloud shadows cover several interesting areas. Until these confirmations can be obtained, the above observations that indicate left-lateral motion within the Tepic-Chapala Rift can only be viewed as preliminary.

11.2.2 Crustal Block Motions

Analysis of the 1:1 million scale TM image mosaic has enabled the detection of three large crustal blocks south of the MVB. From west to east these are the Jalisco, Michoacan, and Guerrero blocks. Relative motion between these blocks and the North American Plate to the north of the MVB has resulted in the formation of major zones of neotectonic deformation within the MVB. It is possible to estimate the magnitudes of the relative motions between the crustal blocks south of the MVB using relative motion vectors from the literature for plates in the vicinity, combined with directions derived from the orientations of recent faulting between the blocks, as seen on the TM images. Figure 41 shows the relative motions between the four plates and three smaller blocks in the region, and Table 3 lists the parameters used to construct Figure 41. In order to create the vector diagram it was necessary to assume that no significant rotations of the components takes place over distances comparable to the dimensions of the area covered. This is probably a valid assumption except for the Cocos plate, which has a pole of rotation located nearby. But, since the velocity of subduction of the Cocos plate varies by less than 15% along the Middle America Trench in this area, the vector diagram is very likely a reasonable approximation.

Table 3 Relative motion parameters for plates and crustal blocks in the region around central Mexico. Bold numbers refer to corresponding vectors in Figure 13. Pac = Pacific; Coc = Cocos; Riv = Rivera; Nam = North America; Gue = Guerrero block; Mic = Michoacan block; Jal = Jalisco block; SC = oceanic spreading Center; RLT = right-lateral transform; LLT = left-lateral transform; S = subduction; CR = continental rift; OS = oblique subduction.

Plate Pair	Rate (mm/yr)	Azimuth	Plate Boundary	Source
1 Pac/Coc	87	84°	SC	Eissler & McNally, 1984
2 Pac/Riv	52	124°	SC/RLT	Klitgord & Mammerickx, 1982
3 Pac/Nam	65	123°†	SC/RLT	Ness et al., 1985
4 Coc/Riv	58†	−131°†	LLT	azimuth similar to Eissler & McNally, 1984
5 Coc/Gue	57†	−146°	S	Chael & Stewart, 1982
6 Coc/Mic	58†	−151°	S	Chael & Stewart, 1982; Dean & Drake, 1978
7 Gue/Nam	2.5†	−15°	CR	this study
8 Gue/Mic	5†	137°	LLT	this study
9 Mic/Nam	7†	−33°	CR	this study
10 Jal/Mic	8†	100°	CR	this study
11 Jal/Nam	7†	40°	CR	this study
12 Riv/Nam	12†	120°	RLT	Klitgord & Mammerickx, 1982
13 Riv/Jal	12†	150°†	OS/CR	this study

†Calculated from vector diagram, Figure 41.

Construction of the diagram in Figure 41 begins by constraining motions of the Cocos and Rivera plates relative to the Pacific plate using spreading rates and transform trends in the Pacific. The Pacific/North America rate is derived from spreading at the mouth of the Gulf of California, and the azimuth of the Rivera/Nam motion is defined by the trend of the Tamayo fracture zone. From this it is possible to determine the Cocos/Rivera motion and the rate of Riv/Nam motion. Slip vectors from Chael and Stewart (1982) and Dean and Drake (1978) are used to constrain the azimuth of convergence between the Cocos plate and the Guerrero and Michoacan blocks. This direction is slightly more easterly for the Guerrero block. The direction of motion of the Guerrero block relative to Nam is assumed to be perpendicular to the trend of the Cuitzeo fault trend, which separates them. This motion may actually be more to the east if significant sinistral motion is occurring on the Chapala-Tula fault zone, but this is difficult to estimate without more detailed field work. Michoacan/Guerrero motion is constrained by the trend of the Chapala-Oaxaca fault zone. The Jalisco/Nam direction is assumed to be perpendicular to the trend of the Tepic-Chapala Rift, and Jalisco/Michoacan motion is perpendicular to the trend of the Colima Rift. Figure 42 shows the geodynamic situation in the region as derived from the velocity triangles in Figure 41. The magnitudes of motions for the blocks south of the MVB are comparable to motions of blocks in areas of active rifting in other parts of the world.
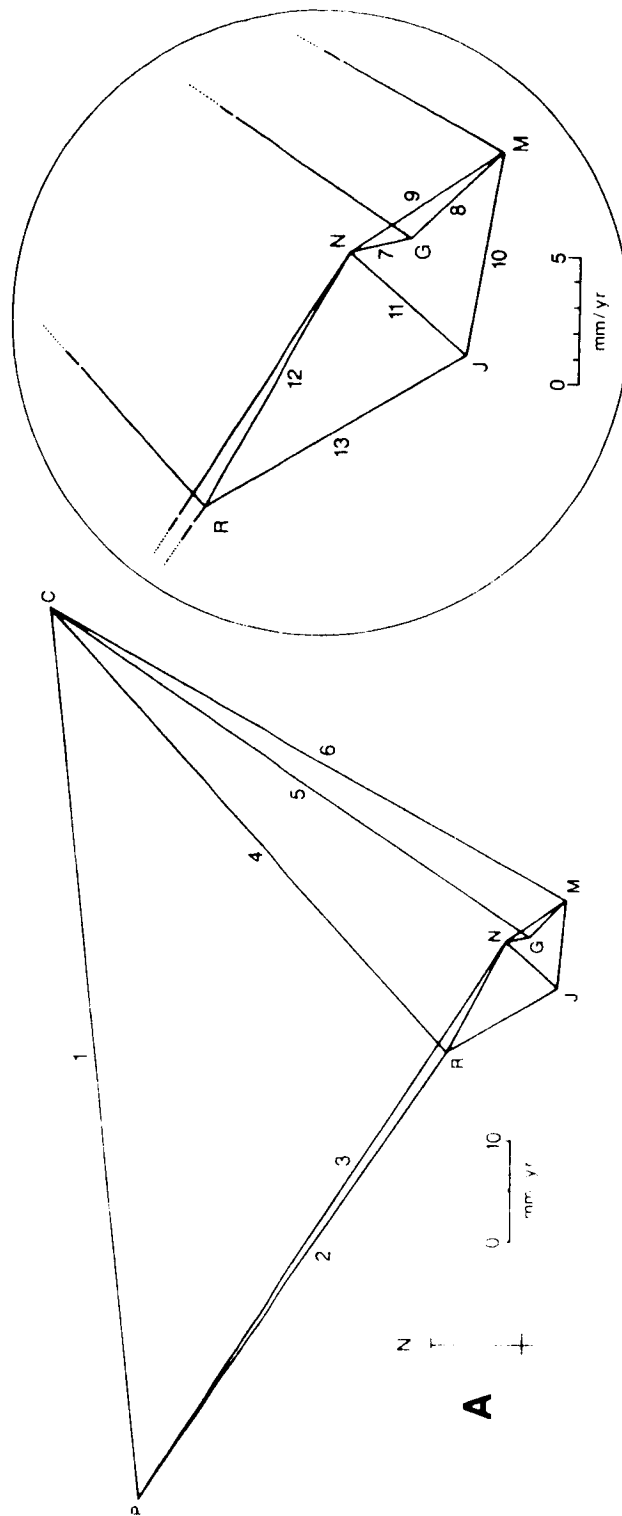
Figure 41: Vector diagram showing relative motions between lithospheric plates and crustal blocks in the region of central Mexico; P, Pacific plate; C, Cocos plate; R, Rivera plate; N, North American plate; J, Jalisco crustal block; G, Guerrero crustal block; M, Michoacan crustal block. Numbers refer to Table 3, where azimuths and magnitudes of relative motion are listed.
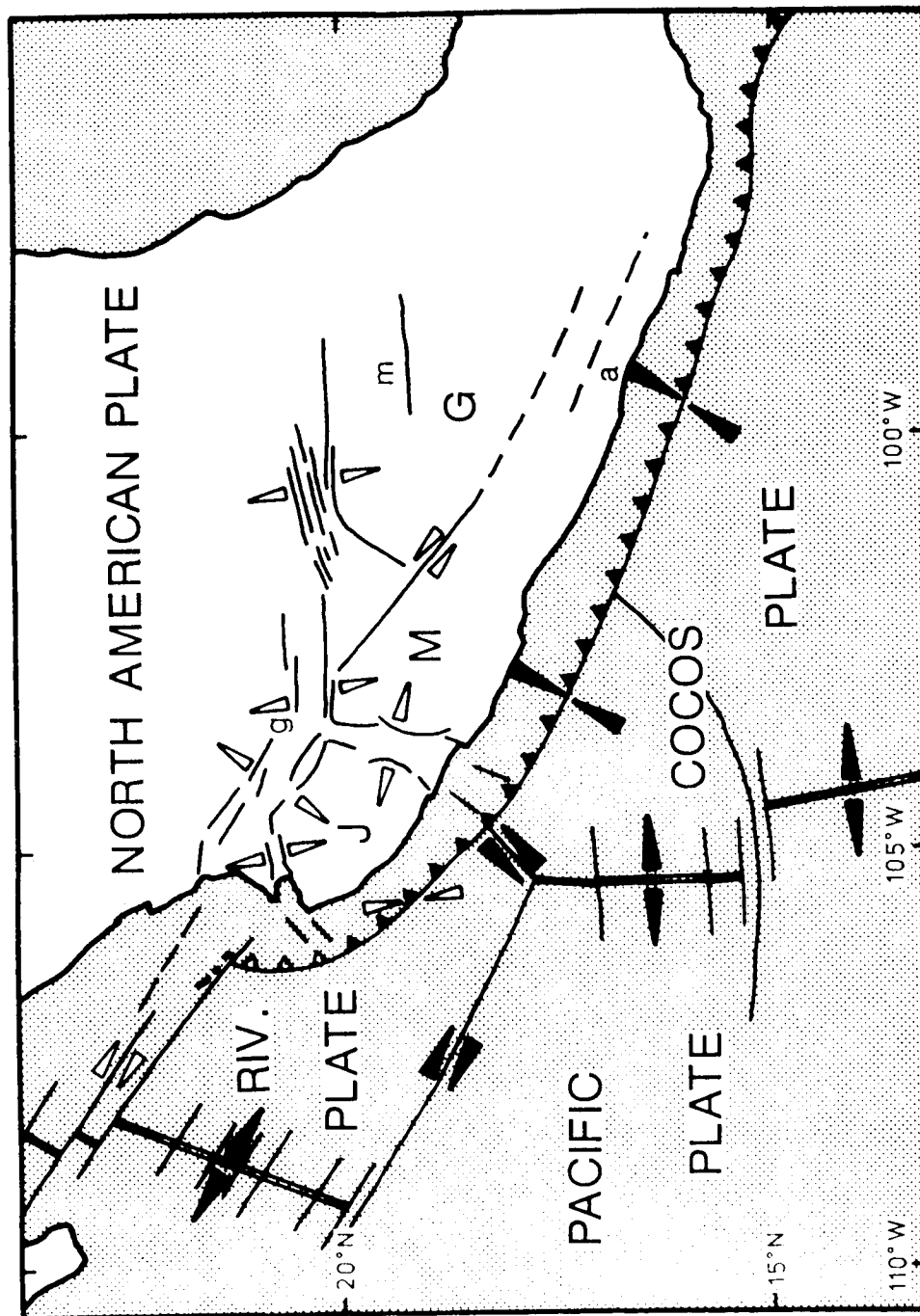
Figure 42: Sketch map of central Mexico and the surrounding region showing relative motions as determined in Figure 41. Letters are the same as in Figure 41; g, Guadalajara; m, Mexico City.

12 Summary: Neotectonics

Interpretation of TM images has enabled the mapping and analysis of major zones of crustal deformation in central Mexico. The deformation is dominated by faulting associated with rifting, transtension and shear, much of it having probable left-lateral components. The faults observed in the region cut the Plio-Quaternary volcanics associated with the Mexican Volcanic Belt (MVB), and many of the faults are still active. This conclusion is based on the morphology of the faults as interpreted on the images, and on the ages of the deposits that the faults have offset.

Neotectonic activity in the MVB can be divided into two regions, eastern and western. In the west, deformation is organized into a triple junction formed by the intersection of three large rift structures. Neotectonic activity in the eastern half of the region is less organized, although its division into four areas with indistinct boundaries is possible. For reference in this section, the reader should refer to Figures 4.7 and 4.8.

12.1 Western Study Area

The geology of this area has been reviewed recently by Allan *et al.* (1987), and the conclusions drawn from the TM study of the region generally echo those of these earlier workers. Deformation in the area is organized into three rifts that intersect to form a triple junction SSW of Guadalajara. This rifting is related to regional uplift and the eruption of small volumes of alkalic volcanic rocks, which indicate that it may be an active form of rifting. This is the only case of African-type rifting that has been documented on the North American continent, although its plate tectonic environment, situated above an active subduction zone, is not typical. This apparent dichotomy is probably related to the subduction of a plate boundary in the vicinity (see the Colima Rift, below).

1. The **Tepic-Chapala Rift** extends from the triple junction NW to the Gulf of California, where it displays a prominent bifurcation near the coast. One branch of the rift continues to the NW, while the other trends WSW and opens into the Bahia de Banderas. The rift forms the active boundary between the North American plate and the Jalisco crustal block. *En echelon* alignments of fault scarps in the Tepic-Chapala Rift show that some motion across the rift may be accommodated by deep-seated sinistral wrench faults. These faults also appear to control the location of many of the volcanic centers within the rift. The rift trends about N130°, and alignments of cinder cones within it having the same trend indicate that the direction of maximum extension across the rift is N40°. These observations are the most significant deviation from the conclusions of Allan *et al.* (1987), who state that motion along the Tepic-Chapala Rift is predominantly right-lateral.

2. The **Colima Rift** extends southward from the triple junction to the Pacific coast, and forms the active zone of faulting that separates the Jalisco and Michoacan blocks. The rift may be divided into northern, central, and southern sections based on structural and volcanic characteristics. The rift as a whole marks a major shift in the location and character of volcanism within the MVB. The rift axis trends about N190°, and extension in the area appears to be roughly perpendicular to this trend. In the southern Colima Rift, however, numerous fault blocks oriented obliquely to the overall trend of the rift indicate that the extension direction may not be oriented strictly perpendicular to the rift axis. The rift overlies the landward extension of the very active Rivera Fracture Zone, which may be causing the rift to form as a tear fault in the overriding plate as the fracture zone is subducted (Nixon, 1982). Alternatively, Luhr *et al.* (1985) have interpreted the rift as an eastward jump of the northern East Pacific Rise to a location beneath the southern edge of the Mexican continent,

implying a mantle plume is responsible for the rifting. Although both factors may contribute to the rifting, the associated uplift and alkalic volcanics suggest that the second interpretation is the more likely of the two.

3. The **Chapala Rift** extends from the triple junction eastward about 130 km, where it is eventually truncated by a prominent N-S trending graben south of the Sierra Penjamo. The zone of deformation is about 50 km wide south of Guadalajara, reaching a maximum width of 100 km east of Lake Chapala. The rift can be divided into three basins or grabens: the Citala Graben, immediately adjacent to the triple junction at the western end of the rift and probably the most active part of the rift; the Chapala Graben, a basin defined by large inward-dipping normal faults at its margins, two-thirds of which is occupied by Lake Chapala; and a broad plain north and east of the lake, interrupted at intervals by normal faults, forming the third major division of the Chapala Rift. The rift represents the zone of extension between the North American plate and the Michoacan crustal block.

12.2 Eastern Study Area

East of Lake Chapala the pattern of faulting becomes more complex. Here, structures within adjacent areas tend to blend and coalesce, making a division into distinct structural entities much more difficult than is possible farther west. It is possible, however, to divide the eastern half of the study area into four areas of internally consistent deformational character.

1. The **Sierra Penjamo** is an area of highlands about 70 km long and 30 km wide, located on the boundary between the Leon-Guanajuato Plateau and the Rio Lerma alluvial plain. It coincides with an area of numerous normal faults that form a distinctive pattern, which is interpreted to indicate localized uplift combined with regional extension in a NNW–SSE direction. The uplift may be the result of a shallow intrusion of a magma body, perhaps accomplished in several pulses.

2. The **Michoacan Triangle** is a triangular area of normal faulting and volcanism located in northern Michoacan state. The area is defined by large marginal fault zones and is situated in the notch between the North American plate and the Michoacan and Guerrero crustal blocks. Faulting in the area lacks a clearly dominant orientation, perhaps indicative of a greater degree of crustal disruption than is expressed elsewhere in the MVB. This conclusion is supported by the absence of large volcanoes in the area. Instead, volcanic activity is characterized by the eruption of hundreds of smaller volcanic centers, which form the densest and most active part of the Michoacan-Guanajuato Volcanic Field (MGVF). This area is a good example of how the character and distribution of volcanism in the MVB is controlled by regional tectonics.

3. The **Cuitzeo fault trend** is a more organized zone of faults trending N70°-80° that extends ENE out of the Michoacan Triangle. Faulting in this area generally has a very youthful expression, particularly between and west of Lakes Cuitzeo and Yuriria, where the faults are smaller and more numerous. South of the city of Queretaro the ENE trending normal faults interact with NNW trending fractures, forming a maze of short horst and graben segments that are tilted and disorganized. The Cuitzeo fault trend is interpreted as a tensional boundary between continental Mexico (the North American plate) to the north, and the Guerrero block to the south. The orientation of faults in the area can be used to 'fix' the direction of extension in the area as about N165°.

4. The **Eastern High Plateau** is a region of broad high plains crossed by volcanic ridges. It extends eastward from about 100°W longitude to beyond the eastern edge of the study area at 98°W. Its elevation is almost entirely above 2000 m, and is much higher in areas where volcanic activity has

been concentrated. The crust in this area is the thickest in Mexico, reaching nearly 50 km, which may explain the progressively less numerous fault scarps east of the Queretaro-Taxco Fracture System; crustal deformation is simply not penetrating to the surface through the entire thickness of crust. Alternatively, the crustal deformation may be migrating eastward at present. Structure on the plateau is dominated by NNW trending fault zones, associated with Mio-Pliocene volcanic ridges, and younger E-W trending fault zones, associated with Quaternary cinder cone fields. Large strato-volcanoes are located where the two trends intersect.

In addition to the four structural divisions mentioned above, at least three major linear fault zones can be discerned on the TM image mosaic east of Lake Chapala.

1. The **Chapala-Tula Fault Zone** is a complex alignment of normal fault scarps that extends eastward out of structures related to the Chapala Rift. These scarps generally trend E-W or ENE-WSW and have vertical offsets of up to several hundred meters. Faults belonging to this fault zone cut Plio-Pleistocene cones southeast of Lake Chapala. The area west of Morelia is characterized by large normal fault scarps in an *en echelon* arrangement, possibly indicating a significant amount of sinistral motion on the Chapala-Tula fault zone. The fault zone continues east of Morelia as a nearly continuous series of major scarps stretching all the way to the Valley of Mexico north of Mexico City.

2. The **Chapala-Oaxaca Fault Zone** extends southeastward out of the southern Chapala Rift and forms the southwestern boundary of the Michoacan Triangle. This system of aligned fractures and narrow *en echelon* graben structures extends for nearly 300 km to where it bends slightly to the east and apparently becomes less active. To the northwest the fault zone is marked by the San Juanico Graben, a narrow structure oriented obliquely to the rest of the fault zone. To the southeast the fault zone is associated with a very prominent, linear valley. The arrangement of faults and small grabens indicates sinistral displacement on the fault zone. The youngest volcanic centers in the MGVF lie along this fault zone: Jorullo (1759-1774) and Paricutin (1943-1952). This fault zone has not been described previously.

3. The **Queretaro-Taxco fracture system** is a series of NNW trending fractures that limits the MGVF on the northeast. It stretches from an area north of Queretaro to the vicinity of Taxco, a distance of roughly 250 km. It varies in width from about 20 km to over 40 km. The generally more eroded nature of scarps associated with this feature indicate that it is a slightly older feature; but since it cuts Pliocene volcanics, the most recent episode of deformation along it cannot be older than Pliocene in age. It is possible that more recent activity has occurred on some of the faults associated with this feature.

13   Conclusions

The results of this study firmly establish a link between deformation in the overriding plate (expressed as neotectonic activity) and the distribution and character of volcanism in the MVB. Volcanism appears to be controlled by tectonics at all scales from local to regional. Nixon *et al.* (1987) describe a southward migration and focusing of volcanism along the volcanic front throughout the MVB since the Pliocene. They argue that this cannot be related to documented plate reorganizations in the Pacific, and that it "occurred much too rapidly to represent a direct response to a significant change in dip of the subducted slab". However, they offer no alternative hypothesis to explain the trend. One possible explanation for this phenomenon is the Quaternary development of the Chapala-Tula fault zone, which is colinear with the volcanic front of the MVB (Figure 43). This interpretation is consistent with observations of the regional development of the Plio-Quaternary arc (Cantagrel and Robin, 1979; Nixon *et al.*, 1987) and suggests that a newly reactivated zone of weakness in the crust of central Mexico is acting as a conduit for rising magmatic fluids generated by the subduction process. The implication is that deformation within the crust of the overriding slab plays a significant part in controlling the location and orientation of the volcanic belt relative to the trench. Thus variations in subduction geometry and velocity along the trench cannot be *solely* responsible for the oblique orientation of the MVB.

The large variation in eruption styles along the MVB may be explained as the result of the influence of various tectonic domains created by differential movement of crustal blocks above a zone of magma production. In general, where crustal extension or disruption is greatest, subduction-related magmas reach the surface over a broad area and no large edifices are likely to result, even if the total amount of erupted material is very large (i.e.: the MGVF). On the other hand, where extension is less, or where (despite significant extension) the crust remains relatively thick, eruptions will be concentrated along zones of crustal weakness such as wrench faults or fracture systems. These eruptions will result in larger edifices, the largest located particularly at places where such faults and fractures happen to intersect (i.e.: Nevado de Toluca, Volcan Popocatepetl).

In addition to the neotectonic synthesis, problems and questions regarding much older deformation may be addressed in unusual ways using the TM images. For example, the Chapala-Tula fault zone is probably the reactivated offspring of one of several major left-lateral faults that segmented Mexico during the early opening of the North Atlantic in the Late Triassic and Early Jurassic (Johnson, 1987). A consensus is emerging that large offsets on such faults are necessary for the reconstruction of Pangea and its break-up in the Mesozoic; and the MVB is a prime candidate for the location of one of these faults (Urrutia-Fucugauchi, 1984). This implies that the entire portion of Mexico south of the MVB is allochthonous relative to the North American craton. This idea is difficult to evaluate directly and test, however, since the MVB effectively obscures structures older than Miocene in age. Our study using TM images provides the first regional observational evidence for an extensive zone of structural weakness in the underlying crust. Conceivably this type of study could provide a similar "window" through volcanic cover in other areas where large reactivated fault zones are thought to be concealed.
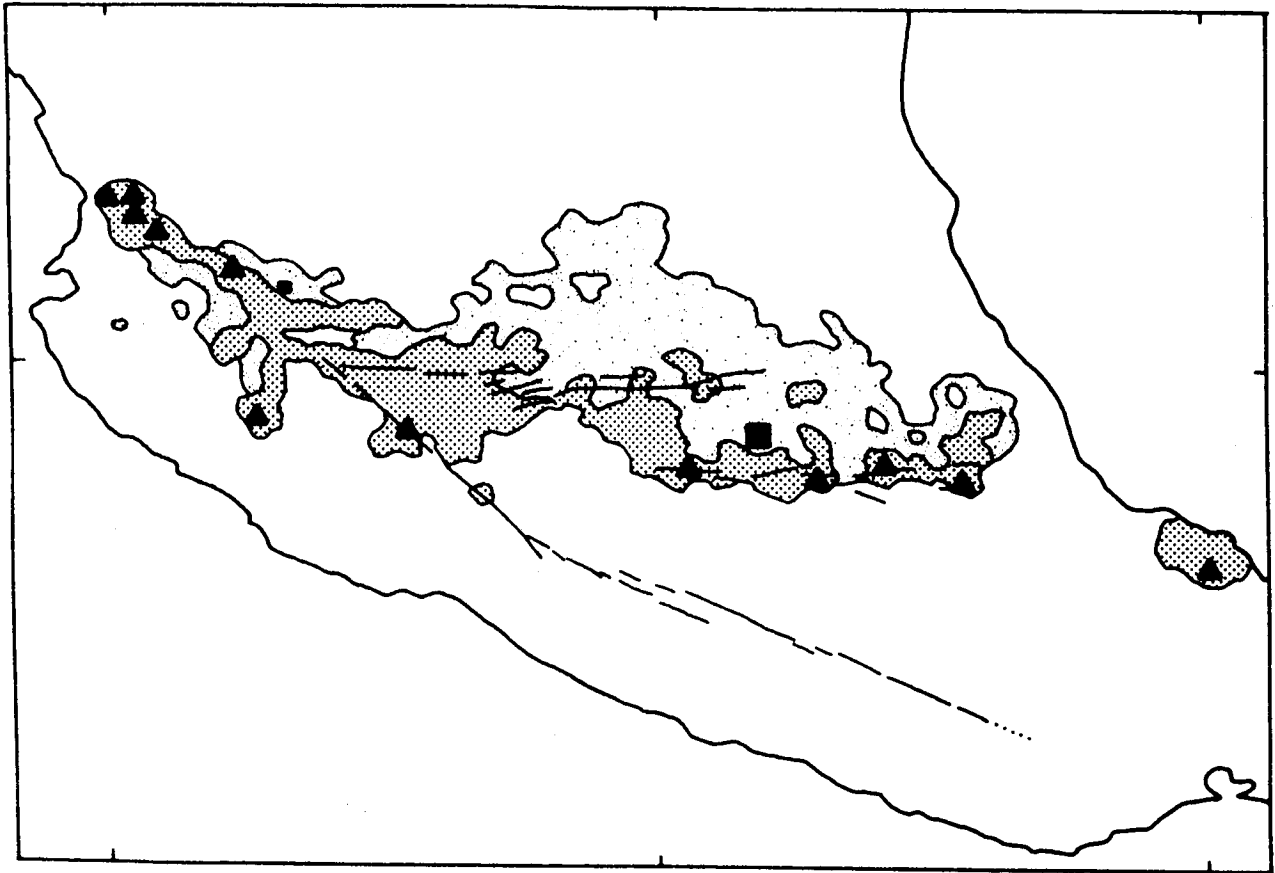
Figure 43: Sketch map showing the relationship between volcanism and neotectonic fault zones in central Mexico. In the Quaternary the volcanic front has migrated southward and focused along a zone colinear with the Chapala-Tula fault zone, east of Lake Chapala. Regular dot pattern shows the distribution of Quaternary volcanics of the MVB. Pliocene volcanics are shown by the lighter, irregular dot pattern. Large volcanoes are shown as triangles. Small square: Guadalajara; large square: Mexico City.

14 Future Work

Much work remains to be done with the Thematic Mapper images. Our growing interest in the very complex geology of central Mexico and our access to the information provided by the TM images has led us to expand the scope of our research there with several related projects. In 1987 Mr. Barros was awarded a fellowship, under NASA's Underrepresented Minority Initiative, to study the history and tectonic evolution of the various components that form the crustal blocks south of the Mexican Volcanic Belt. The geology of this region is among the least known in North America, and its history is closely related to that of neighboring regions such as the Caribbean. Therefore our goal in this project is to use the TM images and field work to refine models of the tectonic evolution of the region. This in turn will allow us to critically evaluate current models of Caribbean tectonic evolution, which must be consistent with our observations in Mexico. Mr. Barros is the ideal individual to accomplish this task. Born in Cuba, he has become one of the leading young researchers interested in the geology of the Caribbean region. He is often sought out by others working in the region for his knowledge of the geology and geologic history of the northern Caribbean, particularly Cuba.

Our group will begin a much more detailed study of Mexico in February. This new effort will involve close collaboration with researchers at NASA/Jet Propulsion Laboratory and at the Institute of Geophysics of UNAM in Mexico. As part of our collaborative arrangement with Mexico we will sponsor a Mexican graduate student, who will work with us at RSMAS. The goal of this project will be to apply new, advanced digital interpretive techniques, developed at JPL by a group headed by Dr. Harold Lang, combined with detailed field investigations to a new and geologically poorly known region (central Mexico). The project will be funded by NASA and all of the members of the group will participate, lending their individual expertise. Dr. Harrison will be Principal investigator for this project and will coordinate the efforts of participants at the three centers (RSMAS, JPL, UNAM).

We also have submitted a proposal in response to an RFP of the State of Florida Technological Research and Development Authority. Notification of awards are scheduled for February. If funded, this grant will allow us to purchase the necessary hardware to establish our own in-house image processing capability. Designed to compliment our research already underway, the planned work would involve further development of digital processing and interpretation techniques. We also plan graduate level courses in geologic remote sensing and digital image processing, which would use the in-house facilities to teach students the fundamentals in an interactive manner.

In short, our current research in Mexico, which is heavily dependent on space technology, has enabled RSMAS to develop close ties with its counterpart in Mexico and with researchers at one of NASA's leading facilities (JPL). Remote sensing is and promises to remain one of the fastest growing fields in the geosciences, and the existence of an active group of researchers using this technology at RSMAS will enable our school to use and develop the latest advances.

15 Publications

in press   Johnson, C. A. and C. G. A. Harrison, Neotectonics in Central Mexico, *Physics of the Earth and Planetary Interiors*, special issue in memory of Daniel Valencio.

Johnson, C. A. and C. G. A. Harrison, Thematic Mapper Studies of Volcanism and Tectonism in Central Mexico, *Advances in Space Research*, Proceedings of the XXVII Plenary Meeting of COSPAR.

1987   Johnson, C. A. and C. G. A. Harrison, Neotectonics in Central Mexico from Landsat Thematic Mapper Imagery, Workshop '87 Report, *Third Annual Landsat Workshop*, 1-3 September 1987, pp. 145-150, published through NASA's Laboratory for Terrestrial Physics.

1986   Harrison, C. G. A. and C. A. Johnson, Structural Geology from Landsat 5 Thematic Mapper Data, *Second Annual Landsat Workshop*, 3-5 September 1986, pp. 69-79, published through NASA's Laboratory for Terrestrial Physics.

Abstracts:

1989   Johnson, C. A., Barros, J. A., and C. G. A. Harrison, "Sunda-Style" Tectonics in SW Mexico: implications for terrane motions and truncation of the southwestern margin of North America, *In:* T. W. Donnelly and B. Burkart, Convenors, The Caribbean-North American Plate Boundary: Terranes and Tectonics, Symposium in South-Central Section Geological Society of America, meeting at Arlington, Texas, 12-14 March, (invited).

1989   Barros, J. A., C. A. Johnson, and C. G. A. Harrison, Tectonic Evolution of South-Central Mexico, *In:* T. W. Donnelly and B. Burkart, Convenors, The Caribbean-North American Plate Boundary: Terranes and Tectonics, Symposium in South-Central Section Geological Society of America, meeting at Arlington, Texas, 12-14 March, (invited).

1988   Johnson, C. A., J. A. Barros, and C. G. A. Harrison, The Chapala-Oaxaca Fault Zone: A Major Trench-Parallel Fault in Southwestern Mexico, *EOS* 69(44): 1450.

1988   Johnson, C. A. and C. G. A. Harrison, Thematic Mapper Studies of Volcanism and Tectonism in Central Mexico, XXVII Plenary Meeting of COSPAR, 18-29 July 1988, Abstracts, p. 312.

1987   Johnson, C. A., Regional Tectonics in Central Mexico: Active Rifting and Transtension within the Mexican Volcanic Belt, *EOS* 68(16): 423.

1986   Johnson, C. A., Active Continental Tectonics in Central Mexico, *EOS* 67(44): 1227.

Acknowlegements

References

Abrams, M. J., D. Brown, L. Lepley, and R. Sadowski, 1983. Remote sensing for porphyry copper deposits in southern Arizona. *Economic Geology*, **78**(4): 591–604.

Allan, J. F., 1985. Sediment depth in the northern Colima Graben from 3-D interpretation of gravity. *Geofisica Internacional*, **24**(1): 21–30.

Allan, J. F., 1986. Geology of the northern Colima and Zacoalco Grabens, southwest Mexico: Late Cenozoic rifting in the Mexican Volcanic Belt. *Geological Society of America, Bulletin*, **97**, 473–485.

Allan, J. F., and I. S. E. Carmichael, 1984. Lamprophyric lavas in the northern Colima Graben, SW Mexico. *Contributions to Mineralogy and Petrology*, **88**: 203–216.

Allan, J. F., S. A. Nelson, J. F. Luhr, I. S. E. Carmichael, and M. Wopat, 1987. Pliocene-Recent Rifting in SW Mexico and associated alkaline volcanism. *in press: The Gulf and Peninsular province of the Californias*, AAPG Memoir Series.

Anderson, T. H. and V. A. Schmidt, 1983. The evolution of Middle America and the Gulf of Mexico-Caribbean Sea region during Mesozoic time. *Geological Society of America, Bulletin*, **94**, 941–966.

Astiz, L., 1986. The 1912 Acambay, Mexico, (M=7.0) earthquake: A reexamination (abstract). *GEOS, Union Geofis. Mex. Reunion Anual*, p. 17.

Bloomfield, K., 1975. A Late Quaternary monogenetic volcano field in central Mexico. *Geol. Rundsch.*, **64**: 476–497.

Campa, M. F., 1985. The Mexican Thrust Belt. *in:* Howell, D. G. (ed.), *Tectonostratigraphic Terranes of the Circum-Pacific Region.* Circum-Pacific Council of Energy and Mineral Resources, Earth Sciences Series, Volume 1, Houston, Texas, 299–314.

Campa, M. F., and P. J. Coney, 1983. Tectono-stratigraphic terranes and mineral resource distributions in Mexico. *Can. J. Earth Sci.*, **26**: 1040–1051.

Cebull, S. E., and D. H. Shurbet, 1987. Mexican Volcanic Belt: an intra-plate Transform? *Geof. Int.*, **26**(1): 1–14.

Chael, Eric P., and Gordon S. Stewart, 1982. Recent large earthquakes along the Middle American Trench and their implications for the subduction process. *J. Geoph. Res.*, **87**(B1): 329–338.

Coney, P. J., 1978. Mesozoic-Cenozoic cordilleran plate tectonics. *Geol. Soc. Amer. Mem.* **152**: 33–49.

Coney, P. J., 1987. Circum-Pacific Tectogenesis in the North American Cordillera. *in:* Circum-Pacific Orogenic Belts and Evolution of the Pacific Ocean Basin, J. W. H. Monger and J. Francheteau (eds.), Geodynamics Series, Volume 18, 59–70.

Connor, C. B., 1984. Structure of the Michoacan Volcanic Field, Mexico (abstract). *EOS, Transactions, Am. Geophys. Union*, **65**(45): 1145.

Cross, T. A., and R. H. Pilger, Jr., 1982. Controls of subduction geometry, location of magmatic arcs, and tectonics of arc and back-arc regions. *GSA Bulletin*, **93**: 545–562.

Cserna, Z. de, 1965. Reconocimento geologico de la Sierra Madre del sur de Mexico, entre Chilpancingo y Acapulco, Estado de Guerrero. *Inst. Geol., UNAM, Bol.*, **62**: 77 pp.

Cserna, Z. de, 1970. Mexico geotectonics and mineral deposits. *New Mexico Geological Society Special Publication*, **6**: 18–25.

Cserna, Z. de, M. Palacios N., and J. Pantoja A., 1978. Relaciones de facies de las Rocas Cretacias en el noroeste de Guerrero y en areas colindantes de Mexico y Michoacan. *Soc. Geol. Mex. libro Guia. Exc. Geol. Tierra Caliente.*

Davis, W. M., 1913. Nomenclature of surface forms on faulted structures. *Bull. Geol. Soc. Am.*, **54**: 205–262.

Dean, B. W., and C. L. Drake, 1978. Focal mechanism solutions and tectonics of the Middle America arc. *J. Geol.*, **86**: 111–128.

Delgado-Argote, L. A., F. A. Gastelum, and M. Orozco-Franone, 1978. Aplicacion de imagenes de satelite Landsat I en la interpretacion de lineamientos y tectonica del Estado de Nayarit. *CRM, VII Seminario Interno Expl. Geol. Min.*, 529–562.

Delgado-Granados, H. and J. Urrutia-Fucugauchi, 1985. The structure of the Chapala Graben, Mexico. *EOS Transactions, American Geophysical Union*, **66(46)**: 1090.

Del Rio, L., 1979. Tectonica del area La Primavera-San Marcos, e implicaciones geotermicas. *in: Reporte de Percepcion Remota, Exploracion Geotermica, Parte II, Seccion C:* Inst. Inv. Elect. e Inst. Geof., reporte interno.

Demant, A., R. Mauvois, and L. Silva, 1976. El Eje Neovolcanico Transmexicano. III Congreso Latinoamericano, Acapulco (Mexico). Guide book 4, 30 p.

Demant, A., 1978. Caracteristicas del eje neovolcanico transmexicano y sus problemas de interpretatcion. *UNAM, Inst. Geol. Rev.*, **2**: 172-187.

Diaz, E. C. and F. Mooser, 1972. Formacion del Graben de Chapala. *Sociedad Geologica Mexicana, Memoria II Convencion Nacional*, 144–145.

Dremer, L. A., and S. A. Nelson, 1985. Geologic and chemical evolution of Volcan Tepitiltic, Nayarit, Mexico. *Geological Society of America Abstracts with Programs*, **17(7)**: 561.

Eissler, Holly K., and Karen C. McNally, 1984. Seismicity and Tectonics of the Rivera Plate and Implications for the 1932 Jalisco, Mexico, Earthquake. *J. Geoph. Res.*, **89(B6)**: 4520–4530.

Elias-Herrera, M., 1987. Metamorphic geology of the Tierra Caliente Complex, Tejupilco region, State of Mexico. *GSA Abstracts with Programs*, **19(17)**: p. 654.

Estela, B. B., J. Pantoja-Alor, and G. Alencaster, 1978. Secuencia estratigrafica del Cretacio Inferior del Cerro de Tuxpan, Jalisco. *Bolletin de Sociedad de Geologia Mexicana, IV Conv. Geologia National Resumenes*, **39(1)**: 12.

Ferriz, H., and G. A. Mahood, 1986. Volcanismo riolitico en el Eje Neovolcanico Mexicano. *Geof. Int.*, **25(1)**: 117–156.

Fielding, E. J., R. N. Alonso, and T. E. Jordan, 1986. Spectral stratigraphy distinguishing sedimentary rocks of the Argentine Puna with TM imagery. *Geological Society of America Abstracts with Programs*, **18(6)**: 601.

Fisher, Robert L., 1961. Middle America Trench: Topography and Structure. *Geological Society of America Bulletin*, **72(5)**: 703–720.

Fries, C., Jr., 1960. Geologia del Estado de Morelos y de Partes adyacentes de Mexico y Guerrero, region central meridional de Mexico. *Univ. Nal. Auton. Mexico, Bol.*, **60**: 326 pp.

Gastil, R. G. and W. Jensky, 1973. Evidence for strike-slip displacement beneath the Trans-Mexican Volcanic Belt. *Stanford Univ. Publ. Geol. Sci.*, **13**: 171-180.

Gastil, R. G., D. Krummenacher, and W. A. Jensky II, 1978. Reconnaissance geology of west-central Nayarit, Mexico. *GSA Map & Chart series MC-24*, 8 p.

Gastil, R. G., D. Krummenacher, and J. Minch, 1979. The record of Cenozoic volcanism around the Gulf of California. *Geol. Soc. Am. Bull.*, **90**: 839-857.

Gilbert, C. M., G. A. Mahood and I. S. E. Carmichael, 1985. Volcanic stratigraphy of the Guadalajara area, Mexico. *Geof. Int.*, **24(1)**: 169-192.

Gillespie, A. R., 1980. Digital techniques of image enhancement. *in: Remote Sensing in Geology* (Siegal, B. S. and A. R. Gillespie, eds.) John Wiley & Sons, 139-226.

Goetz, A. F. H., F. C. Billingsley, A. R. Gillespie, M. J. Abrams, R. L. Squires, E. M. Shoemaker, I. Luchitta, and D. P. Elston, 1975. Application of ERTS images and image processing to regional geologic problems and geologic mapping in northern Arizona, *App. B: NASA TR32-1597*, Jet Propulsion Laboratory, Calif. Inst. of Tech., Pasadena, California, 131-174.

Halbouty, M. T., 1976. Application of Landsat imagery to petroleum and mineral exploration. *AAPG Bull.*, **60(5)**: 745-793.

Hanus, V. and J. Vanek, 1978. Subduction in the Cocos plate and deep active fracture zones of Mexico. *Geofisica Internacional*, **17**: 14-53.

Hanus, V. and J. Vanek, 1984. Subduction induced fracture zones and distribution of hydrothermal activity in Mexico. *Tectonophysics*, **103**: 297-305.

Harding, T. P., 1974. Petroleum traps associated with wrench faults. *American Association of Petroleum Geologists Bulletin*, **58(7)**: 1290-1304.

Hasenaka, T., and I. S. E. Carmichael, 1985(a). A compilation of location, size, and geomorphological parameters of volcanoes of the Michoacan-Guanajuato Volcanic Field, central Mexico. *Geof. Int.*, **24(4)**: 577-607.

Hasenaka, T., and I. S. E. Carmichael, 1985(b). The cinder cones of Michoacan-Guanajuato, central Mexico: their age, volume and distribution, and magma discharge rate. *J. Volcanol. Geotherm. Res.*, **25**: 105-124.

Herrera, C., 1967. *Geologia de los Volcanes de Colima (Thesis Professional)*. Facultad de Ingeniera, Universidad Nacional Autonoma de Mexico, U.N.A.M.

Howell, D. G., D. L. Jones, and E. R. Schermer, 1985. Tectonostratigraphic terranes of the circum-Pacific region. *in:* Howell, D. G., (ed.), *Tectonostratigraphic Terranes of the Circum-Pacific Region.* Circum-Pacific Council of Energy and Mineral Resources, Earth Sciences Series, Volume 1, Houston, Texas, 3-30.

Jackson, J., and D. McKenzie, 1983. The geometrical evolution of fault systems. *Journal of Structural Geology*, **5(5)**: 471-482.

Johnson, C. A., 1987. A Study of Neotectonics in Central Mexico from Landsat Thematic Mapper Imagery. Thesis, University of Miami, Coral Gables, Fla., 112 pp.

Lang, H. R., S. L. Adams, J. E. Conel, B. A. McGuffie, E. D. Paylor, and R. E. Walker, 1987. Multispectral remote sensing as stratigraphic and structural tool, Wind River Basin and Big Horn Basin areas, Wyoming. *Am. Assoc. Pet. Geol. Bull.*, **71(4)**: 389-402.

Larson, R. L., and C. G. Chase, 1970. Relative velocities of the Pacific, North American and Cocos plates in the Middle America region. *Earth Planet. Sci. Lett.*, **7**: 425–428.

Le Pichon, X., and P. J. Fox, 1971. Margin offsets, fracture zones and the early opening of the North Atlantic. *J. Geophys. Res.*, **76**: 6294–6308.

Lomnitz, C., 1982. Direct evidence of a subducted plate under southern Mexico. *Nature*, **296**: 235–238.

Lopez-Ramos, E., 1983. *Geologia de Mexico*. Mexico, D.F., **III**, 453 pp.

Luhr, J. F., and I. S. E. Carmichael, 1980. The Colima Volcanic Complex, Mexico: I. Post-caldera andesites from Volcan Colima. *Contributions to Mineralogy and Petrology*, **71**: 343–372.

Luhr, J. F., and I. S. E. Carmichael, 1985. Contemporaneous eruptions of calc-alkaline and alkaline magmas along the volcanic front of the Mexican Volcanic Belt. *Geof. Int.*, **24(1)**: 203–216.

Luhr, J. F., and P. Lazaar, 1985. The Southern Guadalajara Volcanic Chain, Jalisco, Mexico. *Geofisica Internacional*, **24:4**, 691–700.

Luhr, J. F., S. A. Nelson, J. F. Allan, and S. E. Carmichael, 1985. Active rifting in S.W. Mexico: Manifestations of an incipient eastward spreading-ridge jump. *Geology*, **13**: 54–57.

Mahood, G. A., 1977. A preliminary report on the comenditic dome and ash flow complex of Sierra La Primavera, Jalisco. *UNAM, Inst. Geol. Rev.*, **1**: 177–190.

Mahood, G. A., 1980. Geological evolution of a Pleistocene rhyolitic center–Sierra la Primavera, Jalisco, Mexico. *Journal of Volcanology and Geothermal Research*, **8**: 199–230.

Mahood, G. A., 1981. Chemical evolution of a Pleistocene rhyolitic center: Sierra la Primavera, Jalisco, Mexico. *Contrib. Mineral. Petrol.*, **71**: 129–149.

Mahood, G. A., and R. E. Drake, 1982. K-Ar dating of young rhyolitic rocks: a case study of the Sierra La Primavera, Jalisco, Mexico. *Geol. Soc. Amer. Bull.*, **93**: 1232–1241.

Martin del Pozzo, A. M., 1982. Monogenetic Vulcanism in Sierra Chichinautzin, Mexico. *Bull. Volcanol.*, **45(1)**: 9–24.

McDowell, F. W., and R. P. Keizer, 1977. Timing of mid-Tertiary volcanism in the Sierra Madre Occidental between Durango City and Mazatlan, Mexico. *Geological Society of America Bulletin*, **88**: 1479–1487.

Menard, H. W., 1978. Fragmentation of the Farallon plate by pivoting subduction. *J. Geol.*, **86**, 99–110.

Mohr, P. A., 1974. Structural Geology of the African Rift System: Summary of New Data from ERTS-1 Imagery. in: *Third Earth Resources and Technology Satellite-1 Symposium, Vol. I: Technical Presentations*, S. C. Freden, E. P. Mercanti, and M. A. Becker, eds., National Aeronautics and Space Administration, Washington, D.C., pp. 767–782.

Moik, J. G., 1980. *Digital processing of remotely sensed images*. NASA Special Publication SP-431, National Aeronautics and Space Administration, Washington, D.C., 330 pp.

Molnar, P. and L. R. Sykes, 1969. Tectonics of the Caribbean and Middle American region from focal mechanisms and seismicity. *GSA Bull.*, **80**: 1639–1684.

Mooser, F., 1969. The Mexican Volcanic Belt structure and development, formation of fractures by differential crustal heating. *Mexico, D.F., Pan Am. Symp. on the Upper Mantle (1968)*, pt. 2, 15–22.

Mooser, F., 1972. El eje volcanico Mexicano, debilidad cortical Prepaleozoica reactivada en el Tercario. *Soc. Geol. Mex. Mem.*, **II**, 186–188.

Mooser, F., A. E. M. Nairn, and J. F. W. Negendank, 1974. Paleomagnetic investigations on the Tertiary and Quaternary igneous rocks, VIII. A paleomagnetic and petrologic study of volcanics of the Valley of Mexico. *Geol. Rundsch.*, **63**: 451–483.

Moran-Zenteno, D. J., 1987. Paleogeografia y Paleomagnetismo Precenozoicos Del Tereno Mixteco. Tesis Profesional, U.N.A.M., 177 pp.

Murphy, G. P., and I. S. E. Carmichael, 1984. A Report on the occurrence of maars in the Michoacan-Guanajuato Volcanic Field, central Mexico. *Geol. Soc. Am., Abstracts with Programs*, p. 604.

Nakamura, K., 1977. Volcanoes as possible indicators of tectonic stress orientation-principle and proposal. *Journal of Volcanology and Geothermal Research*, **2**: 1–16.

Negendank, J. F. W., 1972. Volcanics of the Valley of Mexico, Part I: Petrography of the volcanics. *N. Jb. Miner. Abh.*, **116**: 308–320.

Negendank, J. F. W., 1974. Some aspects of the volcanic rocks of the Valley of Mexico. *Proceedings of the Mexican Symposium no Geodynamics*, 292–303.

Negendank, J. F. W., 1976. The crustal origin of the Valley of Mexico volcanics (abstract). *III Congr. Latinoamer. Geol.*, Acapulco, p. 98.

Nelson, S. A., 1980. Geology and petrology of Volcan Ceboruco, Nayarit, Mexico. *Geological Society of America Bulletin, Part II*, **91**: 2290–2431.

Nelson, S. A. and I. S. E. Carmichael, 1984. Pleistocene to Recent alkalic volcanism in the region of Sanganguey Volcano, Nayarit, Mexico. *Contrib. Mineral. Petrol.*, **85**: 321–335.

Nelson, S. A., and R. A. Livieres, 1986. Contemporaneous calc-alkaline and alkaline volcanism at Sanganguey Volcano, Nayarit, Mexico. *Geological Society of America Bulletin*, **97**: 798–808.

Nelson, S. A., and G. Sanchez-Rubio, 1986. Trans-Mexican Volcanic Belt Field Guide: Canadian Geolocgical Assoc., Volcanology Div., 108 p.

Ness, G. E., Lyle, M. W., and Lonseth, A. T., 1985. Revised Pacific, North America, Rivera and Cocos relative motion poles: implications for strike-slip motion along the Trans-Mexican Volcanic Belt. *EOS Transactions, American Geophysical Union*, **66(46)**: 849–850.

Nieto-Obregon, J., L. Delgado A., and P. E. Damon, 1985. Geochronologic, petrologic and structural data related to large morphologic features between the Sierra Madre Occidental and the Mexican Volcanic Belt. *Geofis. Intern.*, **24(4)**: 623-664.

Nixon, G. T., 1982. The relationship between Quaternary volcanism in central Mexico and the seismicity and the structure of subducted ocean lithosphere. *GSA Bull.*, **93**: 514–523.

Nixon, G. T., A. Demant, R. L. Armstrong and J. E. Harakal, 1987. K-Ar and geologic data bearing on the age and evolution of the Trans-Mexican Volcanic Belt. *Geof. Intern.*, **26(1)**: 109–158.

Ontiveros-Tarango, G., 1973. Estudio estratigrafico de la pocion noroccidental de la cuenca de Morelos-Guerrero. *Bol. Asoc. Mex. Geol. Petrol.*, **25**: 189–234.

Ortega-Gutierrez, F., 1986. The geologic regions of Mexico, *in:* Perspectives in Regional Geological Synthesis (Planning for the Geology of North America), Palmer, A. R., (ed.), Geological Society of America, p. 99–104.

Pantoja-Alor, J., 1959. Estudio Geologico de Reconocimiento de la Region de Huetamo, Edo. de Michoacan. *C.R.M. Boletin*, **50**.

Pasquare, G., F. Forcella, A. Tibaldi, L. Vezzoli, and A. Zanchi, 1986. Sturctural behaviour of a continental volcanic arc: the Mexican Volcanic Belt. *in: The Origin of Arcs*, Developments in Geodynamics Series, **21**: 509–527.

Pasquare, G., L. Vezzoli and A. Zanchi, 1987. Morphological and structural model of Mexican Volcanic Belt. *Geofis. Intern.*, **26(6)**: 159–176.

Pasquare, G., V. H. Garduno, A. Tibaldi, and M. Ferrari, 1988. Stress pattern evolution in the central sector of the Mexican Volcanic Belt. *Tectonophysics*, **146**: 353-364.

Paylor, E. D., M. J. Abrams, J. E. Conel, A. B. Kahle, and H. R. Lang, 1986. Performance evaluation and geologic utility of Landsat-4 Thematic Mapper data (abstract). *in: Earth Resources, a continuing bibliography*, NASA SP-7041(50), p. 31.

PeMex, Geologic Guide X, Evaluacion Geologica Petrolera Cuenca de Morelos. Superintendencia de Operacion Geologica, Departmento de Geologia Superficial. Poza Rica de Hgo., 86 pp.

Pilger, R. H., 1978. A closed Gulf of Mexico, pre-Atlantic Ocean plate reconstruction and the early rift history of the Gulf of Mexico and North Atlantic. *Gulf Coast Assoc. Geol. Soc., Trans.*, **28**, p. 385–393.

Pindell, J., and J. F. Dewey, 1982. Permo-Triassic reconstruction of Western Pangaea and the evolution of the Gulf of Mexico/Caribbean region. *Tectonics*, **1(2)**: 170–211.

Podwysocki, M. H., D. B. Segal, and M. J. Abrams, 1983. Use of multispectral scanner images for assessment of hydrothermal alteration in the Marysville, Utah, mining area. *Economic Geology*, **78(4)**: 675–687.

Pratt, W. K., 1978. *Digital image processing*. John Wiley and Sons, 750 pp.

Quennell, A. M., 1985. *Continental Rifts*. Benchmark Papers in Geology; v. 90. Van Nostrand Reinhold, 349 pp.

Ramos, V. A., 1977. Basement tectonics from Landsat imagery in mining exploration. *AAPG Bulletin*, **60(5)**: 745–793.

Robin, C., 1982. Mexico. *in: Andesites* (Thorpe, R.S., ed.), John Wiley and Sons, 137–147.

Rosenfeld, A., and A. C. Kak, 1982. *Digital Picture Processing, 2nd Ed.* Academic Press, **1**: 435 pp. and **2**: 349 pp.

Ruiz, J., P. J. Patchett, and F. Ortega-Gutierrez, 1988. Proterozoic and Phanerozoic basement terranes of Mexico from Nd isotopic studies. *Geol. Soc. Am. Bull.*, **100**: 274–281.

Sabins, F. F., 1978. *Remote Sensing Principles and Interpretation*. W.H. Freeman.

Salinas-Prieto, J. C., 1984. Los limites tectonicos sur y occidental del Terreno Mixteco. *Soc. Geol. Mex. Bol.*, **45**: 73–86.

Schilt, F. S., D. E. Karig, and M. Truchan, 1982. Kinematic evolution of the northern Cocos plate. *J. Geophys. Res.*, **87(B4)**: 2958-2968.

Schowengerdt, R. A., 1983. *Techniques for Image Processing and Classification in Remote Sensing*. Academic Press, 249 pp.

Sengor, A. M. C. and K. Burke, 1978. Relative timing of rifting and volcanism on earth and its tectonic implications. *Geophys. Res. Lett.* **5(6):** 419–421.

Settle, M., 1979. The structure and emplacement of cinder cone fields. *Am. J. of Science*, **279:** 1089–1107.

Settle, M., M. J. Abrams, J. E. Conel, A. F. H. Goetz, and H. R. Lang, 1985. Sensor Assessment Report. *in: The Joint NASA/Geosat Test Case Project, Final Report*, Abrams, M. J., J. E. Conel, and H. R. Lang (H. N. Paley, ed.), American Association of Petroleum Geologists, **2(1):** 2-1–2-24.

Shurbet, D. H. and S. E. Cebull, 1984. Tectonic interpretation of the Trans-Mexican Volcanic Belt. *Tectonophysics*, **101:** 159–165.

Shurbet, D. H. and S. E. Cebull, 1986. Tectonic interpretation of the Trans-Mexican Volcanic Belt–Reply. *Tectonophysics*, **127:** 155–160.

Siegal, B. S. and A. F. H. Goetz, 1977. Effects of vegetation on rock and soil type discrimination. *Photogramm. Engng.*, **43:** 191–196.

Smith, R. L., and R. A. Bailey, 1968. Resurgent Cauldrons. *in: Studies in Volcanology: A Memoir in Honor of Howel Williams*, R. R. Coats, R. L. Hay and C. A. Anderson (Editors), Geol. Soc. Am., Mem., **116:** 613–662.

Stewart, H. E., R. Blom, M. Abrams, and M. Daily, 1980. Rock type discrimination and structural analysis with Landsat and Seasat data: San Rafael swell, Utah. *in: Radar Geology: an assessment.* NASA Jet Propulsion Laboratory Publication 80-61, p. 151-167.

Stewart, J. H., 1978. Basin-range structure in western North America: A review: *Geological Society of America Memoir 152*, 1–31.

Suarez, G. and S. K. Singh, 1986. Tectonic interpretation of the Trans-Mexican Volcanic Belt–Discussion and Reply. *Tectonophysics*, **127:** 155–160.

Tchalenko, J. S., 1970. Similarities between shear zones of different magnitudes. *Geological Society of America Bulletin*, **81:** 1625–1640.

Thornbury, W. D., 1969. *Principles of Geomorphology*, Second Edition. John Wiley and Sons, Inc., 594 p.

Thorpe, R. S. and P. W. Francis, 1975. Volcan Ceboruco: A major composite volcano of the Mexican Volcanic Belt. *Bulletin Volcanologique*, **39:** 201–213.

Thorpe, R. S., 1977. Tectonic significance of alkaline volcanism in eastern Mexico. *Tectonophysics*, **40:** 19–26.

Urrutia-Fucugauchi, J., 1981. Preliminary paleomagnetic study of lower tertiary volcanic rocks from Morelos and Guerrero state. *Geof. Int.*, **22:** 81–110.

Urrutia-Fucugauchi, J., 1984. On the tectonic evolution of Mexico: Paleomagnetic constraints. *in: Plate Reconstruction from Paleozoic Paleomagnetism*, Van der Voo, R. *et al.*, eds., A.G.U. Geodynamics Series, Vol. 12, p. 29-47.

Urrutia-Fucugauchi, J., 1986. Late Mesozoic-Cenozoic evolution of the northwestern Mexico magmatic arc zone. *Geof. Int.*, **25(1):** 61–84.

Urrutia-Fucugauchi, J., 1986. Crustal thickness, heat flow, arc magmatism, and tectonics of Mexico–preliminary report. *Geof. Int.*, **25(4):** 559–573.

Urrutia-Fucugauchi, J., and H. Bohnel, 1987. Tectonics along the Trans-Mexican Volcanic Belt according to paleomagnetic data. *in press: Physics of the Earth and Planetary Interiors.*

Verma, S. P., 1983. Magma genesis and chamber processes at Los Humeros Caldera, Mexico-Nd and Sr isotope data. *Nature*, **301**: 52–55.

Verma, S. P., 1984. Alkali and alkaline earth element geochemistry of Los Humeros Caldera, Puebla, Mexico. *J. Volcanol. Geotherm. Res.*, **20**: 21–40.

Verma, S. P., 1985. Mexican Volcanic Belt (preface). *Geofis. Int.*, **24(1)**: 7–20.

Vincent, R. K., 1975. The potential role of thermal infra-red multispectral scanners, in geological remote sensing. *Proc. IEEE*, **63**: 137–147.

Walker, G. P. L., J. V. Wright, B. J. Clough, and B. Booth, 1981. Pyroclastic geology of the rhyolitic volcano of La Primavera, Mexico. *Geol. Rundsch.*, **70**: 1100–1118.

Walper, J. L., 1980. Tectonic evolution of the Gulf of Mexico. *in: The Origin of the Gulf of Mexico and the Early Opening of the Central North Atlantic*, R. H. Pilger, ed., *Houston Geol. Soc. Contin. Ed. Ser.*, **1**: 87–98.

Watkins, N. D., B. M. Gunn, A. K. Baksi, D. York and J. Ade-Hall, 1971. Paleomagnetism, geochemistry, and potassium-argon ages of the Rio Grande de Santiago volcanics, central Mexico. *Geol. Soc. Am. Bull.*, **82**: 1955-1968.

Wilcox, R. E., T. P. Harding, and D. R. Seely, 1973. Basic Wrench Tectonics. *American Association of Petroleum Geologists Bulletin*, **57(1)**: 74–96.

Williams, H., 1950. Volcanoes of the Paricutin region, Mexico. *U.S. Geol. Surv. Bull.*, **965-B**: 165–279.

Williams, R. S., 1983. Geological Applications. *in: Manual of Remote Sensing, 2nd Edition, Vol. II: Interpretation and Applications, Chapter 31*, 1667–1954.

Withjack, M. O., and C. Scheiner, 1982. Fault patterns associated with domes–An experimental and analytical study. *Am. Assoc. Pet. Geol. Bull.* **66(3)**: 302–316.

Wright, J. V., 1981. The Rio Caliente ignimbrite: analysis of a compound Intrapinian ignimbrite from a major Late Quaternary Mexican eruption. *Bulletin Volcanologique*, **44**: 189–212.
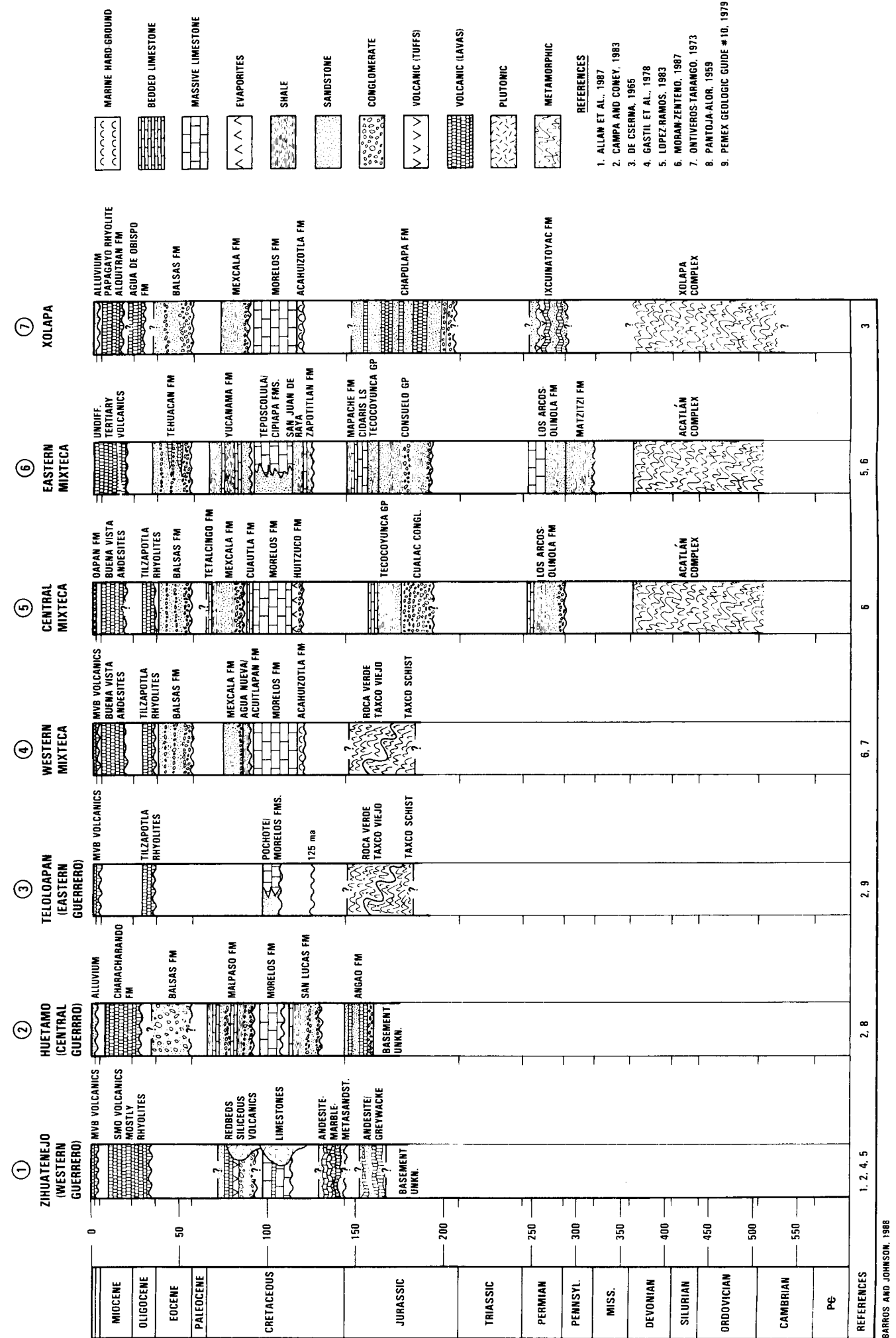
Figure 40: Phanerozoic stratigraphy south of the MVB.

NEOTECTONICS IN CENTRAL MEXICO

KEY TO VOLCANIC FEATURES

1. VOLCAN SAN JUAN
2. VOLCAN SANGANGUEY
3. VOLCAN TEPILTIC
4. VOLCAN CEBORUCO
5. VOLCAN TEQUILA
6. LA PRIMAVERA CALDERA
7. NEVADO DE COLIMA
8. VOLCAN DE COLIMA
9. TANCITARO
10. PARICUTIN
11. JORULLO

12. LOS AZUFRES CALDERA
13. AMEALCO CALDERA
14. HUICHAPAN CALDERA
15. NEVADO DE TOLUCA

16. IZTACCIHUATL
17. POPOCATEPETL
18. CERRO MALINCHE
19. PICO DE ORIZABA

Figure 11: Sketch map showing neotectonic deformation in central Mexico, simplified from Figure 10.
Also shown are interpretations of four images not included in Figure 10, continuing the trace of the
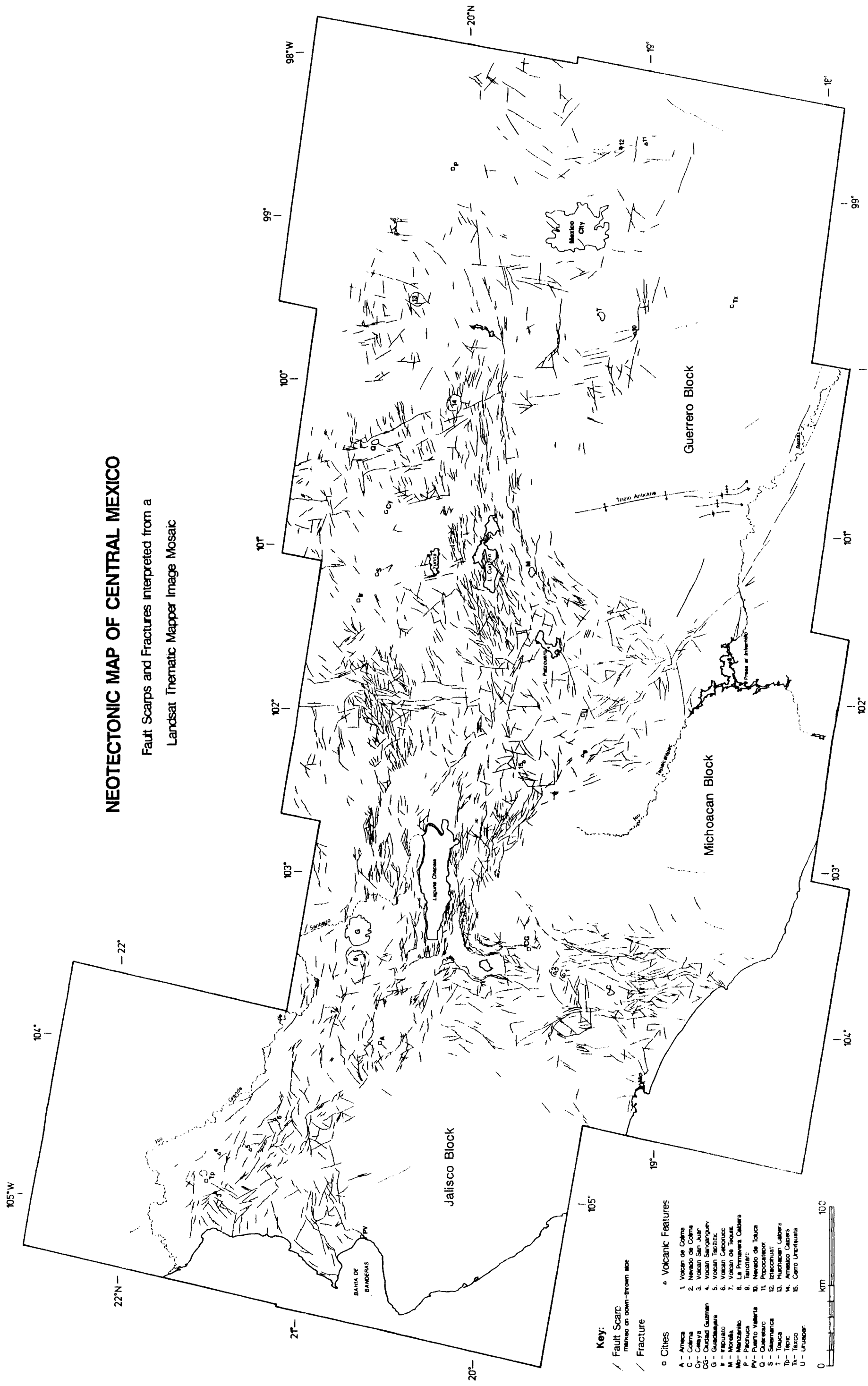Chapala-Oaxaca fault zone to the southeast.

39

Figure 10: Neotectonic map of central Mexico derived from the interpretation of Landsat Thematic Mapper imagery at a scale of 1:1 million. The locations of major cities and volcanic features are marked on the map for help in location.
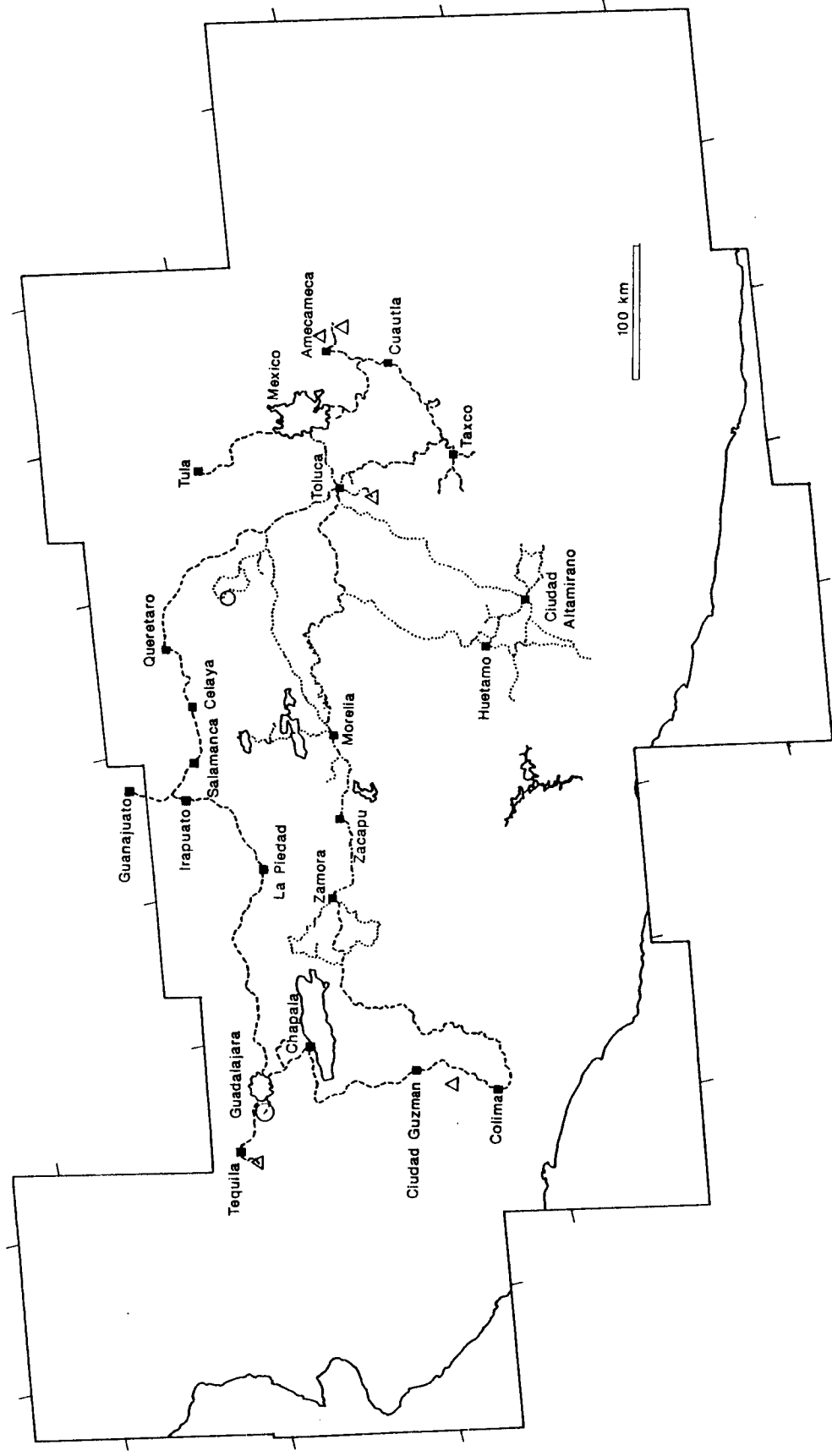
Figure 9: Sketch map of the study area showing the regional coverage of the two field seasons, which were held during the Spring of 1986 (dashes)and 1988 (dots). Reconnaissance geology and Ground-truth data was collected over much of the central and western parts of the volcanic belt, as well as from a large portion of the region south of the MVB. M, Mexico City; G, Guadalajara. Refer to Figure 11 for comparison with the neotectonic deformation in the region.